ORNL-3385

Contract No. W-7405-eng-26

CHEMICAL TECHNOLOGY DIVISION
METALS AND CERAMICS DIVISION

STATUS AND PROGRESS REPORT FOR THORIUM FUEL CYCLE DEVELOPMENT FOR PERIOD ENDING DECEMBER 31, 1962

Compiled by
D. E. Ferguson

DATE ISSUED

OCT 28 1963

OAK RIDGE NATIONAL LABORATORY
Oak Ridge, Tennessee
operated by
UNION CARBIDE CORPORATION
for the
U. S. ATOMIC ENERGY COMMISSION

DISCLAIMER

CONTENTS

CONTENTS (Continued)

CONTENTS (Continued)

1.0 ABSTRACT

Sol-Gel Process Development. -- The sol-gel process, developed for the preparation of thoria or uranium oxide--thorium oxide particles suitable for filling nuclear reactor fuel elements by vibratory compaction, has been successfully scaled up to the preparation of 15 kg per batch. Starting with the products of the Thorex process (uranyl nitrate and thorium nitrate), the process produces the dense oxides in four simple steps that can be readily carried out behind shielding. In engineering and chemical development, the optimization of procedures and equipment for the preparation of oxide (3/97 U/Th weight ratio) at the rate of 10 kg/day for the Kilorod Project was emphasized. Each unit operation required for the sol-gel process was demonstrated at full scale. In the course of these studies, materials were made available for fuel element fabrication development and for in-pile testing of sol-gel-prepared materials.

In the rotary denitrator, batches of thorium nitrate containing 15 kg of ThO_2 were dehydrated in heated air as the temperature was increased to 180°C, and then denitrated in superheated steam as the temperature was increased to 475°C and held for 1 hr. The design and operation of the calciner was unusually successful and trouble-free. More than 400 kg of highly dispersible ThO_2 that had a reproducible residual NO_3^-/ThO_2 mole ratio of from 0.025 to 0.03 was prepared.

Uranium oxide--thorium oxide sol was prepared in a specially-designed and developed critically safe slab tank. A precisely measured volume of uranyl nitrate solution, analyzed for uranium and nitrate content, was added to water and circulated through the tank and a heater. While heating to 85°C, the nitrate content of the solution is adjusted to give an NO_3^-/ThO_2 mole ratio of 0.077 for the finished sol. A weighed batch (10 kg) of ThO_2 was flushed slowly into the tank with the correct amount of water to give a 2 M ThO_2 sol. After digestion at 90°C with recirculation for 1 hr, sufficient NH_4OH was added to give a 0.017 NH_4OH/ThO_2 mole ratio. The nitrate adjustment ensures complete dispersion, and the NH_4OH adjustment fixes uranium on the surface of the thoria. This optimized procedure gives sols that lead to homogeneous oxide products whose particles vary in U/Th weight ratio by less than 1%. The oxides from these sols likewise

consistently have particles of maximum density (9.9+ g/cc), and are easily packed to densities of 9.0 g/cc in fuel rods.

The adjusted sol was pumped to the top of a series of sol-dryer trays arranged in cascade and connected by overflow tubes so that the sol, containing 10 to 15 kg of oxide, was distributed equally among them. The sol was dried to gel at 85 to 90°C in a stream of heated air. In 48 hr of drying time, gel particles ranging in size from 1 cm down to about 100 U.S. mesh size (about 90% of particles larger than 16 mesh) were produced, and they had 4 to 6% volatile matter and a density of 6 to 7 g/cc. Laboratory experiments indicated that particle size may be controlled by specifying conditions of sol-drying.

Gels were calcined in air at a relatively slow rate of increase in temperature (100°C/hr) up to 500°C, and then at 300°C/hr up to 1150°C. After 1 hr in air, the atmosphere was changed to noncombustible 4% H_2--Ar and calcination continued at 1150°C for 4 hr. The furnace and charge were cooled under argon to about 200°C before being removed from the furnace.

Laboratory experiments showed that calcinations and cooldowns conducted entirely in argon or nitrogen produced oxide products that had a density of as high as 9.9+ g/cc, an O/U ratio of 2.0500 or less, and a residual gas content of 0.005 cc/g or less, comparable with the results of calcinations in 4% H_2--Ar. However, in a larger furnace, where the atmospheres and the temperatures were cycled, good results were not achieved with inert gases because good control of atmosphere in contact with the charge was impossible.

In testing calcined oxides to determine the quantities and species of gases contained in them, they were heated to 1200°C in vacuum. These quantities and species of gases were shown to depend on the furnace atmospheres used during the calcination and cooling steps, on size of the oxide particles, and on blanket gases in contact with the oxide during comminution to obtain optimum particle size distribution. The evolution of hydrogen and carbon monoxide were strongly indicated to be due to a reaction between carbon in the oxide and the water adsorbed during grinding. Water and carbon dioxide were the major gases released from oxides in which the O/U ratios were high. The bulk of water and carbon dioxide adsorbed by the oxide during grinding was evolved in vacuum at temperatures below 400°C.

Fabrication and Material Development. -- Research and development on this program in the Metals and Ceramics Division has been carried out in three general areas. One effort has been the development of process schemes and equipment for the remote fabrication of fuel elements containing mixtures of thorium and uranium oxides.

During the past year, equipment for crushing, classifying, and vibratory compaction of oxides, plus equipment for welding, cleaning, and inspection of fuel rods have been developed and installed in a lightly shielded facility. Approximately 1100 fuel rods containing U^{233} will be fabricated for criticality, zero power experiments at Brookhaven National Laboratory.

The prime developmental work centered around the solution of the proper particle-size distribution to be fed to the fuel rods during vibratory compaction, and the establishment of optimum welding conditions.

The second area of major concern has been the irradiation performance of mixed oxides of thorium and uranium produced by the sol-gel process. Over 30 capsules containing various versions of sol-gel-prepared oxides were irradiated. Most of these were conducted at process-water temperatures and with rather modest heat ratings. In comparison with mixed oxides obtained by standard methods, the sol-gel-derived fuel proved to be at least as good and, in some cases, slightly better in retaining fission gases. Because of the modest heat ratings, no sintering of the loose fuel particles has been observed.

Thoria pellet development work was originally undertaken, with the goal of achieving a dense spherical particle having a high attrition resistance. The ultimate purpose was to use these pellets in a fluidized blanket system of a breeder reactor. Fabrication methods were developed whereby density and grain size could be controlled. The use of coatings were investigated and then evaluated by attrition tests. Encouraging results were obtained just prior to the termination of the project.

Efforts to improve the resistance of thorium metal to irradiation-induced swelling involve the use of dispersion hardening. The dispersoid selected is thoria in the submicron-particle-size range. The problem involves the development of fabrication procedures to achieve the fine particle size of metal and oxide and to fabricate shapes containing an optimum dispersion of oxide in the metal.

2.0 INTRODUCTION AND SUMMARY

The ORNL Fuel Cycle Program has been directed toward process development of the sol-gel process for preparing ThO_2-UO_2 reactor fuels, and evaluation of the product obtained. Process development has included studies of the variables important to sol preparation and gel formation, gel calcination, and gas retention by the product. A preliminary comparative evaluation of radiation stability of sol-gel process ThO_2-UO_2 and of ThO_2-UO_2 mixed oxides prepared by other methods has also been made.

A request to ORNL to prepare about a thousand tubes filled with oxide containing 3 wt % $U^{233}O_2$--97 wt % ThO_2 has provided an opportunity to demonstrate a sol-gel--vibratory-compaction procedure for preparing reactor fuels with U^{233} at the 10 kg of fuel per day scale. The fuel prepared by this procedure will be used in zero power criticality experiments at Brookhaven National Laboratory. This program has been dubbed the Kilorod Program, and has required the construction of a shielded, completely contained facility which has been named the Kilorod Facility.

The construction of the structural components in the Kilorod Facility were completed during this report period. All operations involved in manufacture of the reactor fuel will be done in Building 3019, the chemical engineering pilot plant building at ORNL. They consist of (1) a solvent extraction cycle employing 2.5% di-sec-butylphenyl phosphonate for the removal of the daughter activities of U^{233} and U^{232}; (2) preparation of reactor grade UO_2-ThO_2 (3 wt % U^{233}), using the ORNL sol-gel process; (3) sizing and classification of the resultant solids; and (4) compaction of the solids by vibratory compaction in Zircaloy-2 tubes.

2.1 Solvent Extraction

The solvent extraction pilot plant is now in a condition suitable for operation, but is untested under the conditions required by the process flowsheet. All equipment modifications have been completed, and additional equipment has been installed. The status of this part of the program may be summarized as follows:

1. All equipment and piping has been leak tested with water.

2. All vessels and instruments have been calculated.

3. The flowsheet to be used for the purification of the U^{233} has been validated.

4. A hazards review has been prepared, setting out the process hazards and methods of control. Operation approval for criticality control methods has been received from the Criticality Review Committee.

5. Run sheets, data sheets, and operations manuals have been prepared.

6. A program of operator training by means of lectures and in-plant training involving the unit operations has been completed.

2.2 Sol-Gel Process

All equipment has been located within the sol-gel cubicle in cell 4 of Building 3019 and installation is underway. Piping within the cubicle is about 10% complete. Electrical work, including installation of the west control panel, has been completed. The estimated completion date for this facility is December 30, 1963. Following the equipment-installation phase, 20 kg of 3 wt % natural urania-thoria will be prepared to provide material for vibratory compaction studies and to gain in-plant operability information.

2.3 Rod Fabrication

The installation of the manipulator ports and windows has been completed and the structural steel racks to be used for the equipment have been placed. All equipment items tested in the mockup have been cleaned and await installation.

2.4 Radiation-Monitoring Program

In addition to the preparation of the fuel elements, an additional objective of the Kilorod Program is to gain practical radiation hazards information connected with the handling of recycled U^{233}.

An inherent problem of thorium fuel cycles is the radioactivity associated with the recycled fuel. The radioactive substances include

the U^{233} and U^{232}, any recycled thorium, and fission products. However, the U^{233} to be used in the Kilorod Program is free of fission products and contains only 38 ppm of U^{232}. Solvent extraction purification just prior to use will remove thorium and the U^{232} daughter products, which will grow back during the process. Since, in the absence of fission products, these daughters are the major gamma sources, it is desirable to obtain data on both the actual gamma dose rates and the cumulative doses to workers at each operation in the Kilorod Facility. As a result, a series of calculations of dose rates received by operators of the equipment to be used in the solids-handling cubicles were made. With some assumptions as to exposure times, a probable cumulative dose to an operator's hands and arms has been estimated. Calculated dose rates and total exposures will be greatest for the operations in the chemical cubicle, that is, for the sol-gel-process lines. Ten sol-gel batches will be made from each lot of decontaminated uranyl nitrate hexahydrate (UNH), the first only a few hours after solvent extraction, the second about ten days later. The results of the calculations for the first and tenth of these batches are summarized in Fig. 2.1. Here the bars show the dose rates, while the solid lines show the accumulated dose at each operation. The solid bar and lower line are for the first sol-gel batch, the open bar and upper line for the tenth batch.

On the basis of the calculations, a program has been prepared for alpha and gamma spectrometric measurements on samples of UNH product, sol, gel, and fired solids, and for direct monitoring of the gamma dose rates from the same materials in-process. Cumulative doses to personnel at each station will be measured by use of film badges and pocket dosimeters. The data obtained should facilitate the estimation of activity in and dose rates from unshielded sol-gel lines that transport UNH with higher U^{232} concentrations.

3.0 SOL-GEL PROCESS DEVELOPMENT

(O. C. Dean, A. T. Kleinsteuber, J. W. Snider, C. C. Haws, P. A. Haas)

3.1 Description of the Process

The sol-gel process was developed to convert uranyl and thorium nitrates to dense ThO_2 or UO_2-ThO_2 particles suitable for the filling

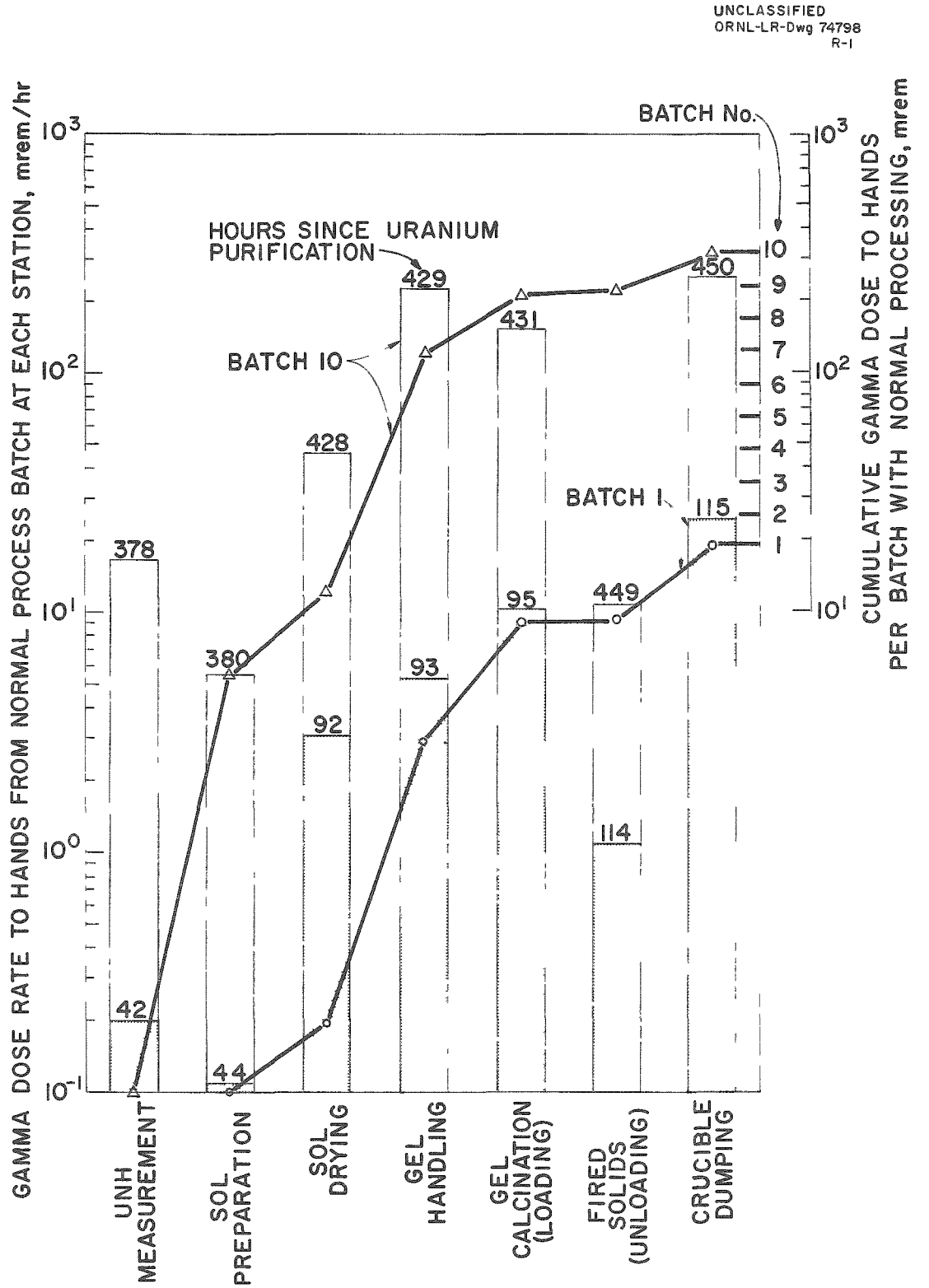

Fig. 2.1. Gamma Dose Rate and Cumulative Hand Exposure During Sol-Gel Processing.

of fuel tubes by vibratory compaction. It consists of four simple steps (Fig. 3.1): thorium nitrate, a product of the Thorex process,[1] is heated to about 200°C in a stream of air and then is denitrated with superheated steam to produce ThO_2 that contains a closely controllable 2-to-3 mole % of residual nitrate. This ThO_2 is dispersed to a stable oxide sol by agitation in dilute uranyl nitrate solution at 80°C. After dispersion and adjustment to a pH of 3.9, the sol is evaporated at 85 to 90°C to produce a gel that on drying breaks up into pieces approximately 1/2 in. across. This gel contains about 5 wt % of residual water and has a density of about 5 g/cc. The gel is calcined in air, the temperature being increased 300°C/hr to 1150°C and held for 1 hr. The blanket gas is then changed to argon containing 4% H_2 for 4 hr to reduce the uranium oxide to UO_2. The optimized product then is a completely homogeneous solid solution of UO_2 in ThO_2, practically free from pores. The particle density of the product is greater than 9.9 g/cc, or 99% of theoretical density.

The process has good flexibility. Thorium nitrate crystals or solution can be denitrated with equal ease to a dispersible oxide. Mixed thorium and uranium nitrates have been co-denitrated to a dispersible mixed oxide powder. The uranium content of the sol can be varied from 0 to 10 at. %. A flowsheet similar to the one shown in Fig. 3.1 was used to prepare 4 wt % plutonium-thorium oxide that had a particle density of 98% of theoretical. This material was packed into irradiation capsules which are now being irradiated in the NRX reactor.

3.2 Engineering Development

The primary purpose of this part of the program was to develop equipment and operating procedures for the Kilorod Program. This development has culminated in a full-scale demonstration of each unit operation required for the process. In the course of these studies, materials were made available for programs to develop vibratory compaction and for in-pile tests of oxides prepared by the sol-gel process.

[1] F. R. Bruce, "The Thorex Process," Symposium on the Reprocessing of Irradiated Fuels, Brussels, Belgium, May 20-25, 1957, TID-7534, Book I, p 180.

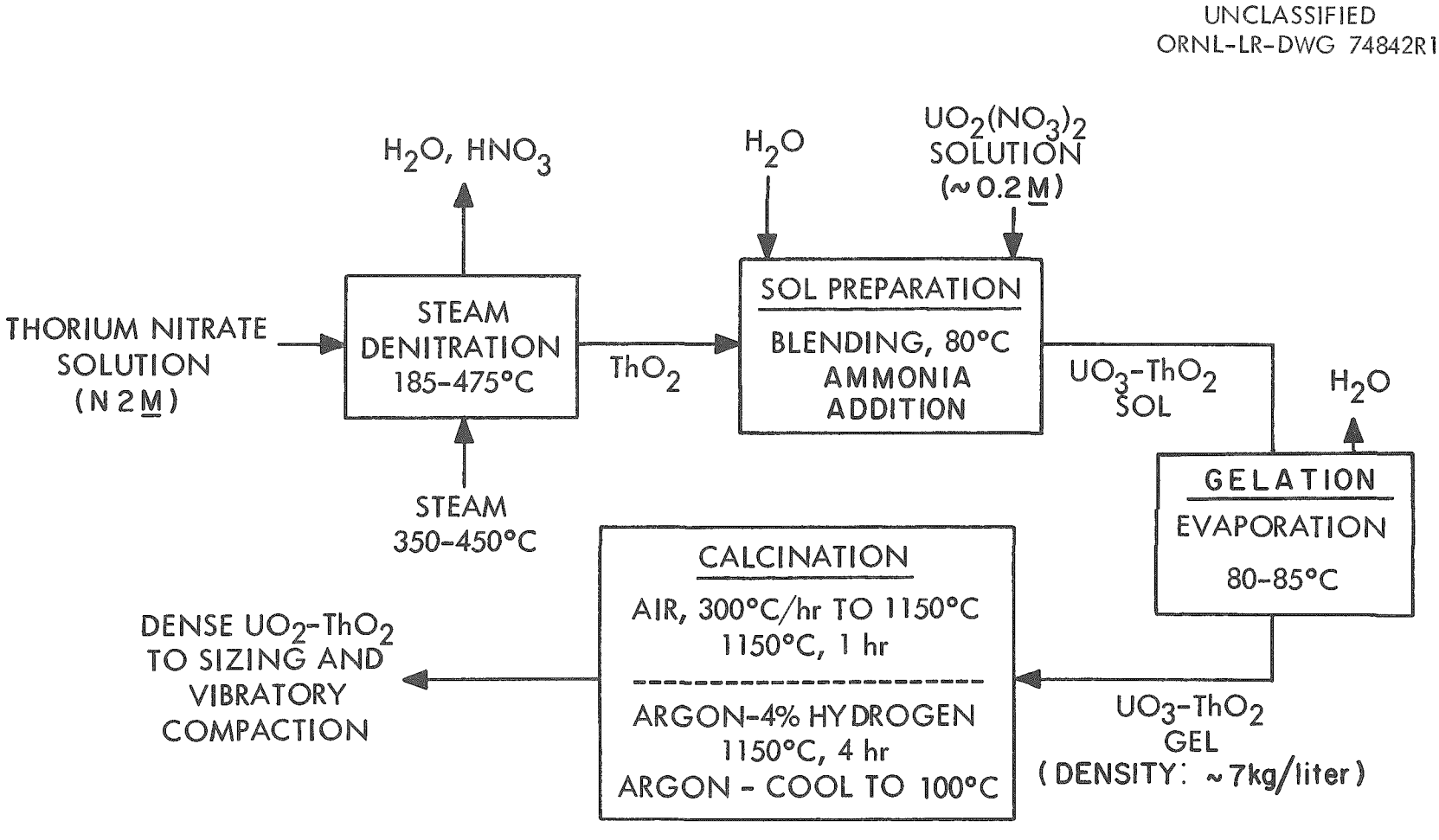

Fig. 3.1. Flowsheet for the Sol-Gel Process.

3.2.1 Denitration of Thorium Nitrate

A 14-in.-diam rotary denitrator was designed, built, and operated at the capacity required for the Kilorod Program. The denitrator was operated in two phases. The first consisted of a series of runs in which operating variables were studied to find those which produced denitrated products with good sol-producing characteristics. The second phase was a series of runs to demonstrate consistent and dependable operation. About 400 kg of ThO_2 powder with good sol-producing characteristics was prepared. Results and conditions for all runs are tabulated in the Appendix (Tables A.1, A.2, and A.3).

Description of Equipment. -- A diagram of the rotary denitrator and auxiliary equipment is shown in Fig. 3.2, and the rotary denitrator in the unloading position is shown in Fig. 3.3. Electrical heaters on a stationary shell around the drum, the rotation of the drum, and the gas annulus between the drum and the heaters ensures uniform temperatures for the charge. The rotary drum is 14 in. in diameter and 31 in. long, with a 60° tapered inlet end and a 22.5° tapered exit end. The overall length is 45 in.

Seven thermocouples (1/16-in.-OD stainless steel sheath with MgO filling) were installed on the drum to measure the skin temperature. One was also placed inside the steam-supply line. Short-circuiting of the thermocouples to the stainless steel sheath was a frequent problem, and was attributed to vibration at the end of the commutator. In all 32 runs, at least one of the drum thermocouples performed satisfactorily.

An inlet steam baffle, 4 in. in diameter, was installed and used for most of the runs. The baffle is located in the enlarging inlet section such that about 1 in. of clearance exists between the baffle and conical section of the drum. A smaller 2-in.-diam baffle is located about 4 in. from the steam-exit point. The purpose of the baffles was to deflect the steam and prevent channeling at the low flow rates.

Denitrations were also made in an agitated trough (of the type used for the denitration of uranyl nitrate) and in smaller laboratory apparatus. The results of the rotary denitrator runs were more reproducible due to

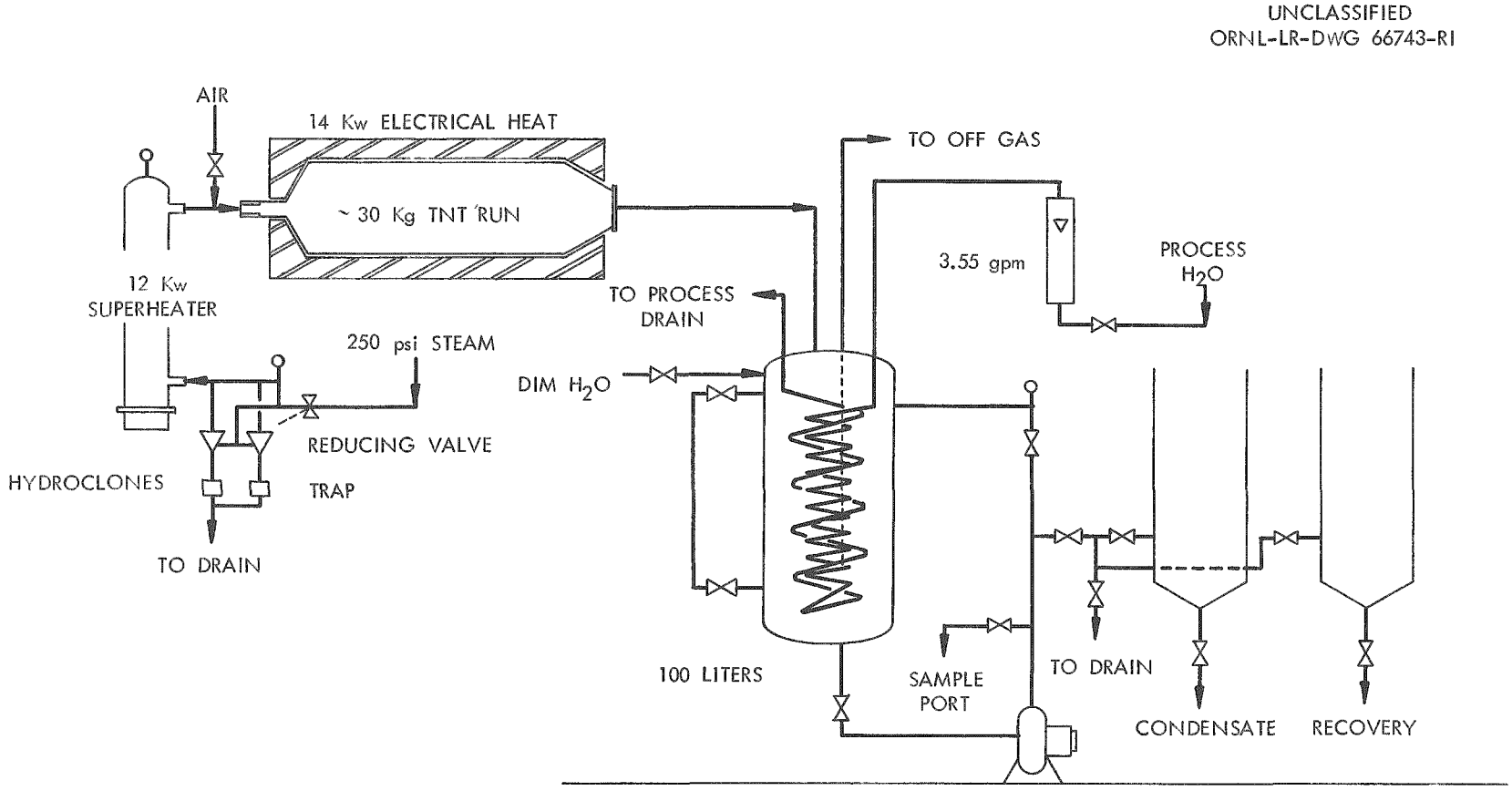

Fig. 3.2. Fourteen-Inch-Diameter Rotary Denitrator and Auxiliary Equipment.

UNCLASSIFIED
PHOTO 55878

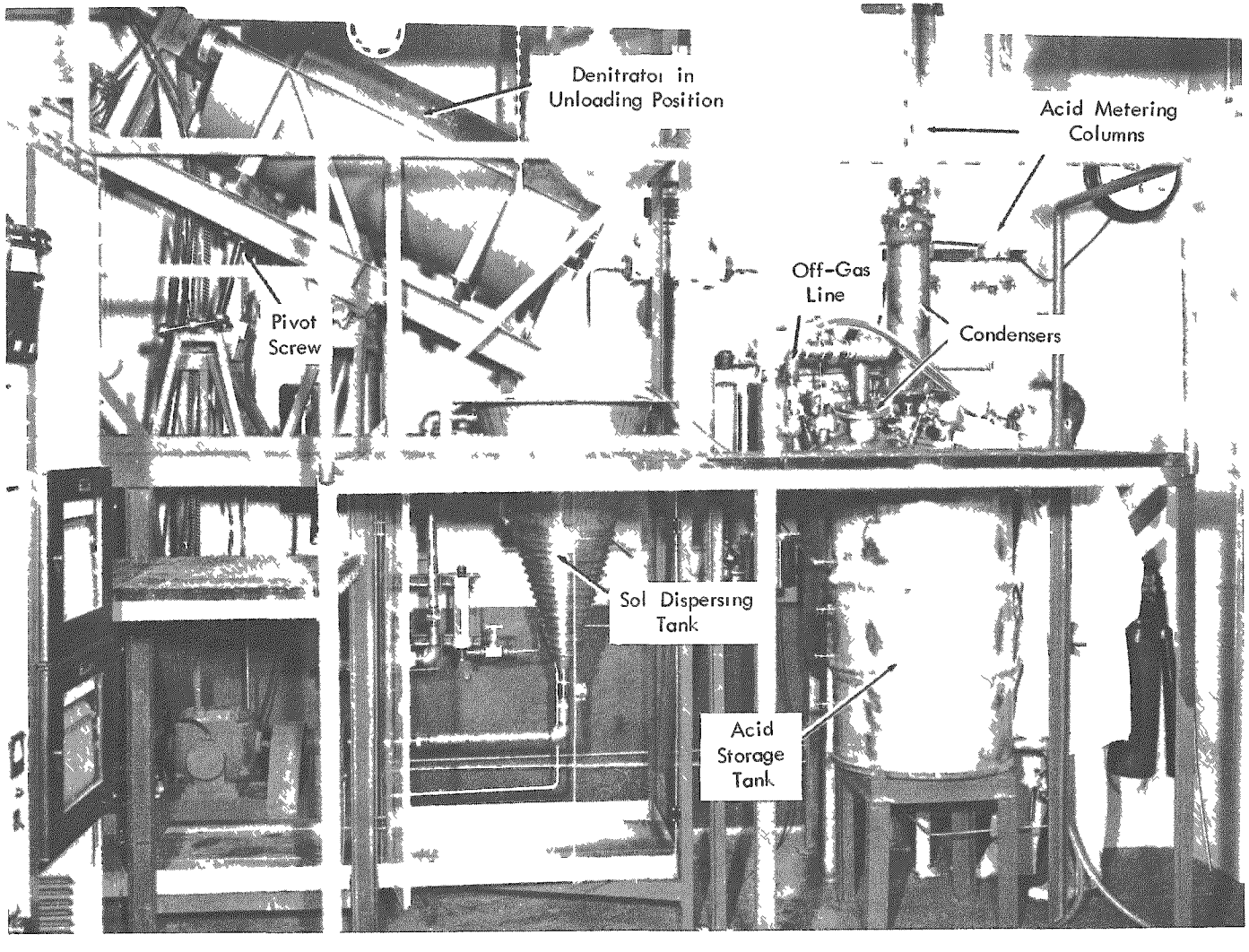

Fig. 3.3. Rotary Denitrator in the Unloading Position.

more uniform heat fluxes and temperatures; therefore, discussions of results refer principally to the runs in this large unit. The ranges of acceptable operating conditions were determined by earlier experiments in the smaller units.

The Effects of Operating Conditions. -- The ThO_2 products from the rotary denitrator runs may be grouped into those that have good sol-producing characteristics and those that do not. The first type was characterized by almost complete dispersion into a stable sol that had a characteristic blue color when observed by transmitted light. The second was characterized by incomplete dispersion and had a white appearance when observed by transmitted light. The difference between the two types was not evident from chemical analyses (Appendix, Table A.3).

For most of the denitration runs, 30 kg of thorium nitrate crystals were charged to the discharge end of the drum, which was tilted upward. About 14.5 kg of ThO_2 product was obtained from this size charge. However, charges of up to 45 kg were denitrated to yield about 21.5 kg of ThO_2. Operation of the denitrator in a manner that provided good sol-producing products required heating the thorium nitrate crystals to drum temperatures of about 200°C under an air purge prior to steam contact. Partial dehydration occurred during this interval. Superheated steam was then introduced to effect denitration. The temperature continued to increase from heat added as superheated steam and through the heated drum walls. At about 250 to 300°C, the crystals melted into a syrup and remained syrupy until, at about 350°C, solid ThO_2 was formed. The steam flow was continued for an additional 3 to 4 hr, during which the temperature increased to 450 to 475°C. When this procedure was used, the variations in product analyses were small and dispersion into good thoria sols was achieved. One run was made with a $Th(NO_3)_4$ solution instead of thorium nitrate crystals as feed. The solution was evaporated without difficulty. After 180°C was reached, procedures, temperatures, nitrate evolution, and the product properties were indistinguishable from those for runs with thorium nitrate crystals.

The temperature profiles and condensate volumes for two representative runs (one, RDB-14, which gave a good product, and the other, RDB-16, which

gave an undesirable product) are shown in Fig. 3.4. There are two significant differences in the heating profiles of these runs. The temperature profile for run RDB-14 shows a hold, indicating an endothermic reaction at about 290°C, whereas that for RDB-16 does not. Also, run RDB-14 shows a more endothermic reaction at 325°C than did run RDB-16.

In Fig. 3.5 the nitrate evolution rate vs run time for a good and poor run are compared. The run that gave undesirable sol-producing properties had a nitrate evolution rate which was higher for the first 1-1/2 hr of denitration and decreased for the remainder of the run. The run that gave desirable sol-producing properties had a lower nitrate evolution rate for the first 1-1/2 hr of denitration, and two extremely high nitrate evolution rates for short time intervals corresponding to the ≥90°C hold and the 325°C hold. The off-gas condensate collected for the good run up to the time corresponding to the ≥50°C hold period was less than for the poor run.

Uniformity of the Product. -- Thirty to 50 wt % of the product from the first five runs was not dispersible by the usual method nor by a vigorous fume-down method. This fraction was thought to be produced by contamination of the charge or the steam by a component which sorbed on the ThO_2 surface so strongly that nitrate could not displace it.

The products from the rotary denitrator were remarkably reproducible in nitrogen content for a given run time (Table 3.1). The effect of run

Table 3.1. Product Uniformity of Denitrated Thorium Nitrate

Rotary denitrator: 14 in. in diameter and 36 in. long
Steam: 350°C and 1 atm
Temperature: increasing to 475°C

No. of Runs	Total Run Time (hr)	Time Above 450°C		Product	
		Steam (hr)	Air (hr)	Wt (kg)	NO_3^-/Th Mole Ratio
11	6	3	0	14	0.027 ± 0.009
5	4	0	1	14	0.059 ± 0.005
3	6.5	2.5	0	22	0.050 ± 0.007

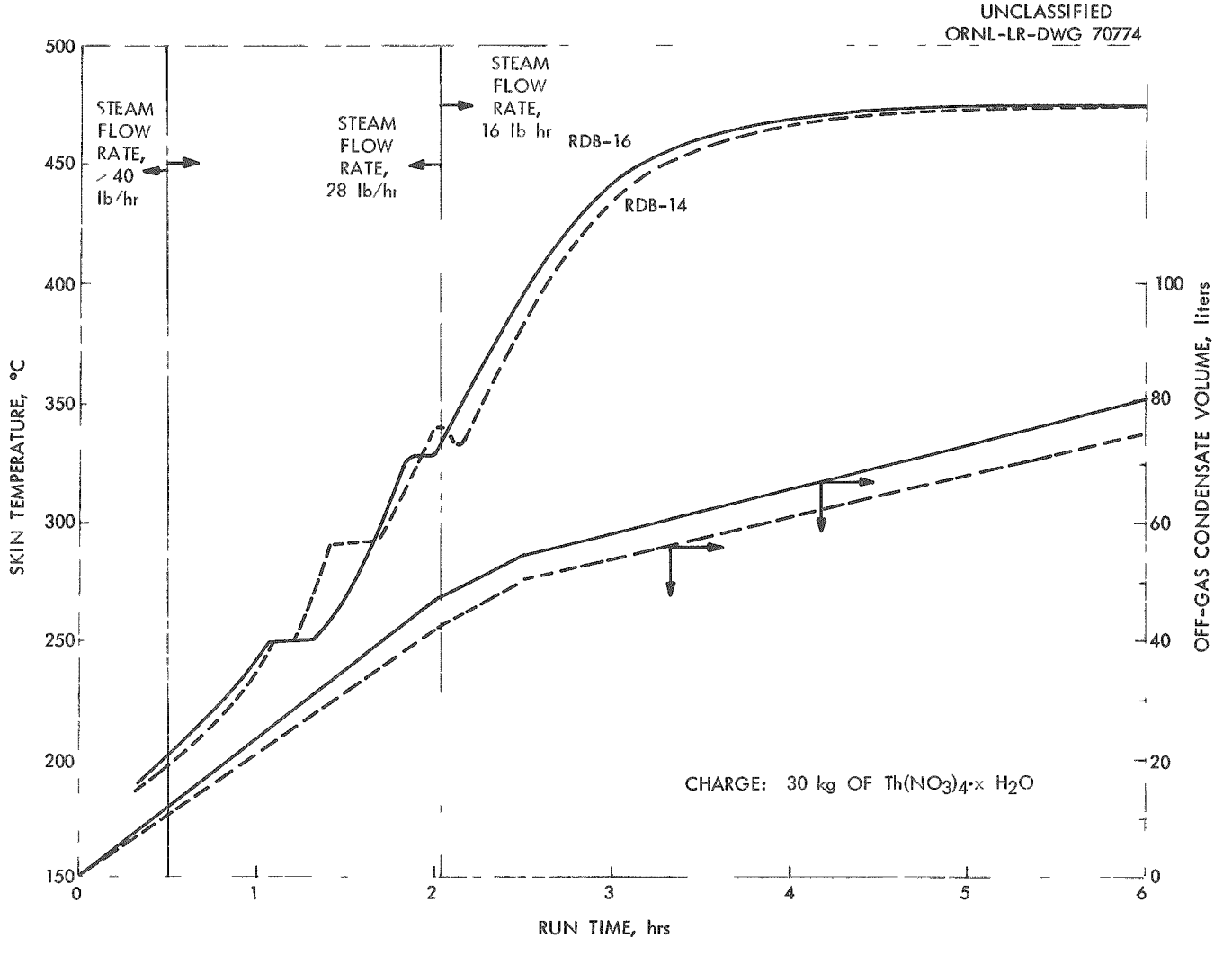

Fig. 3.4. Rotating-Drum Temperature and Condensate Volume Collected vs Run Time for Runs RDB-14 and RDB-16.

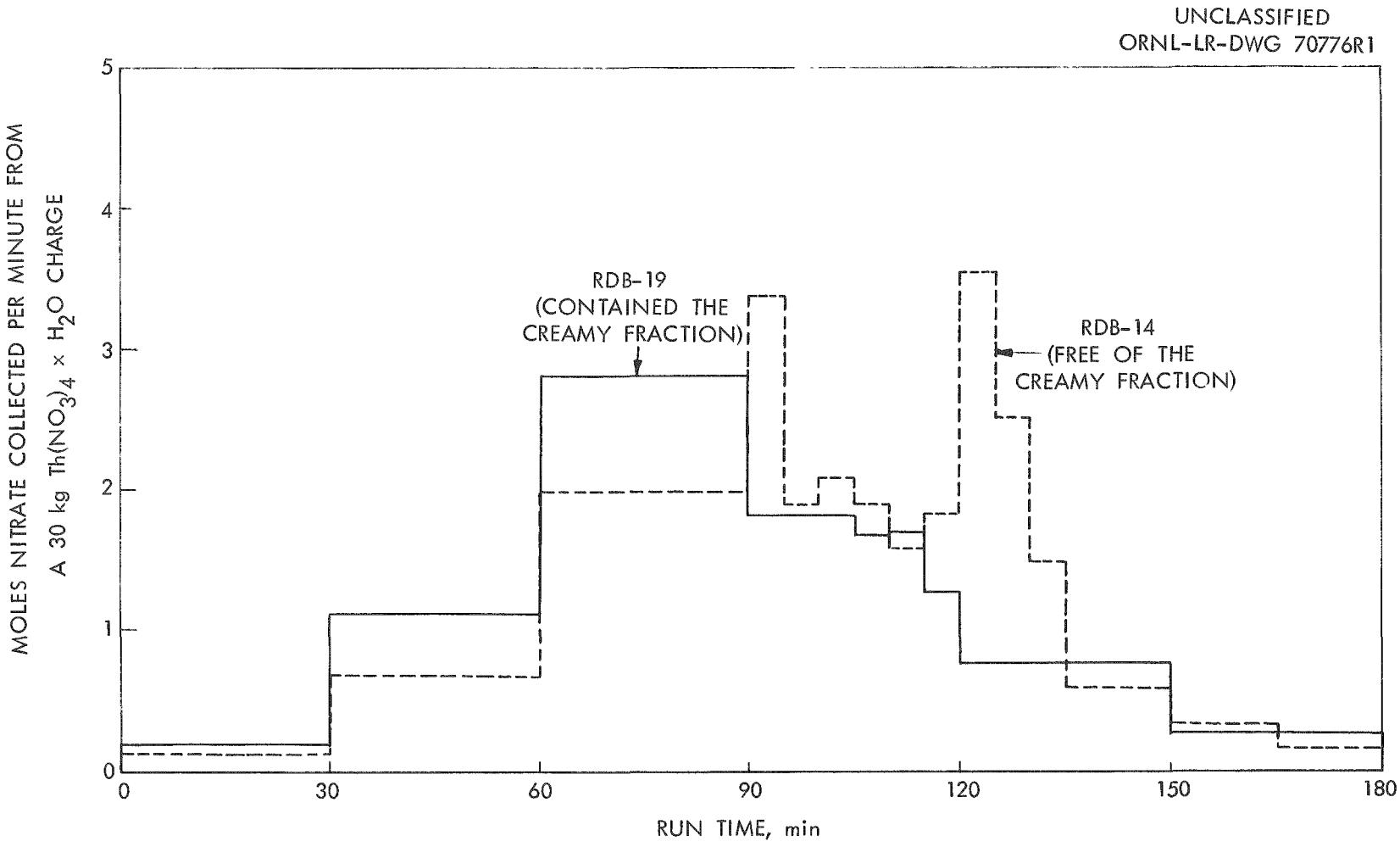

Fig. 3.5. Nitrate Evolution Rate as a Function of Run Time for a Run Free of the Creamy Fraction and for One Containing the Creamy (Nondispersible) Fraction.

time on the N/Th mole ratio is shown in Fig. 3.6. The run time to be used for the Kilorod Program, compatible with plant throughput and an 8-hr shift, should be: 5-1/2 hr in steam; no air at 475°C. This will give a product containing about 0.03 mole of nitrogen per mole of thorium. Products from the rotary denitrator are so uniform in sol-producing characteristics from batch to batch that the residual nitrate may be ignored in sol preparations. The uniformity will be further increased by blending several denitrator batches together for ThO_2 feed to the plant.

Several products from a variety of run times and conditions were dispersed and allowed to stand 24 hr in a sol column not exceeding 5 in. of height, at a concentration of about 2 M ThO_2. All products with good sol properties left heels upon decantation which showed that more than 99.5% dispersion was achieved at an added nitrate-to-thoria mole ratio of 0.07. Above this nitrate level very little additional dispersion was achieved (Fig. 3.7). Run ATC-58, which was made in the agitated trough calciner, is included to emphasize the superiority of the products of the rotary denitrator. Both methods of denitration give products that disperse at an added NO_3^-/Th mole ratio of about 0.07; however, the rotary denitrator products are more completely dispersible.

Results of Co-denitrating Thorium and Uranyl Nitrates. -- Three runs were made in the agitated trough to study the co-denitration of thorium and uranyl nitrates [3 to 15 mole % $UO_2(NO_3)_2$] (Table 3.2). The first

Table 3.2. Run Conditions and Analyses of Co-denitration Runs

	TU-1	TU-2	TU-3
Time in steam, min to go from 180 to 350°C	180	180	180
Time in air, min above 350°C	180	180	180
Percent thorium by weight	82.34	76.95	72.00
U/Th mole ratio	0.0292	0.0948	0.176
Percent nitrogen by weight	0.32	0.27	0.25
N/Th mole ratio	2.0644	0.0582	0.0575
Crystallite size, A	58	55	55
Surface area (BET, N_2), m^2/g	41.8	48.8	52.4

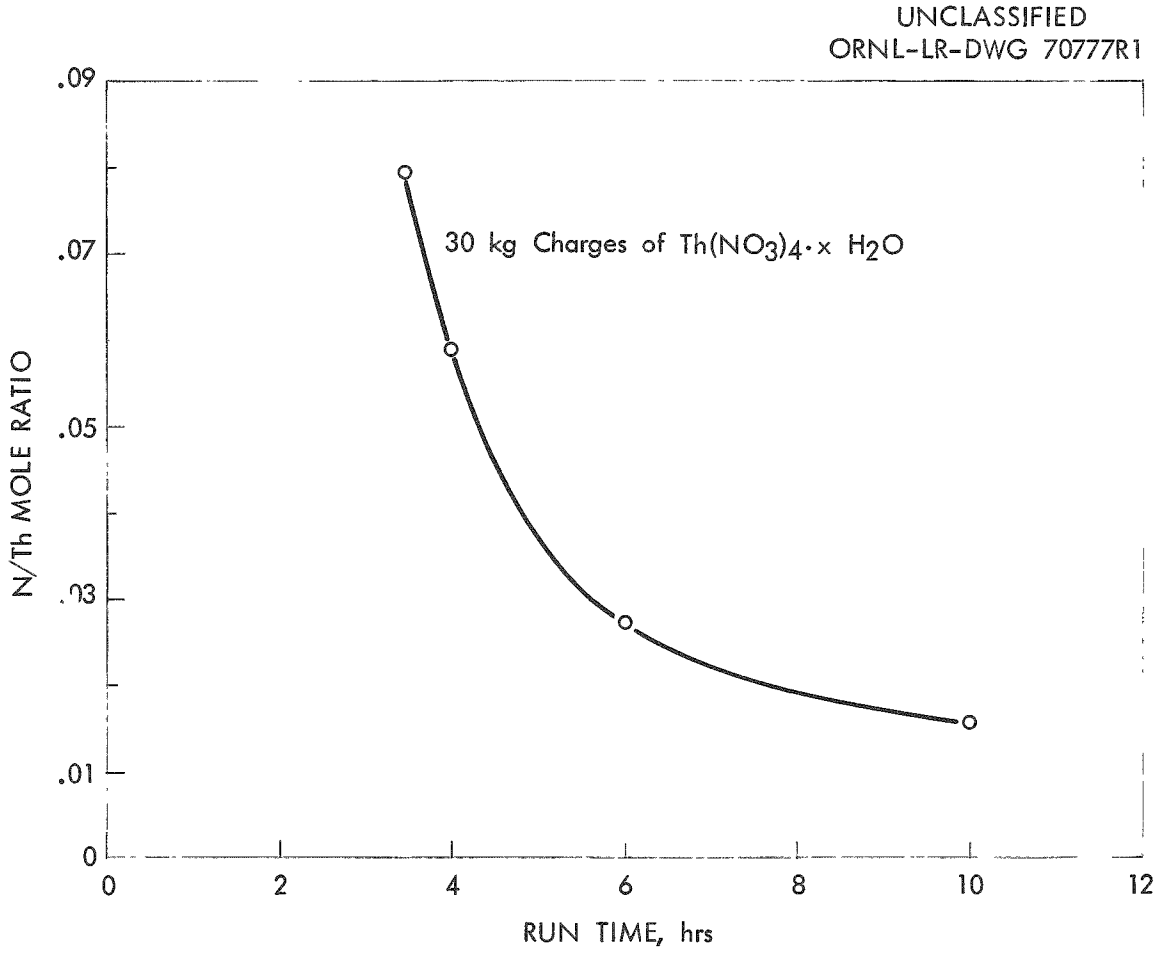

Fig. 3.6. Nitrogen-to-Thorium Mole Ratio vs Run Time for 30 kg Charges of $Th(NO_3)_4 \cdot xH_2O$.

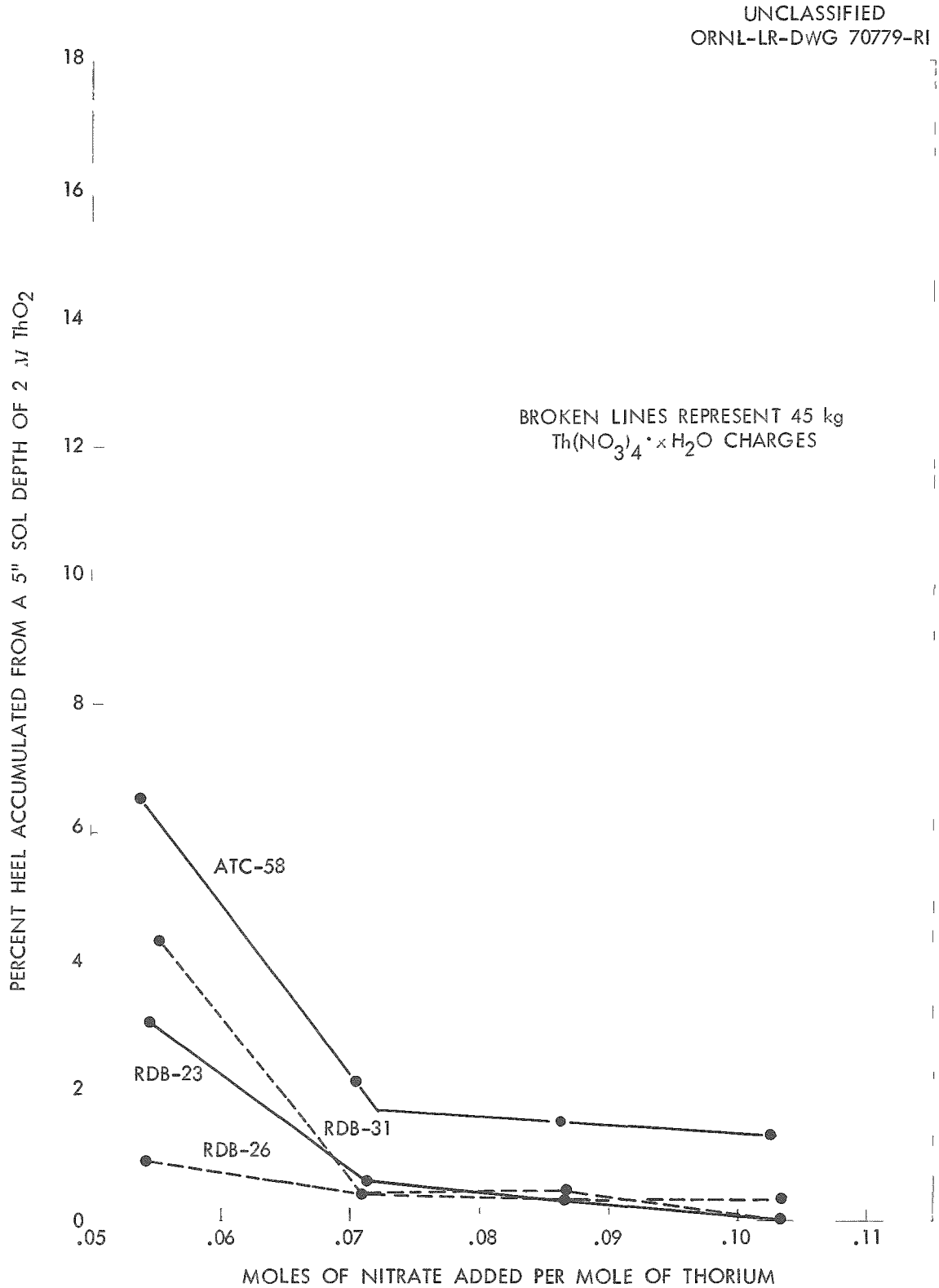

Fig. 3.7. Percent Heel Accumulated in 24 hr for Various Steam-Denitrated Products vs Added Nitrate-to-Thorium Mole Ratio.

run, TU-1, was a nominal 3% urania--97% thoria preparation. This product dispersed easily and produced a fired product that had the characteristics of fired particles produced from a thoria sol with a high nitrate content. Run TU-2 product, 9% urania--91% thoria, was not completely dispersible; the product of run TU-3, a 15% uranium-thorium oxide, was dispersed very little by normal sol-gel dispersion methods.

3.2.2 Sol Preparation

Apparatus. -- The prototype sol mixing tank, designed with a slab configuration to be critically safe (Fig. 3.8), is a full-size model of the one to be installed in the Kilorod Facility. The glass front (absent in the actual Kilorod tank) allowed observation of dispersion and sol adjustment as conditions and design were varied during development of equipment and process. The total capacity of the tank is about 30 liters, and the effective capacity for a sol batch is 20 liters of 2 M ThO_2 (about 10 or 11 kg of ThO_2). Optimum operation requires that the sol level be below the inlet pipe (pump discharge) at the upper right. In operation, the sol is circulated from the bottom of the tank through the centrifugal pump and a shell-and-tube steam-heated heat exchanger in the discharge line of the loop and returned to the tank above the sol surface. Four spray nozzles near the top admit water to wash down any solids adhering to the tank walls. The funnel (top right) is fitted with an interior stopper that permits charging with water with thoria product from the denitrator. After the powder is wetted, the stopper is lifted, permitting the slurry to flow by gravity into the hot circulating uranyl nitrate solution in the tank. No mechanical difficulties were encountered with this apparatus in more than 25 preparations. One modification in equipment was the substitution of a centrifugal recirculating pump for the Vanton peristaltic pump whose Neoprene and Hypalon liners were eroded badly by the sol. Centrifugal pumps gave excellent dispersion and introduced only negligible problems. In another modification, ammonia was added at the pump intake rather than at the top of the tank to prevent the formation of curds, which tended to collect on the wall of the tank at the sol level.

UNCLASSIFIED
ORNL-PHOTO 59412R2

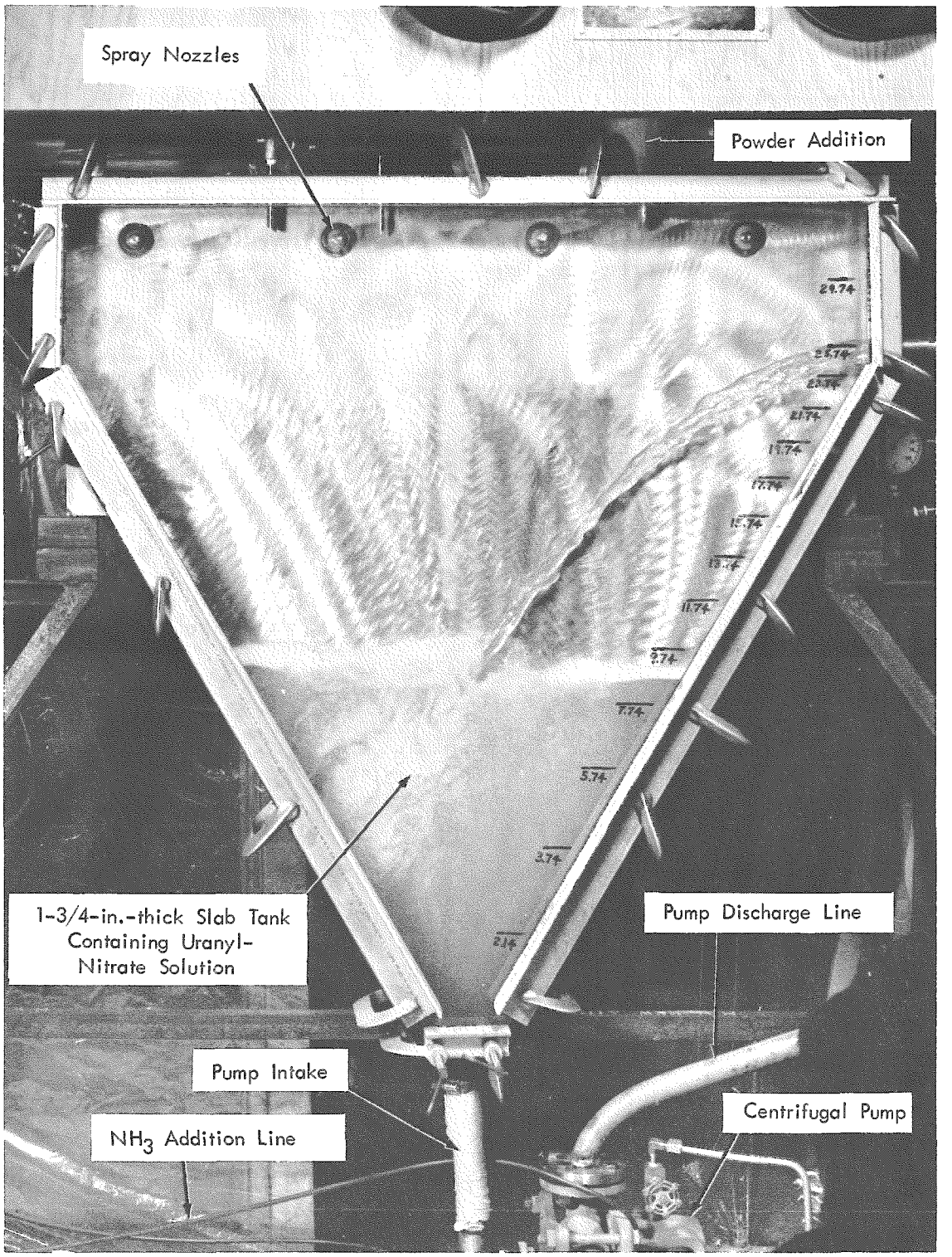

Fig. 3.8. Tank for Preparing the Sol.

3.2.3 Procedure for Preparing the Sol

The procedure discussed below was the preferred one of two developed for the preparation of the 2 M, 3 at. % uranium-thorium oxide sol required for the Kilorod Program, and is known as the slurry addition method. In the alternative procedure, preferred for the preparation of 4 to 10 at. % oxide containing more than about 5% uranium-thorium oxide sols, ThO_2 is dispersed in HNO_3, then ammonium diuranate or UO_3 is blended in. The slurry addition method is preferred because in it the control of the NO_3^-/ThO_2 mole ratio is relatively easy.

In preparing sol for the Kilorod Program by the slurry addition method, the amounts of U^{233}, ThO_2, and nitrate charged to the tank must be accurately known. The nitrate-to-thoria mole ratio of the steam denitrator product is so controllable and uniform that it may be assumed to be 0.03 without analysis, and the ThO_2 content is determined by ignition at 900°C for 2 hr. Since the maximum permissible total NO_3^-/ThO_2 mole ratio is 0.107 for 3% uranium-thorium oxide sols where the average ThO_2 crystallite size is 70 A (see Section 3.3), and since a 0.03 mole ratio exists in the denitrated product, the maximum NO_3^-/ThO_2 mole ratio which may be added is 0.077. The dilute uranyl nitrate solution is made up in a calibrated, critically safe metering vessel and analyzed for uranium and nitrate content. An accurately measured volume of the uranyl nitrate solution containing about 265 g of U^{233} is charged to the sol make-up tank. The metering vessel, connecting lines, and the walls of the sol make-up tank are flushed with deionized water sufficient to make the volume of solution about 6 liters; the pump is then started, and the steam is admitted to the heat exchanger. When the solution temperature reaches 90°C, a water slurry of about 10.5 kg of previously analyzed and weighed ThO_2 denitrator product is added slowly from the funnel. Sufficient flush water is then added to bring the total sol volume to about 20 liters. Recirculation is continued until dispersion of the ThO_2 is complete, as determined by a settling test on a sample. The impeller of the centrifugal pump was an effective device for dispersing the ThO_2. For most denitrator products the dispersing time is 1 hr.

After complete dispersion, 0.015 to 0.02 mole of NH_3 per mole of thoria is added at the intake of the pump to bring the pH of the sol to

about 3.9. Recirculation is then continued for about 1 hr to homogenize the sol, especially with respect to uranium distribution.

With the composition of the product for the Kilorod Program fixed at 2 M ThO_2 and with a U/U + Th atom ratio of 0.03 ± 0.0003, the remaining independent variables for control of compactability and uniformity of U/Th atom ratio over the entire particle-size range of the fired and sized oxide are: NO_3^-/ThO_2 mole ratio, NH_3/ThO_2 mole ratio, and pH.

The sources of nitrate ion in the sol are the residual nitrate in the steam denitrator product, nitrate associated with the uranyl nitrate, and any nitric acid added to adjust the NO_3^-/ThO_2 ratio. The variation in nitrate in the ThO_2 powder was small, and there was some evidence that this nitrate was not readily available for stabilizing the sol. The nitrate demand for the optimum dispersion of steam denitrator products as determined by conductimetric titration corresponded to an NO_3^-/ThO_2 mole ratio of 0.07 ± 0.002. Most of the nitrate was supplied by the uranyl nitrate solution, a product of solvent extraction in which the nitrate/uranium ratio was above 2. With a permissible over-run of 10% of the optimum NO_3^-/ThO_2 mole ratio, the maximum allowable NO_3^-/U ratio is 2.56 for sol-gel products containing 3 at. % uranium.

Twenty-five batches (3 to 5 kg each) of about 3% uranium-thorium oxide were prepared for studying vibratory compaction. Data for these batches are fully tabulated in Table A.4 of the Appendix. In preparing these batches, the final sol-gel procedure was developed. An upper limit on the allowable nitrate/thorium mole ratio was set by the appearance of a high viscosity which made mixing and transfer of the sol very difficult. When an added NO_3^-/ThO_2 mole ratio of about 0.12 was exceeded, an instantaneous increase in viscosity was noted. The addition of NH_4OH did not reverse the increased viscosity, but led to a thixotropic sol. One such thixotropic sol, which had a setting time of about 3 min, was made by adding a NO_3^-/ThO_2 mole ratio of 0.12 followed by neutralizing a third of the added nitrate with ammonia. The variables, added NO_3^-/ThO_2 mole ratio and added NH_3/ThO_2 mole ratio, were carefully optimized in order to prepare calcined oxides of maximum particle density and compactability. Table 3.3 contains data for seven typical batches selected to show the

Table 3.3. Effect of Sol-Preparation Conditions on Density of Sol-Gel Oxides

3-7 kg batches; 3 at. % U--ThO_2

Batch No.	Sol Conditions			Density (% of Theoretical)	
	Moles Nitrate Added per Mole ThO_2	Moles NH_3 Added[a] per Mole ThO_2	Adjusted pH[b]	Particle[c]	Vibrated Bulk
20-5M	0.067	0	3.31	99.3	90.6
21	0.086	0	2.90	99.9	89.6
22	0.093	0	2.90	96.5	86.0
8A	0.170	0.041	2.72	97.9	83.4
8C	0.170	0.093	3.45	97.5	87.8
31	0.080	0.020	3.80	98.6	87.8
28	0.077	0.015	3.48	99.5	89.4

[a] Added after dispersion of ThO_2.

[b] Taken just prior to evaporation of sol.

[c] Determined by toluene immersion.

effect of these variables on density and compactability. Batches 20-5, 21, 22, and 28 show that the optimum added NO_3^-/ThO_2 ratio is probably somewhere between 0.067 and 0.086. Higher nitrate concentration decreased particle density, and in addition gave particles of irregular shape with rough, cracked surfaces. All these particle properties are unfavorable for high compactability. Neutralization of high nitrate with ammonia improved particle shape and surface character, but when used in amounts greater than 0.015 mole per mole of thoria, produced particles of low density. Ammonia also imparted added toughness to the particles, so that in vibration, points and edges did not break off as readily; some degradation is desirable to allow increased bulk density of the compacted material. The optimum conditions for the preparation of 3 at. % uranium-thorium oxide sols are represented in batch 28, where about 10% excess nitrate is used to hasten dispersion of the ThO_2, and the excess nitrate is neutralized by a minimum of ammonia.

Sol-preparation conditions must also be optimized for a uniform uranium-to-thorium ratio in all particles of the product. For the Kilorod Program, the maximum allowable deviation in uranium percentage for any particle sample is only 1% of the 3% overall uranium content. Table 3.4 contains a set of selected batches to show the variability of uranium distribution under various conditions. Similar data for the remaining batches are in Tables A.5 and A.6 of the Appendix. High nitrate-to-thoria mole ratios favored concentration of uranium in the fine-particle fraction. The use of ammonia to neutralize excess nitrate improved the uranium distribution. As mentioned earlier, the apparent pH of the sol at the optimum adjustment was 3.8 to 4.0. Batch 28 represents optimized variables for uniform distribution, and since these conditions also produce a compactable oxide, they are the conditions recommended for the Kilorod preparation.

Two sol preparations (batches 19-4M and 20-5M) were made in which the ThO_2 concentrations were 4 and 5 M, respectively. As shown in Tables 3.3 and 3.4, batch 20-5M was satisfactory with respect to compactability and uranium distribution. No mechanical problems were encountered in the preparations.

Table 3.4. Sol Preparation Conditions and Uranium Distribution in Sol-Gel Oxides

Typical batches of 3-7 kg oxide, 3 at. % U

Batch No.	Sol Conditions			Uranium Distribution in Product, % Deviation from Mean U/Th		
	Moles Nitrate Added per Mole ThO_2	Moles NH_3 Added[a] per Mole ThO_2	Adjusted pH	Coarse Fraction[b]	Medium Fraction[c]	Fine Fraction[d]
28	0.077	0.015	3.92	+0.03	+1.18	-0.03
31	0.080	0.020	3.80	-0.40	+1.09	+1.56
9-AB	0.096	0	2.82	-4.37	+6.58	+6.58
20-5M	0.067	0	3.31	-1.62	+3.76	+1.75
14-H	0.086	0.014	4.18	-0.70	+1.92	+0.46

[a] Added after dispersion of ThO_2.

[b] 6/16 mesh, 60 wt %.

[c] 50/140 mesh, 15 wt %.

[d] -200 mesh, 25 wt %.

3.2.4 Evaporation of the Sol

The digested, pH-adjusted sol is batch-evaporated to gel in trays under a stream of heated air at 85 to 90°C. The trays are arranged in cascade so that sol from the top tray overflows to the one immediately under it. Twenty liters of sol, containing 10 kg of oxide, are pumped into the top tray. The optimum depth of sol in the trays is 3/4 to 1 in. A drying time of 48 hr is used to prevent the formation of bubbles in the gel product and to remove all except 4 to 6% of the volatile matter. The particle-size ranges from more than 1/2 in. down to about 35 mesh, about 90% of which is larger than 16 mesh. The density of the gel is about 5 g/cc, giving a concentration factor during drying of about 3.5. The particle size is affected by the drying rate, which in turn is dependent on air temperature, flow rate, and humidity. These factors are being studied for their possible use in the control of particle size.

3.2.5 Calcination of the Dried Sol (Gel)

The dried gel from a single batch (10 kg of oxides) is dumped from the trays into a funnel that directs the charge to two crucibles, each of 6 kg capacity. The volatile material is removed, and the oxide is densified in air by increasing the furnace temperature 300°C/hr to 1150°C and holding 1 hr. After flushing the furnace for 10 min with argon, the charge is reduced in an atmosphere of argon containing 4% hydrogen at 1150°C for 4 hr. At this composition, the blanket gas is noncombustible. After cooling to below 100°C in argon, the product is dumped to a hopper that feeds the sizing equipment.

In a laboratory study using 55-g samples of 3% uranium--thorium oxide, the densification, reduction, and degassing of the oxide were nearly complete with 20 min of heating at 1150°C in air (Table 3.5). Densification and degassing were complete with an additional 3-1/2 hr of heating in nitrogen or argon--4% hydrogen. The highest possible temperature of withdrawal of the cooled charge without serious reoxidation was 200°C (Table 3.6). Although the data from small-scale firings show that a blanket of nitrogen is as effective for eliminating sorbed gases from the products as one of argon--4% hydrogen, Table 3.7 shows that firing large batches in a blanket of argon or nitrogen in a large

Table 3.5. Effects of Calcination Atmosphere on Particle Density and Residual Gas Content

Samples: 55 g 3% U--ThO_2

Firing: 300°C/hr to 1150°C; at 1150°C, 20 min in air; then in indicated gases for the indicated times

Cooling: in indicated atmospheres to < 200°C

Calcination Atmosphere	Calcination Time (hr)	Cooling Atmosphere	Particle Density (g/cc)	Gas Release at 1200°C in Vacuum (std cc/g)
Air	0.5	Argon	9.91	0.14
Air	0.5	Nitrogen	-	0.037
Argon	0.5	Argon	9.92	0.024
Argon	1.5	Argon	9.94	0.014
Nitrogen	3.5	Nitrogen	9.95	0.001
Argon--4% H_2	3.5	Argon	9.95	0.001

Table 3.6. Effect of Temperature of Exposure to Air on Residual Gas Content

Samples: 55 g, 3 at. % U--ThO_2

Firing: air, 300°/hr to 1150°C; 20 min at 1150°C, air; 3 hr at 1150°C, argon; cooled to indicated temperature; exposed to air

Temperature of Exposure to Air (°C)	Residual Gas Released at 1200°C in Vacuum (cc/g)
500	0.036
400	0.024
315	0.017
< 200	0.005

Table 3.7. Oxygen:Uranium Ratio and Residual Gas Content of Calcined Product

Batch size: 5-7 kg

Composition: 3 at. % U--ThO_2

Firing procedure: 300°C/hr to 1150° and held for 1 hr in air; calcined in indicated gases 4 hr; cooled in same gas to <100°C

Calcination Atmosphere	O/U Ratio			Gas Release at 1200°C in Vacuum (std cc/g)		
	+16 mesh[a]	16/35 mesh[b]	-35 mesh[c]	+16 mesh[a]	16/35 mesh[b]	-35 mesh[c]
Argon--4% H_2	2.026	2.027	2.019	0.004	0.004	0.067
Nitrogen	2.099	2.087	2.157	0.018	0.055	0.120
Argon	2.220	2.267	2.308	0.030	0.047	0.050

[a]Represents about 92 wt % of product.

[b]Represents about 5 wt % of product.

[c]Represents about 3 wt % of product.

[d]Cooled in argon containing no hydrogen.

furnace gave products of higher residual gas content than in argon--4% hydrogen. The fines had more residual gas than the coarse particles, which indicated that gases were reabsorbed subsequent to calcination. This would be possible and probable in the cooling step if the blanket gas contained absorbable gases, if the furnace were not well sealed, or if the furnace refractories supplied gases during the cooling cycle. More detailed gas-release data are presented in Tables A.7 to A.10 of the Appendix. The O/U ratios shown in Table 3.7 also show that nitrogen and argon are not as effective as argon--4% hydrogen in reducing the ratio under the calcination conditions used. These data also show higher oxygen content for the smaller-size particles, suggesting oxygen reabsorption during cooling. Thus, the use of hydrogen in the calcination blanket gas appears to be justified at present for the Kilorod flowsheet.

3.3 Studies of Dispersion of Thoria

Studies were made in order to determine optimum conditions for the complete dispersion of ThO_2 in dilute HNO_3 and $UO_2(NO_3)_2$ solutions. Sol-gel prepared uranium-thorium oxide products were previously observed to have good compactability, optimum shape (blocky and smooth), and uniformity in uranium-to-thorium ratio when the nitrate-to-ThO_2 mole ratio used in sol preparation was at some optimum value which depended on the surface area of the powder. Complete and stable dispersion of ThO_2 in dilute nitric acid was also obtained only at about the same NO_3^-/ThO_2 mole ratio. The surface area of ThO_2 powder prepared by steam denitration of thorium nitrate (Curve B, Fig. 3.9) as measured by the BET (nitrogen adsorption) method was from 50 to 67% that of gels prepared from it by dispersion with dilute nitric acid and evaporation at 90°C (see also Table 3.8). The measured surface areas of the gels approached the values calculated from average crystallite sizes (see Curve A, Fig. 3.9), using the $6/\rho d$ relationship. This suggests that the thoria powder particles are aggregates of crystallites bonded in a manner that does not permit access of all of their surface to nitrogen. When dispersed with nitric acid the aggregates are broken up, rendering nearly all of the crystallite surface available to nitrogen adsorption.

The surface areas of gels obtained from evaporation of thoria sols (Fig. 3.10) prepared with added increments of nitric acid, increased to

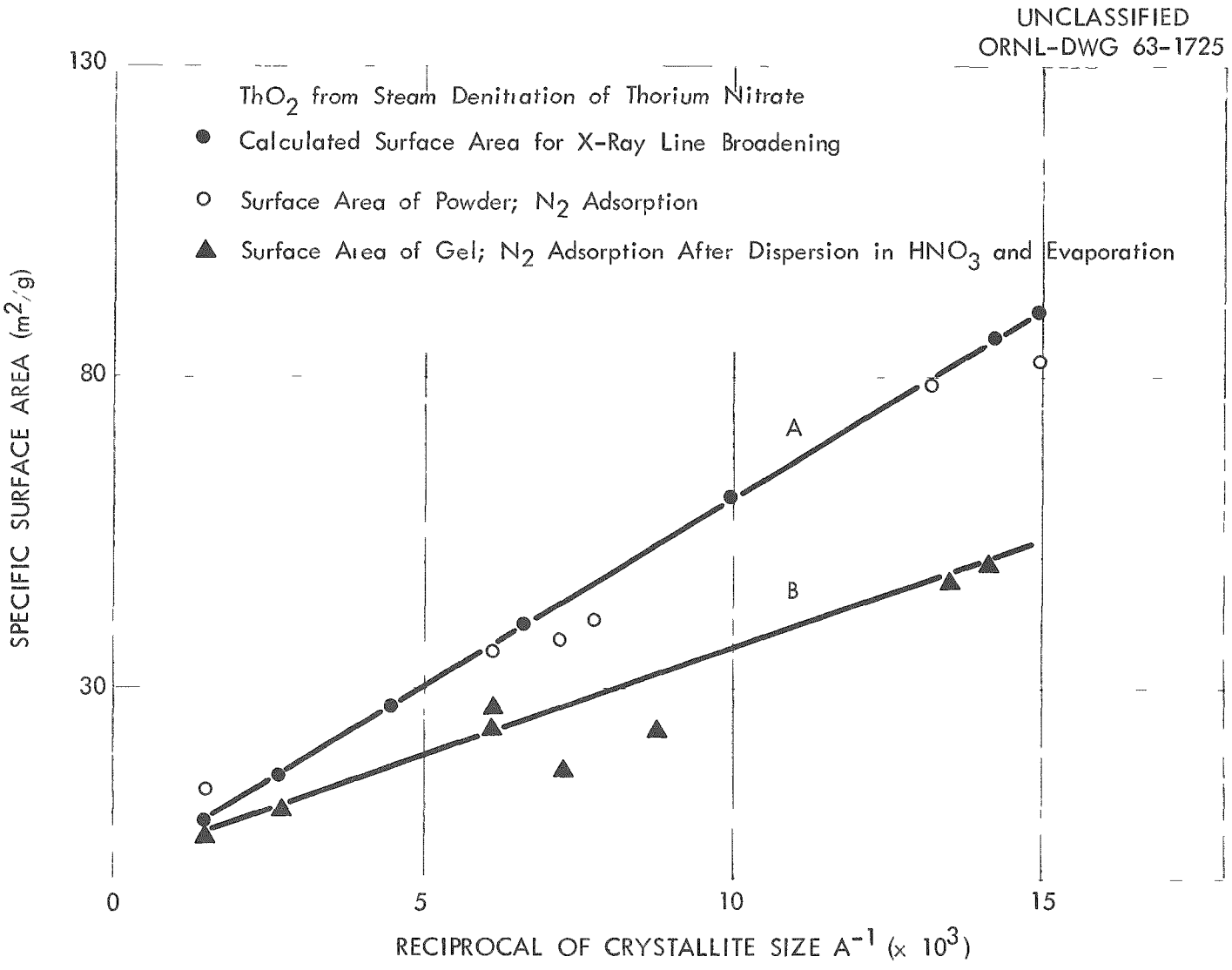

Fig. 3.9. Availability of Surface of ThO_2 to Nitrogen.

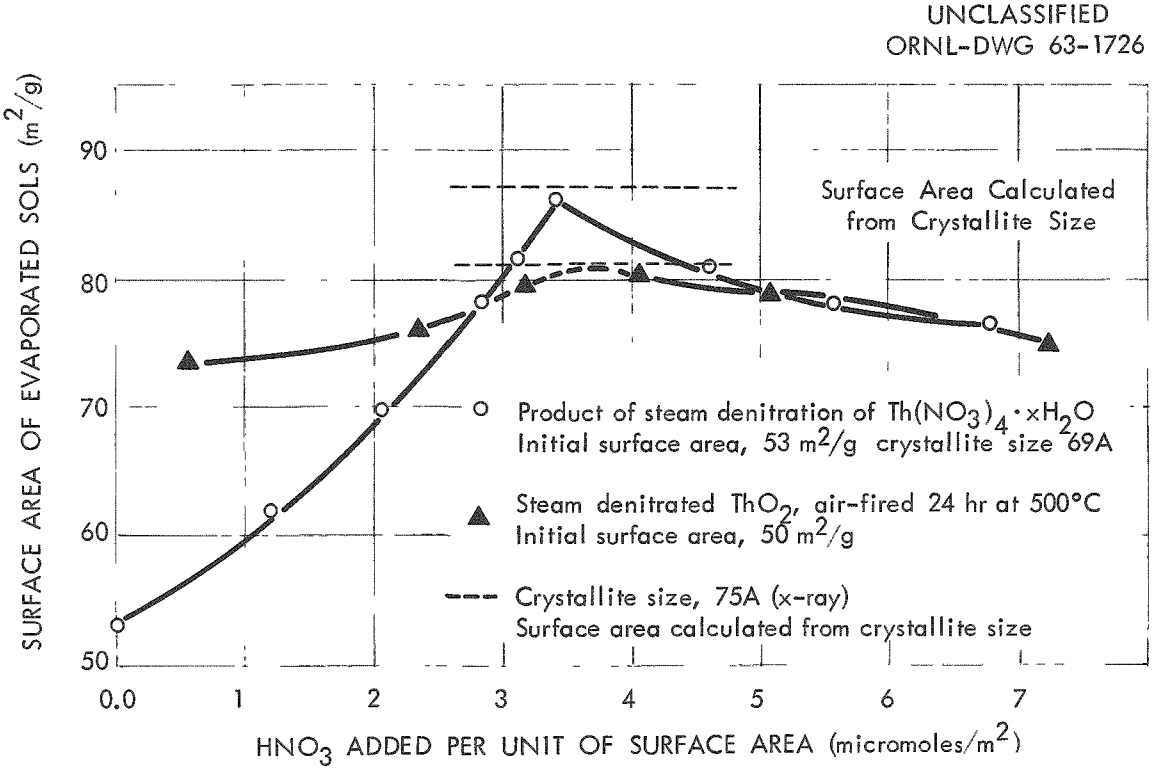

Fig. 3.10. Effect of Added Nitric Acid on Conductivity and Surface Area of Gels Prepared from Them.

Table 5.3. Surface Area and Crystallite Size of ThO_2 Used in the Preparation of ThO_2 Sols

Sample No.	Preparation Method[a]	Maximum Temperature (°C)		Time of Temperature (hr)		Crystallite Size (A)	Specific Surface Area (m^2/g)		
		Steam	Air	Steam	Air		Calculated[b]	Before Dispersion[c]	After Dispersion[d]
D-19	SD	380	-	1.5	-	52	115	75	-
RD-23	SD	475	500	1	1	70	86	50	77
RD-27	SD	475	-	3	-	70	86	50.8	80
RD-33	SD	475	-	2	-	67	90	47.4	8. .4
RD-10	SD	475	700	3	1	100	60	32	48
RD-17	SD	475	700	3	4	127	47	23.1	41
RD-33	SD	475	700	2	4	138	43.5	16.7	38.4
RD-40	SD	475	700	2.5	4	135	44.5	20.3	43.1
DT-78	Ox	-	1000	-	4	702	8.6	7.1	13.3

[a] SD = steam denitrated in rotary calciner; Ox = oxalate-precipitated, then air-calcined.

[b] Calculated from crystallite size, $6/\rho d$. Crystallite size determined by x-ray diffraction line-broadening.

[c] Before dispersion, powder, as calcined, N_2 adsorption.

[d] Dispersed in dilute HNO_3 at 90°C, evaporated to gel at 90°C.

maxima and then decreased. One curve represents ThO_2 produced by the rotary calciner in a routine run (see Section 3.1). The other curve is for the same ThO_2 powder that had been previously dispersed in dilute nitric, evaporated, then fired at 500°C for 24 hr. The residual nitrate contents of the powders were not taken into account in the plots because of the scatter of analytical results. This scatter was thought to be due to a time-dependent release of bound nitrate to the solution during digestion. If the highest nitrate value determined for the original thoria is added, the surface area maxima occur at about 5×10^{-6} mole of nitrate per square meter. The Spaepen-Wimber-Wadsworth estimate[3] of chemisorption sites on thoria surfaces is 10.6×10^{-6} mole/m^2. The maximum surface measured approached the value calculated from average x-ray crystallite size (from $6/\rho d$), indicated by the dashed lines of the plots, and appears to occur when about half the chemisorption sites are occupied by nitrate ions. Maximum surface area was assumed to be evidence of maximum dispersion of ThO_2.

The NO_3^-/ThO_2 mole ratio used in sol preparation strongly influenced the quality of fired oxide product, and it had a sharp optimum. Conductimetric titration of a water slurry of ThO_2 appeared to be a convenient and accurate method for determining the NO_3^-/ThO_2 mole ratio optimum for complete dispersion of any steam-denitrated product. A typical plot of conductivity vs nitric acid added is shown in Fig. 3.11 along with a typical plot of surface area vs added nitrate. As nitric acid is added in increments to the ThO_2 slurry, the electrical conductivity at first increased only slowly up to a critical NO_3^-/ThO_2 mole ratio. Beyond this ratio the conductivity increased rapidly as though nitric acid were being added in the absence of ThO_2. The break in the conductivity curve coincides closely with the maximum in relative surface area. For ordinary products of steam denitration runs the "nitrate demand" value is very close to 0.07 mole/mole ThO_2. When uranium was present in the sol, the break occurred at a lower NO_3^-/ThO_2 mole ratio, and was not as sharp. The nitrate demand, however, appears to be the same for complete dispersion in the presence or absence of uranium.

---

[3] G. J. Spaepen, R. T. Wimber, and M. E. Wadsworth, Adsorption of Silicic Acid on Thoria Determined by Infrared Spectroscopy, Technical Report No. V, Univ. of Utah (June 30, 1959).

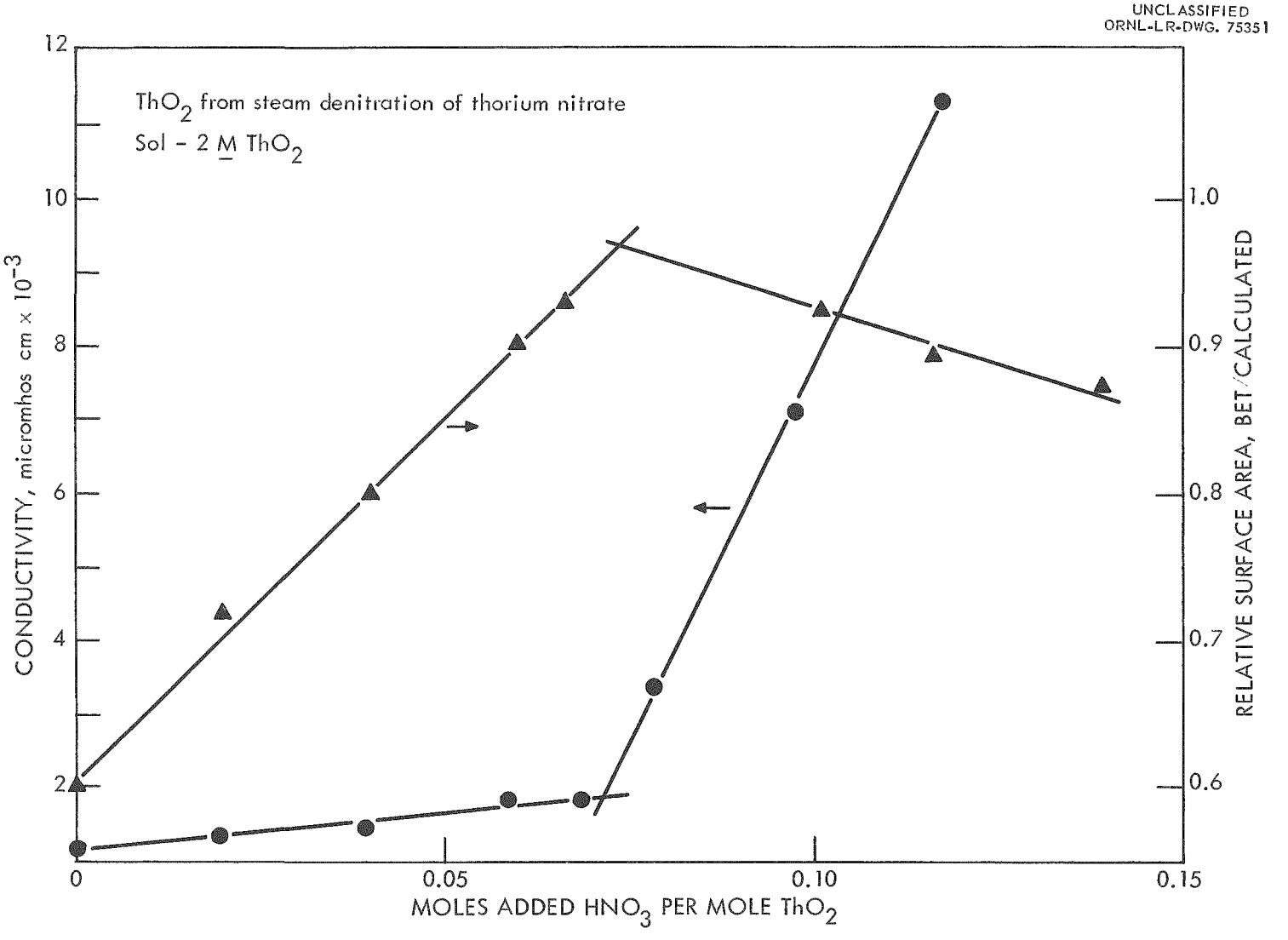

Fig. 3.11. Effect of Added Nitric Acid on Conductivity and Surface Area of Thoria.

The scattering of light by sol particles is a directly observable criterion of degree of dispersion. A brief study was made of the extent of light-scattering by thoria sols. The intensity of transmitted light at 6700 A was measured in a Beckman DU spectrophotometer for sols of varying ThO_2 concentrations and NO_3^-/ThO_2 mole ratios. Typical Beer's law plots are shown in Fig. 3.12 for the thoria samples of two average crystallite sizes. Slopes (indicating degree of dispersion) vary with NO_3^-/ThO_2 mole ratios and show a broad minimum. Figure 3.13 is a plot of optical density vs the nitrate/surface area ratio for a sol of ThO_2 product of steam denitration which had been fired 4 hr at 700°C. A typical minimum is shown at about 5 micromoles of nitrate per square meter of ThO_2 surface, giving support to the indication of complete dispersion of ThO_2 when half the chemisorption sites are occupied by nitrate. The minimum, however, is probably not sharp enough to be useful in a routine determination of nitrate demand.

Thoria slurry samples, when titrated slowly with dilute nitric acid at 90°C showed equivalence points at apparent pH values of 3.1 to 3.35. The NO_3^-/ThO_2 ratios at the equivalence point varied with the surface area (see Fig. 3.14). A sol, stable at the end point, flocculated and settled at a pH of about 2. When back-titrated with NH_3 the sol again became stable, but the NO_3^-/ThO_2 ratio at equivalence for the back titration was greater, though at the same pH as for the initial acid titration. It is thought that the NO_3^-/ThO_2 mole ratio equivalence inflection shown by the ammonia back titration is more nearly characteristic of the nitrate demand of the ThO_2 powder for complete dispersion than that of the initial acid titration. The addition of excess acid and the allowance of more digestion time apparently caused further dispersion. Rates of dispersion are apparently dependent on acid concentration.

Well-digested sols of ThO_2 or ThO_2 containing up to 5 at. % uranium appear to change in pH with dilution. The magnitude and direction of change in apparent pH depends on the NO_3^-/ThO_2 mole ratio and the ThO_2 molar concentration (Fig. 3.15). For sols in which the NO_3^-/ThO_2 mole ratio is less than equivalent to half occupancy of active surface sites by nitrate, the apparent pH is decreased by dilution with water, and the rate of decrease with dilution increases with dilution. If the nitrate-

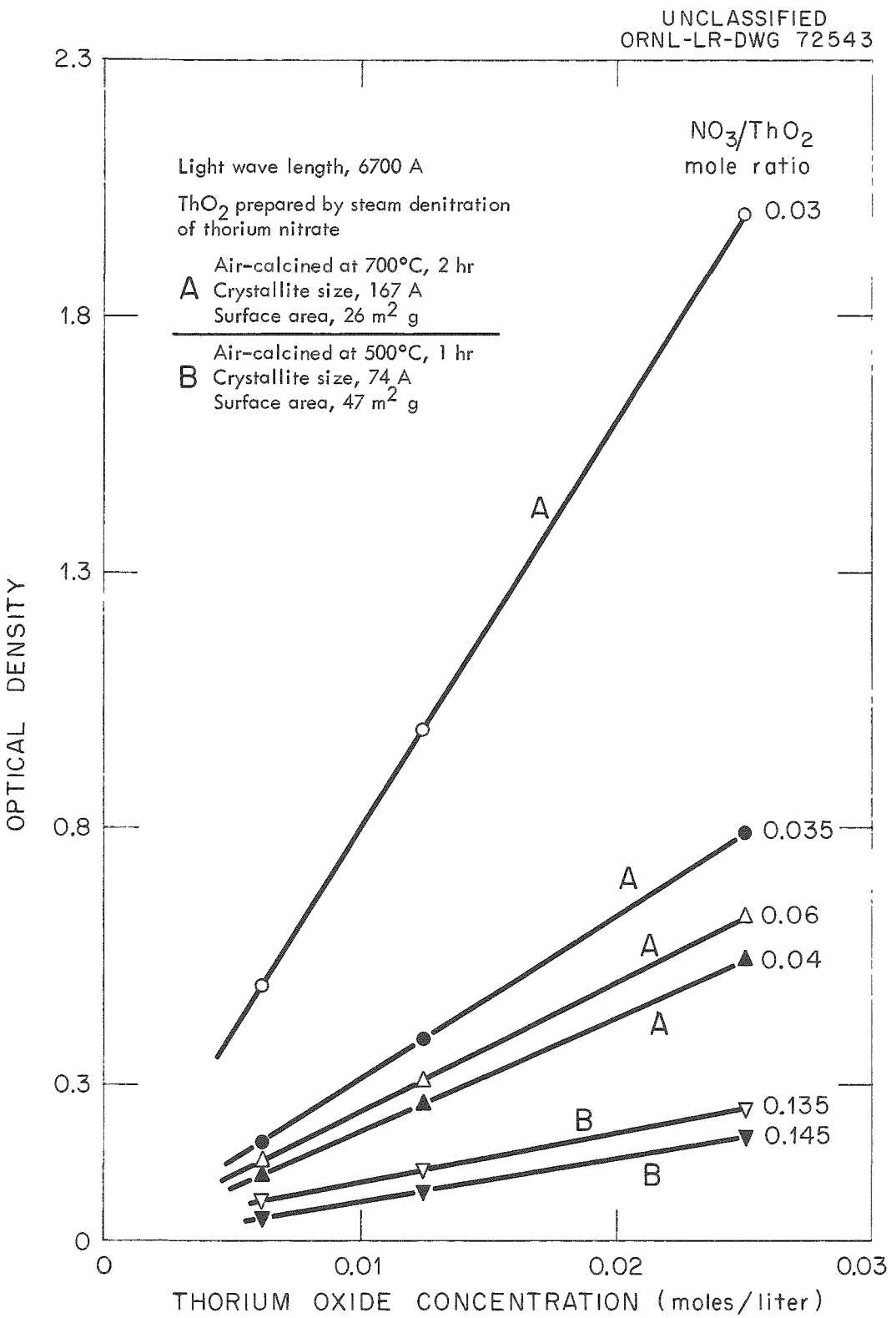

Fig. 3.12. Effect of ThO_2 Concentration and Nitrate on Optical Density of ThO_2 Sol.

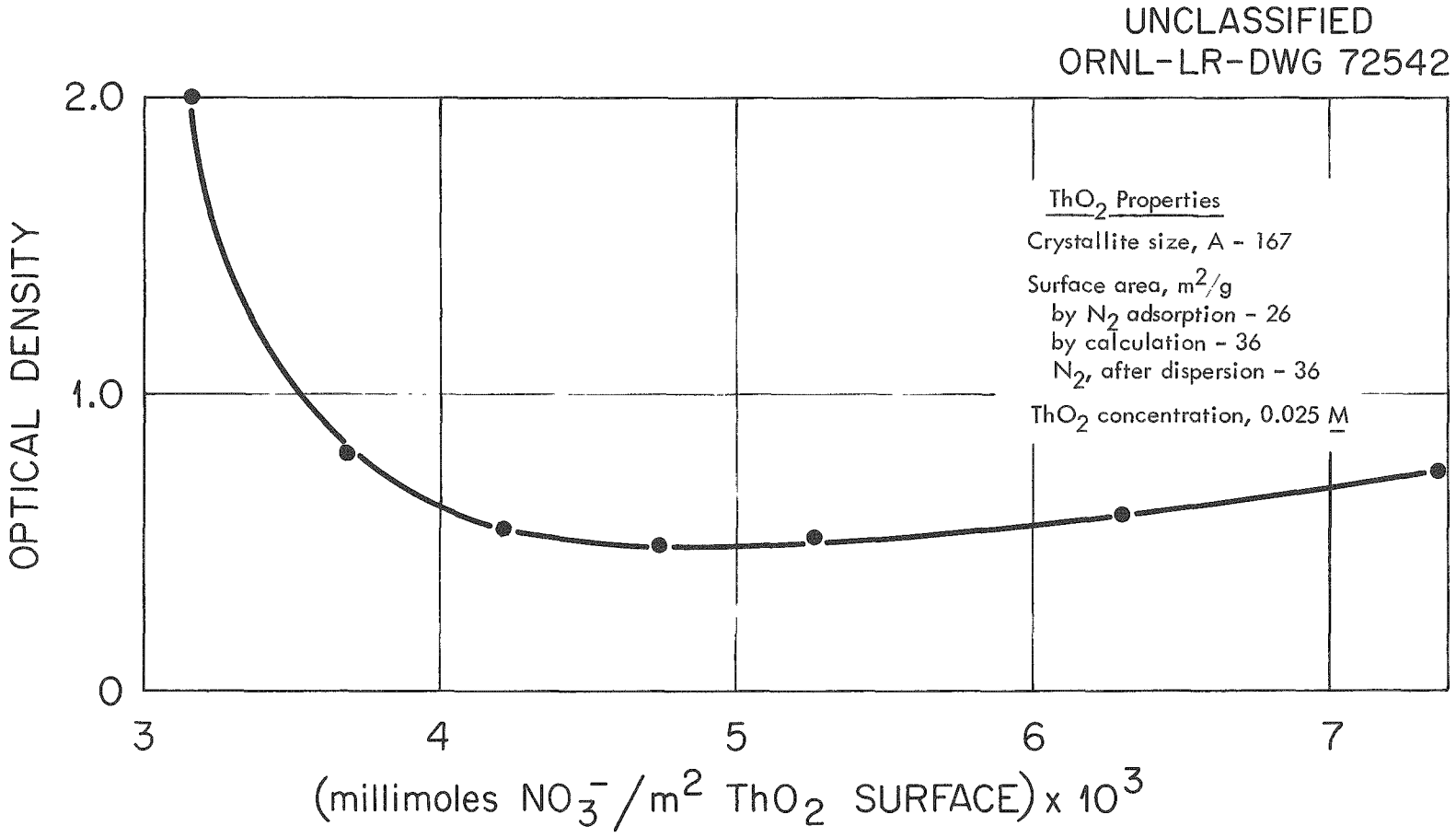

Fig. 3.13. Effect of Nitrate on Optical Density of ThO_2 Sols.

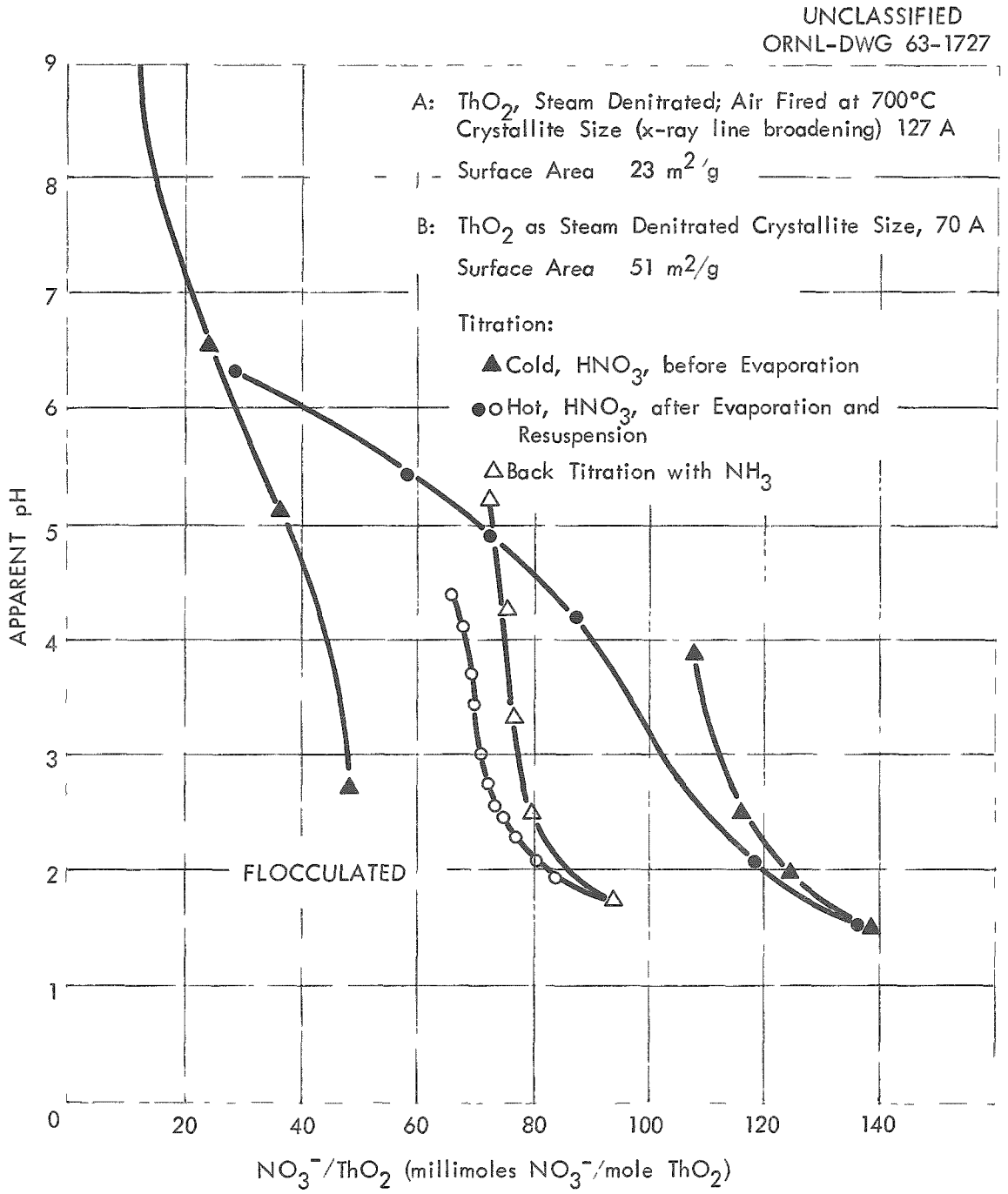

Fig. 3.14. Acidimetric Titration of ThO_2 Products of Steam Denitration.

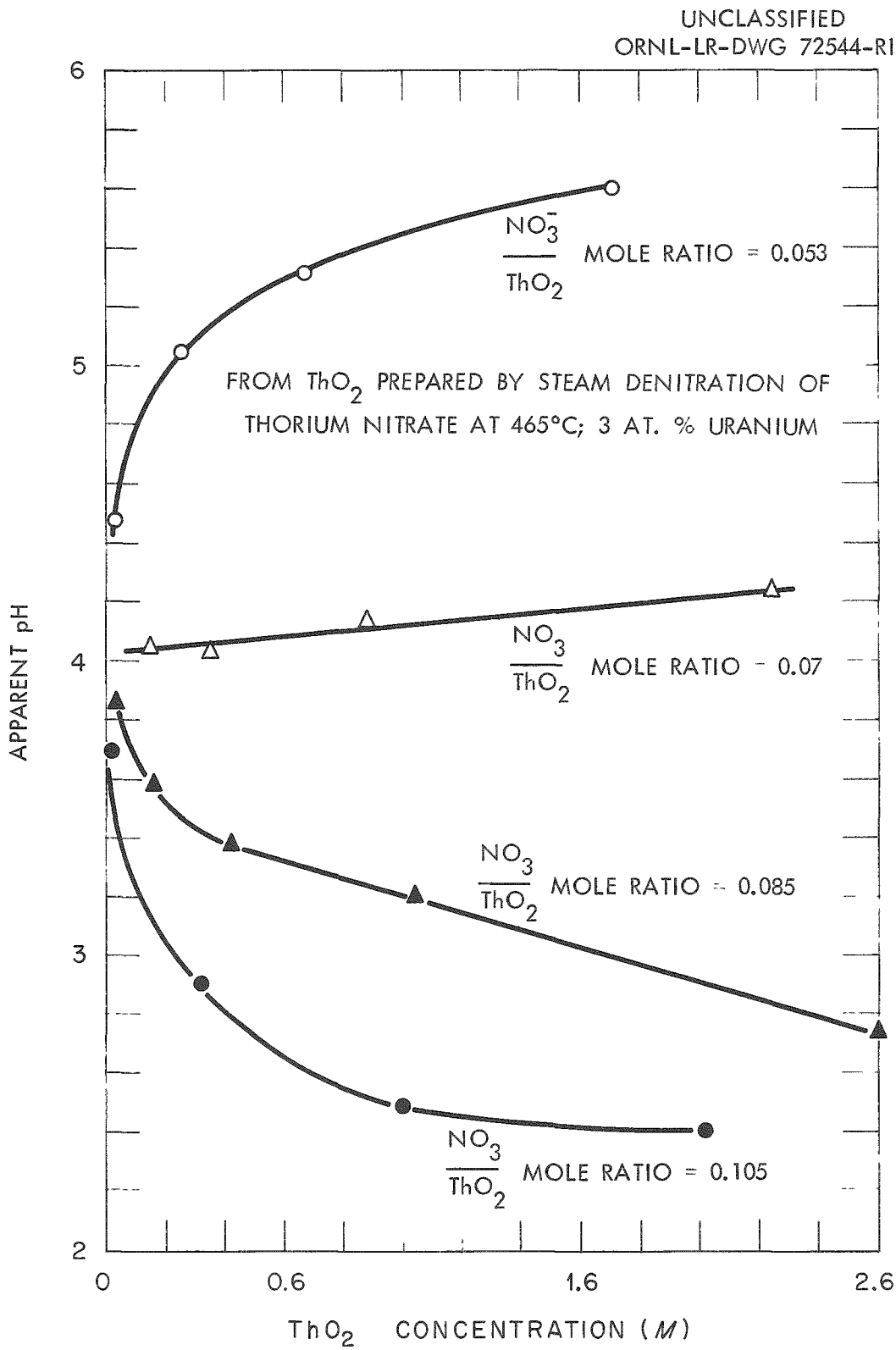

Fig. 3.15. The Effect of ThO_2 Concentration and NO_3/ThO_2 Mole Ratio on Apparent pH.

to-thoria mole ratio is greater than half-occupancy equivalency, the pH increases with dilution, which is expected. If NO_3^-/ThO_2 is at equivalency, the pH appears to be relatively unchanged by dilution. This effect of dilution on apparent pH is useful in adjusting the sol so that flocculation or uranium segregation will not occur during evaporation of the sol. Sols having a small excess NO_3^-/ThO_2 mole ratio can be adjusted by the addition of ammonia. An apparent pH of 3.9 for a sol which shows little change on dilution indicates that the net nitrate is at or is close to equivalence. Sols of 3 at. % uranium-thorium oxide having this property can be evaporated without flocculation or segregation.

3.4 Properties of the Product

Products containing 3 at. % uranium prepared by the flowsheet shown in Fig. 2.2 had uniformity of uranium distribution in all size fractions to within ±1% of the mean; the particle density was more than 99% of theoretical; the sized oxide vibratorily compacted consistently to 90% of theoretical density; the gas released at 1200°C in vacuum was 0.10 cc/g or less; and the O/U ratio was less than 2.03 (Table 3.9). One of the

Table 3.9. Properties of Batch-26 Sol-Gel Oxide
Total batch weight = 4.5 kg; uranium is 93% U^{235}
Batch prepared for fabrication of irradiation test specimens by vibratory compaction

Screen Size U.S. Standard	Uranium (wt %)	Percent Deviation of U from Mean U/U + Th Atom Ratio	BET (N_2) Surface Area (m^2/g)	Particle Density (g/cc)	Total Gas Evolved at 1200°C Vacuum (cc/g)	O/U Ratio
			As Calcined			
+16	5.50	-0.94	-	9.98	0.004	-
16/35	5.62	+4.35	-	9.98	0.004	-
-35	6.03	+11.1	-	-	0.067	-
			Sized			
6/16	5.30	-1.81	0.015	-	0.012	2.026
50/140	5.53	+0.55	0.065	-	0.062	2.027
-200	5.51	+0.19	0.488	-	0.170	2.019

large batches prepared for irradiation specimens was exhaustively analyzed, and it had a total impurity content of 1050 ppm, of which 640 ppm were aluminum, iron, and sodium. The macroscopic neutron cross sections of the total impurities was equivalent to that of 5 ppm of boron (Table 3.10).

All evidences from x-ray diffraction, metallography, petrography, and electron micrography show the sol-gel product to be a single-phase solid solution. At up to 500X magnification, etched sections show no large grain structure (Fig. 3.16). At 69,000X magnification a fractured surface showed grains ranging in size from 5000 to 7500 A, with the grains fitted so that they suggested some degree of ordering of sol particles during evaporation and calcination.[4]

3.4.1 Gases Evolved from Sol-Gel Uranium-Thorium Oxide Fuels

The evolution of gases from solid fuels in service affects the fuel economy and operational safety of the reactor adversely because all gases increase pressures within the cladding, and some promote corrosion of the cladding material. Studies were made of the gases evolved from heated samples of small and large batches of oxide products. The weighed samples were evacuated at room temperature, then heated to 1200°C until there was no further increase in pressure. Gases were withdrawn, the volumes at standard conditions were determined, and then the components were determined by mass spectrography. The quantities and species of gases trapped in the oxides were shown to be related to atmospheres used in calcination, to particle size, and to methods used in sizing the particles for vibratory compaction.

3.4.2 The Effect of Size of Batch and Calcining Furnace on the Gas Content of the Product

In laboratory-scale experiments where control of furnace atmosphere was maintained, particles of high density and low gas content were produced equally well by heating and cooling the charge in inert atmosphere (argon or nitrogen) or in argon--4% hydrogen (see Section 3.2.5 and Table 3.5). When larger batches (3 to 7 kg) were calcined in a larger furnace with its much larger volume of porous insulation, gases in contact with the oxides could not be so well controlled. The change from air to inert atmosphere could not be effected rapidly. The gas contents and O/U

[4] D. E. Ferguson et al., Preparation and Fabrication of ThO_2 Fuels, ORNL-3225 (1961).

Table 3.10. Trace-Element Analyses of Batch-26 Sol-Gel Uranium-Thorium Oxides

Crushed and sized for vibratory compaction; uranium, 93% enriched; batch prepared for irradiation test

Element	Cross Section Barns[a]	Screen Fraction 6/16 ppm	Screen Fraction 50/140 ppm	Screen Fraction -200 ppm
Al[b]	2.3×10^{-1}	13	42	110
B[b]	7.55×10^{2}	< 0.5	< 0.5	< 0.5
Ba[b]	1.20	< 10	< 10	< 10
Be[b]	1.0×10^{-2}	$< 10^{-2}$	$< 10^{-2}$	$< 10^{-2}$
C	3.7×10^{-3}	30	30	70
Ca[b]	4.3×10^{-1}	30	52	49
Cd[b]	2.5×10^{3}	< 10	< 10	< 10
Cl	3.4×10	< 5	< 5	< 5
Co[b]	3.7×10	< 5	< 5	< 5
Cr	3.1	< 5	< 5	10
Cu	3.8	44	40	43
F	9.0×10^{-3}	< 20	< 20	< 20
Fe	2.6	118	340	363
K	2.1	38	38	114
Li	7.1×10	< 5	< 5	< 5
Mg[b]	6.3×10^{-2}	43	80	90
Mo	2.7	6.9	7.6	6.9
N	1.9	16	11	6
Na	5.3×10^{-1}	223	223	283
Ni	4.6	17	54	27
P	2.0×10^{-1}	13	13	13
Si	1.6×10^{-1}	< 25	< 25	< 25
Sn	6.3×10^{-1}	< 65	< 55	< 55
V	4.9	< 2	< 2	< 2

[a] Cross sections from Chart of the Nuclides, KAPL, 6th ed., December 1961.

[b] Spectrographic analysis; all others by wet analysis.

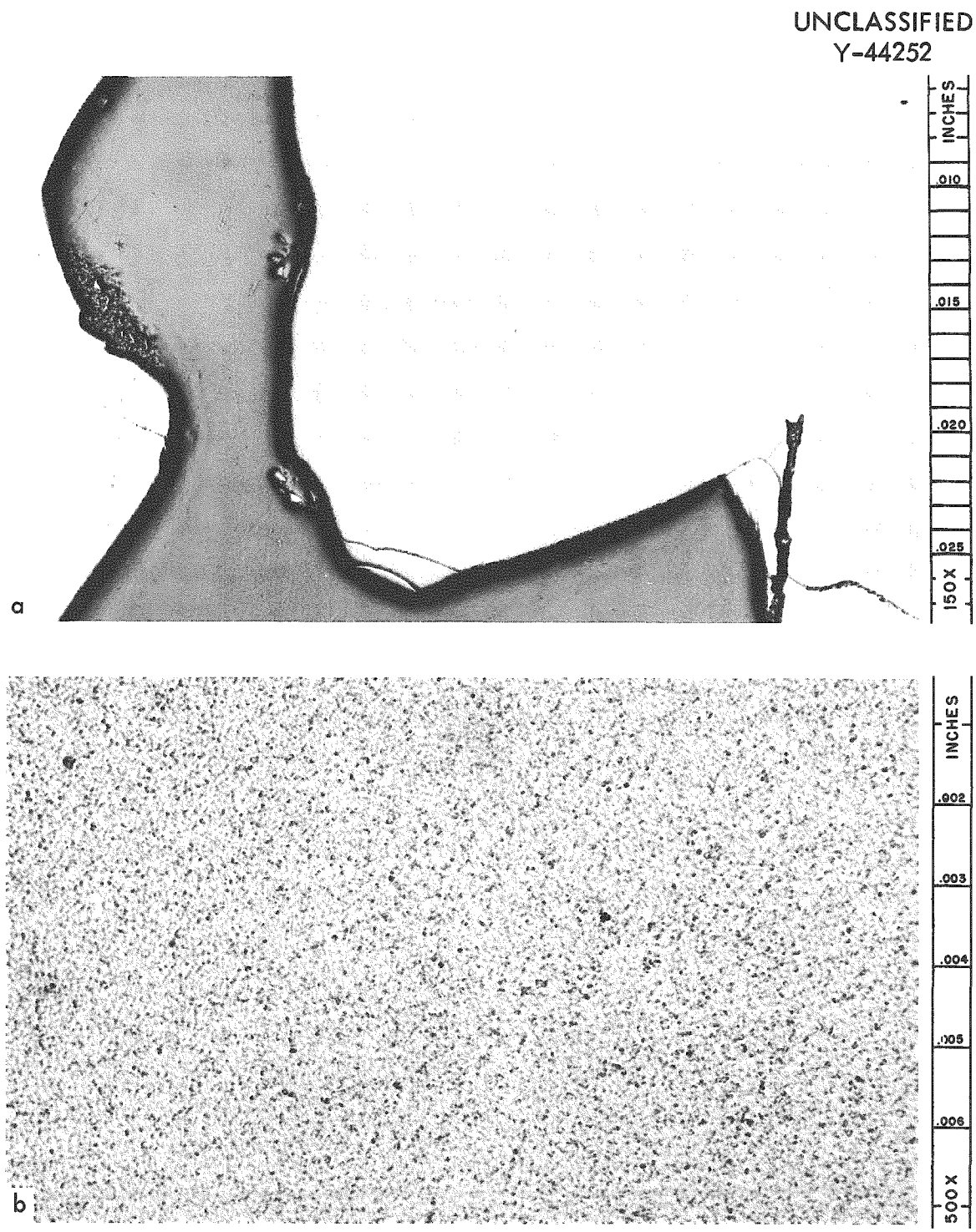

Fig. 3.16. Sol-Gel E ThO_2--4.5 Wt % UO_2 Powder. No impurities were found in this material. Small surface cracks may be seen in the particles. (a) 150X. As-polished. (b) 500X. Etchant: boiling HNO_3-HF. At higher magnification, the particles show a very fine natural porosity, and extremely fine crystallites (spheroidal white particles) may be observed. No large grain boundaries are evident.

ratios of the products were unsuitably high when calcined and cooled in nitrogen or argon but satisfactory in 4% hydrogen--argon.

In studies of gases from calcined sol-gel uranium-thorium oxides in larger batches than 1 kg, the effects of particle size of oxide, calcining and cooling atmospheres, and grinding on total gases and species evolved at 1200°C in vacuum were estimated. Detailed data on gases evolved from large batch preparations are given in Tables A.7 to A.10 in the Appendix.

3.4.3 The Effects of Particle Size on Gases in Calcined Sol-Gel Oxides

As removed from the furnace, the oxides had particle sizes ranging from larger than 4 mesh (about 3/8 in.) downward to about 100 mesh. Comparison of coarse with medium and fine fractions (Table 3.11) of oxides calcined under like conditions, as represented by samples 32C with 32F, shows that particles of the fine fractions liberate about twice the volume of gas as coarse ones, but that the quantities are not proportional to particle size or surface area. Small particles evolved more CO and CO_2 than large particles. The probable sources of carbon were CO_2 in furnace gases or air and volatile carbon compounds in blanket gases. Smaller particles, with their greater specific surface, would be expected to have more capacity for adsorption of either CO_2 or H_2O or for the deposition of carbon. Calculations showed that even for the smallest particles of highest specific surface, complete monolayer coverage with CO_2 (ref 5) could not account for more than 20% of the carbon present in the evolved CO + CO_2. It was concluded that the decomposition of carbon compounds during calcination was the major source of carbon.

3.4.4 The Effects of Calcination and Cooling Atmospheres on Gases in Calcined Sol-Gel Uranium-Thorium Oxides

Oxides calcined and cooled in argon and nitrogen evolved more total gas when heated and had a higher residual O/U ratio (about 2.3 vs 2.02) than those calcined in hydrogen or 4% H_2--argon (Table 3.11). Gases evolved from oxides calcined in inert atmosphere contained only minor amounts of water and carbon monoxide, and were composed mostly of carbon dioxide and free oxygen. The smaller particles evolved less free oxygen and a correspondingly larger amount of CO + CO_2. In cases of particularly low free oxygen, less CO_2 and more CO were found.

[5] C. H. Pitt and M. E. Wadsworth, Carbon Dioxide Adsorption on Thoria, Technical Report No. I, Univ. of Utah (1958).

Table 3.11. Effect of Particle Size and Calcination Atmosphere on Gas Evolution from Sol-Gel Oxides

Calcination program: 1 hr in air at 1150°C; 4 hr in a specified atmosphere; cool down to 25°C in atmosphere

Oxide samples evacuated at 25°C; heated to 1200°C and held there until pressure became constant

Oxide Sample[a]	Calcination Atmosphere[b]	O/U Ratio	Surface Area (m^2/g)	Gases Evolved at 1200°C and Under Vacuum (std cc/g)					
				Total	H_2	H_2O	CO + N_2	CO_2	O_2
32C	A-N	-	0.002	0.033	0	0.0004	0.001	0.006	0.025
32F	A-N	-	0.014	0.067	0	0.0007	0.003	0.022	0.040
71C	N-N	2.244	0.002	0.023	0	0.0003	0.0007	0.003	0.019
71M	N-N	2.285	0.005	0.033	0	0.0003	0.0009	0.005	0.027
71F	N-N	2.304	0.014	0.039	0	0.0003	0.0020	0.029	0.008
26C	$4H_2$-A	2.026	0.015	0.004	-	-	-	-	-
26M	$4H_2$-A	2.027	0.065	0.004	-	-	-	-	-
26F	$4H_2$-A	2.019	0.048	0.067	-	-	-	-	-
26 comp[c]	$4H_2$-A	2.025	0.047	0.206	0.100	0.003	0.083	0.011	0.001
E comp	H_2-A	2.020	0.015	0.027	0.009	0.0007	0.012	0.006	0.0
D-C	H_2-A	2.01	0.008	0.012	0.004	0.0005	0.007	0.0001	0.0

[a] C = coarse, 4 to 16 mesh; M = medium, 50-140 mesh; F = fine, 35-100 mesh; comp = mixed sizes.

[b] A-N, calcined in argon, cooled in N_2; N-N, calcined and cooled in N_2; $4H_2$-A, calcined in 4% H_2-argon, cooled in argon; H_2-A, calcined in H_2, cooled in argon.

[c] Sized by crushing and ballmilling, then blended.

When calcined in a reducing atmosphere and cooled in inert gas (Table 3.11, 26C to D-C), the major components of gases evolved were H_2, H_2O, and CO. There was little CO_2 and, of course, no free oxygen.

The distribution of gases evolved by heating some hydrogen-calcined oxides in vacuum to various temperatures was determined. The results for two oxide samples are presented in Table 3.12. The gases were removed at the end of each temperature interval and consequently could not interact with those evolved at the next higher interval. The results indicate that up to 300°C the gases removed were mainly those physically adsorbed or weakly chemisorbed. At 300 to 1000°C, the likely sources of gases were the CO and H_2 from the reaction of carbon with water, and the strongly chemisorbed CO_2.

The conditions likely to be produced inside a fuel element upon heating may be estimated from the O/U ratio. In Table 3.13, oxides which were calcined in inert atmosphere and those calcined in reducing atmosphere are compared. The excess oxygen indicated by the O/U ratio above 2.00 is assumed to be a potential source of available oxygen. Oxides calcined in inert atmosphere had O/U ratios of about 2.3 and generated oxidizing conditions (oxidizing gases greatly in excess) in the gases evolved by heating. Oxides calcined in hydrogen evolved reducing gases, including hydrogen. Hydrogen and water are known to cause hydriding of Zircaloy, while the presence of small excesses of free oxygen is known to inhibit the reaction of Zircaloy with water.[6] It is therefore desirable to handle the oxide product so that it will not absorb water. Further, excess oxygen may be desirable in the fuel if it can be shown not to cause the migration of uranium in the system or to adversely affect fission-gas retention. Table 3.14 shows that preparations having O/U ratios up to 2.43 evolve only a minor percentage of their potential oxygen excesses (less than 15%) as free oxygen or carbon-oxide gases and that nonstoichiometric urania may act as a sink or source for oxygen. Properly controlled conditions, produced by calcination in inert atmosphere, promise to give a slight, regulated oxygen excess within the fuel cladding during service.

[6] F. H. Kreuz, Can Hydrogen Pickup in Zircaloy be Prevented? GRGM-1081 (October 1962).

Table 3.12. Fractions of Each Gas Evolved from Sol-Gel-Prepared Uranium-Thorium Oxides at Various Temperatures

Calcined in 100% H_2; cooled in argon; approximately 4 at. % U, 93% enriched; heated to various temperatures in vacuum

Oxide Sample	Temperature (°C)	Gases Evolved, % of Total for Each[a]										Total Gas, std cc/g	
		H_2		H_2O		H_nC_{n+x}		CO		CO_2			
		A	B	A	B	A	B	A	B	A	B	A	B
Sol-gel	25-300	0.8	1.6	59.1	55.5	None	None	4.1	1.8	41.5	31.4	17.6	17.2
	300-500	10.7	20.0	33.4	31.8	69.1	56.7	23.6	20.0	51.6	50.5	25.6	25.8
	500-750	72.0	64.3	6.4	8.3	30.0	42.7	33.2	58.3	5.2	16.3	40.0	43.7
	750-1010	16.6	15.0	1.1	2.1	0.9	0.6	39.0	19.8	0.3	1.9	16.8	13.2

[a]Volume of individual gas evolved at temperature divided by the total volume of that gas evolved over the entire temperature range.

Table 5.13. Effects of Calcination Atmosphere, Particle Size, Sizing Procedure, and O/U Ratio on Oxidation-Reduction Conditions in Atmosphere over Heated Sol-Gel Oxide Fuel

Oxide No.	O/U Ratio	Calcination Atmosphere	Cooling Atmosphere	U... Sieve Size Mesh	Available Oxygen[a] (μg atoms/g)	Free H_2 (micromoles/g)	H_2O (micromoles/g)	Free Oxygen (μg atoms/g)	Oxidizing Gases[b] / Reducing Gases (mole/mole)
—	2.0	Hydrogen	Argon	-30 +100	3.	0.38	0.09	0.0	0.51
A-G	2.005	Hydrogen	Argon	-30 +3_5	0.76		0.833	0.0	0.49
6	2.0_5	4% H_2-argon	Argon	-6 to -.00	6	4.46	0.134	0.09	0.8_
D-G	.2_66	Nitrogen	Nitrogen	-5 +16	74	0.0	0.055	8.0	37._
D-F	2.36	Nitrogen	Nitrogen	-35 +100	110	0.0	0.0_3	1.75	13.7
D-Fg	2.36	Nitrogen	Nitrogen	-200 +3_5	110	0.0	1._4	0.0 3	11.0

[a]Available oxygen = μg-atoms of oxygen on the basis of oxygen in excess of that of $UO_{2.00}$.

[b]Oxidizing gases = free O_2 + CO_2 + H_2O; reducing gases = free H_2 + CO.

Table 3.14. Effects of Excess Oxygen in Sol-Gel-Prepared Oxides on the Evolution of Oxygen-Containing Gases upon Heating

Oxide Number[a]	O/U Ratio	Excess O_2 in UO_{2+x} (cc/g)	Gases Evolved at 1200°C, Vacuum		
			Total cc/g	Free Oxygen (% of excess O_2)	$CO + CO_2$ (% of excess O_2)
71 C	2.24	0.76	0.023	2.60	0.4
71 Cg	2.24	0.76	0.061	7.70	0.2
70 Cg	2.27	0.83	0.094	10.60	0.6
70 C	2.29	0.90	0.044	4.56	0.4
71 M	2.29	0.90	0.033	3.03	0.7
70 Mg	2.32	1.03	0.091	2.10	6.6
71 Mg	2.32	1.03	0.091	2.16	7.8
70 M	2.33	1.04	0.047	4.06	0.3
70 F	2.36	1.24	0.039	1.53	1.5
70 Fg	2.36	1.24	0.220	0.002	14.7
101 F	2.43	1.97	0.160	5.62	2.5

[a] C = coarse particles unground; Cg = coarse particles, crushed; M = -16 +35 mesh particles unground; Mg = -50 +140 mesh, crushed; F = -35 +100 mesh particles unground; Fg = -200 mesh particles, ball milled.

3.4.5 The Effects of Grinding Sol-Gel-Prepared Oxides on Gas Evolution

After calcination, the sol-gel oxides are prepared for vibratory compaction by crushing or ball milling to the desired size fractions. Grinding, particularly ball milling, in ambient air increased the total gas evolution more for the smaller particles than for the larger (Table 3.15). Water and carbon dioxide were the gases absorbed in the size-reduction step. For oxide that had been calcined in inert atmosphere and ball milled in air, the evolution of water, carbon dioxide, and carbon monoxide was greatly increased, but the evolution of free oxygen was correspondingly decreased. For oxides calcined in reducing atmospheres, ball milled in air, then heated, the evolution of water and carbon monoxide was increased and hydrogen and carbon dioxide decreased.

Table 3.15. Effect of Grinding on Gas Evolution from Sol-Gel-Prepared Oxides

Calcination program: 1 hr at 1150°C in air; 4 hr in atmosphere at 1150°C; cool down to ~25°C in atmosphere

Oxide Sample[a]	Calcination Atmosphere		Grinding Method	O/U At. Ratio	Particle Size	Surface Area (m^2/g)	Gases Evolved at 1200°C in Vacuum (std cc/g)					
	Calc	Cool					Total	H_2	H_2O	CO + N_2	CO_2	O_2
26 C	$4H_2$-A	A	None	2.026	6/16	0.015	0.004	-	-	-	-	-
.6 comp	$4H_2$-A	A	Crush and ball mill	2.025	6/325	0.047	0.206	0.100	0.003	0.0830	0.011	0.001
26 F	$4H_2$-A	A	None	2.019	35/100	0.067	0.067	-	-	-	-	-
A comp	H_2	A	Crush and ball mill	2.005	10/200	0.220	0.125	0.0024	0.062	0.0080	0.051	0.0
DC	H_2	A	None	2.01	4/50	0.008	0.012	0.0041	0.0005	0.0070	0.0001	0.0
71 C	N_2	N_2	None	2.244	6/16	0.002	0.023	0.0	0.0003	0.0007	0.0025	0.0195
71 Cg	N_2	N_2	Crush	2.308	6/16	0.002	0.061	0.0	0.0010	0.0020	0.0006	0.0573
71 F	N_2	N_2	None	2.304	35/100	0.014	0.039	0.0	0.0003	0.0015	0.0293	0.0078
70 Fg	N_2	N_2	Ball mill	2.307	-200	0.077	0.220	0.0	0.0274	0.0183	0.1731	0.0002
32 C	A	N_2	None	-	4/16	0.002	0.033	0.0	0.0004	0.0010	0.0064	0.0251
31 Cg	A	N_2	Crush	-	6/16	0.002	0.019	0.0	0.0003	0.0006	0.0030	0.0151
32 F	A	N_2	None	-	35/100	0.014	0.067	0.0	0.0007	0.0026	0.0024	0.0403
31 Fg	A	N_2	Ball mill	-	-200	0.077	0.246	0.0	0.0039	0.0706	0.1616	0.0004

[a]C, coarse fraction; F, fine fraction; Cg, coarse, crushed; Fg, fine ground; comp, mixture of sizes.

In order to prevent the development of conditions in the oxides detrimental to their service in Zircaloy, grinding in an atmosphere free of water and carbon dioxide is recommended. Gas evolution from sol-gel-prepared oxides would be minimized by sizing the dried gel prior to calcination.

3.4.6 Effects of Excess Oxygen on O/Metal Ratio and Gas Volumes Inside of Fuel Elements Filled with Sol-Gel-Prepared Oxides

In uranium dioxide fuel technology, a rigid specification for the O/U ratio of less than 2.02 is imposed. The reason is that excess oxygen beyond 0.02 causes excessive release of fission product gases, uranium migration due to sublimation of UO_3, and resultant excessive pressures in the fuel element. While the effects of excess oxygen in the UO_2-ThO_2 system on the above factors are not known from in-pile experience, evidence from chemical properties of solid solutions of thoria and urania indicates that a higher O/U ratio may be tolerated. The thoria lattice is larger than that of urania; consequently, it may behave as a "sink" for gases, including fission products and excess oxygen. Since urania-thoria systems may form solid solutions in the 3 to 10 at. % uranium range, the vapor pressure of UO_3 may be depressed from its normal value as a pure uranium oxide. Uranium, therefore, would not migrate readily in the presence of excess oxygen. Figure 3.17 (curve A) shows that for a 3% uranium--thorium oxide an O/U ratio as high as 2.3 (calculated assuming O/Th = 2) would correspond to an O/U ratio of less than 2.02 in a fuel composed of pure UO_2. Curve B in the same figure shows the potential volume of excess oxygen vs the O/U ratio. Although this calculated volume per gram is high, and would generate high pressures within fuel pins at reactor operating temperatures if it were released from the fuel, it appears that only a small percent is released, as shown by the data of Table 3.14. In this table, amounts of gases actually released at 1200°C and under vacuum from oxides which contained 7 and 10 wt % uranium and which were calcined in nitrogen in large batches are compared with the amounts which the excess oxygen represents if it were completely evolved. In all cases, less than 11% of the oxygen was released as free oxygen, and less than 15% as carbon oxide gases. In these same oxides, no hydrogen, and negligible water were evolved.

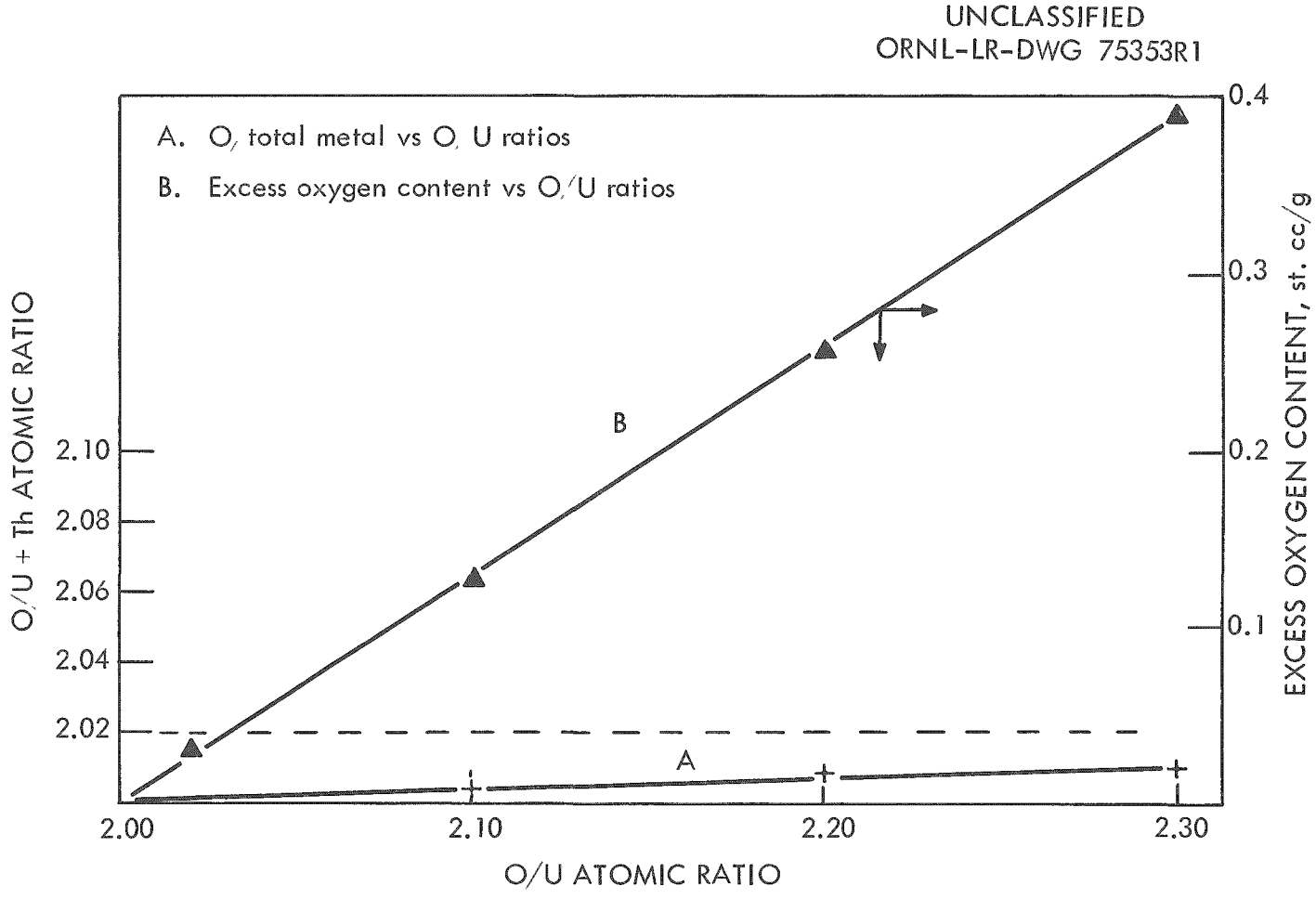

Fig. 3.17. Oxygen/Uranium Ratio in 3 at. % U-ThO_2: Effect on Oxygen/Metal Ratio and Excess Oxygen Volume. Gases released at 1200°C, vacuum.

3.4.7 Estimated Total and Partial Pressures of Evolved Gases Within Fuel Elements at Pressurized-Water-Reactor Temperatures

Estimates were made of total and partial pressures of evolved gases from sol-gel oxides calcined in various atmospheres within fuel elements (pins) of the Kilorod element dimensions, loadings, and void spacings. For the pin having an overall cavity length and diameter of 45-1/16 in. and 0.43 in., respectively, and with two end spacers having a volume sum of 1.95 cc and a maximum loaded length of 43 in., the total void space for gas in each pin was 13.9 cc. The weight of fuel was taken to be 944 g per pin. The Indian Point Consolidated Edison PWR was taken as representative of pressurized-water-reactor conditions. With a fuel center-line temperature of 3600°F and a maximum clad temperature of 675°F, a mean operating temperature was calculated as 1670°F. It was assumed that the volumes of gases released in the pins would be the same as those released in vacuum at 1200°C (probably too high) and that one atmosphere (at STP) of helium was present in the pin. Total and partial gas pressures were plotted vs the volumes of gases released for oxides calcined in hydrogen, in 4% hydrogen--argon, and in inert gases (argon or nitrogen) in Figs. 3.18, 3.19, and 3.20.

For oxides calcined in hydrogen or hydrogen--argon, gases attaining the highest estimated internal pressures were hydrogen and carbon monoxide, reaching 50 psi even at an acceptably low total gas volume. At volumes of gases evolved by ball milled oxides, the partial pressures of hydrogen and water approached 200 psi. Such pressures of hydrogen and H_2O would be certain to cause Zircaloy corrosion.

The major gases evolved from oxides calcined in nitrogen or argon were CO_2 and oxygen (Fig. 3.20). No hydrogen was present, but water had partial pressures in the troublesome range at gas release volumes characteristic of ball milled oxides.

3.5 Sampling Methods

The two feed streams (uranyl nitrate solution and thoria powder) used for sol preparation can be analyzed easily and should provide adequate basis for control of average batch composition. A study was

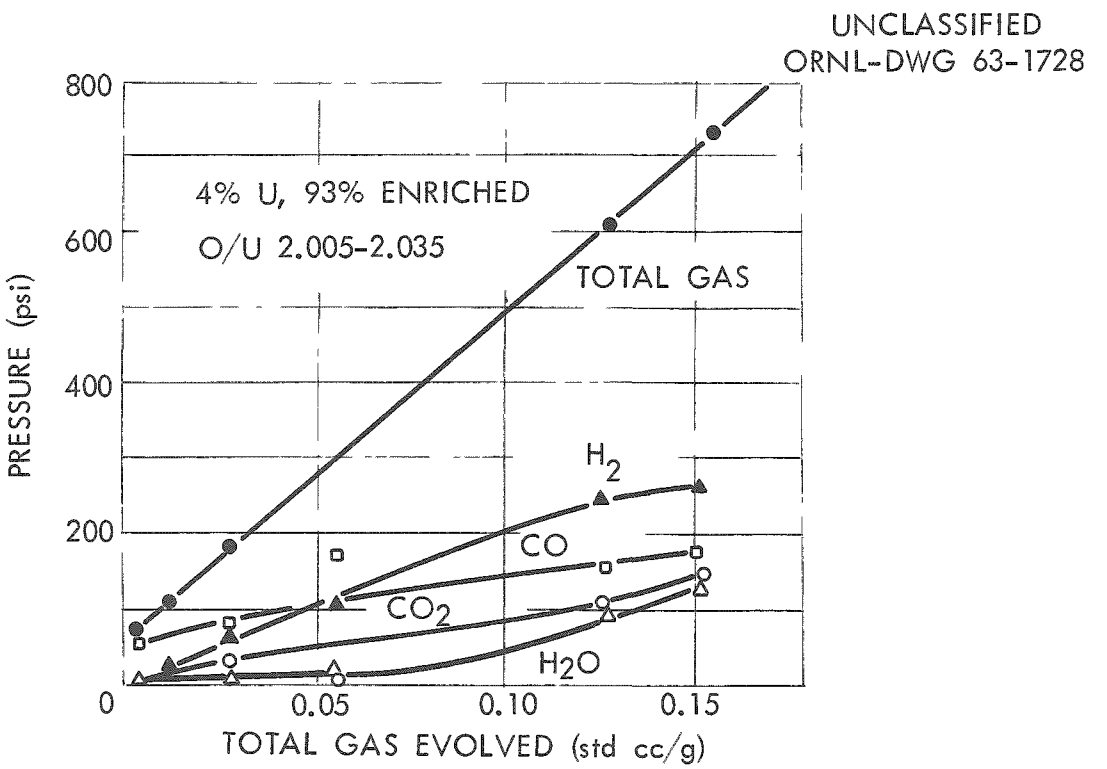

Fig. 3.18. Expected Gas Pressures Inside Kilorod Fuel Elements at 1670°F Mean Temperature, for H_2-Calcined Sol-Gel Oxides.

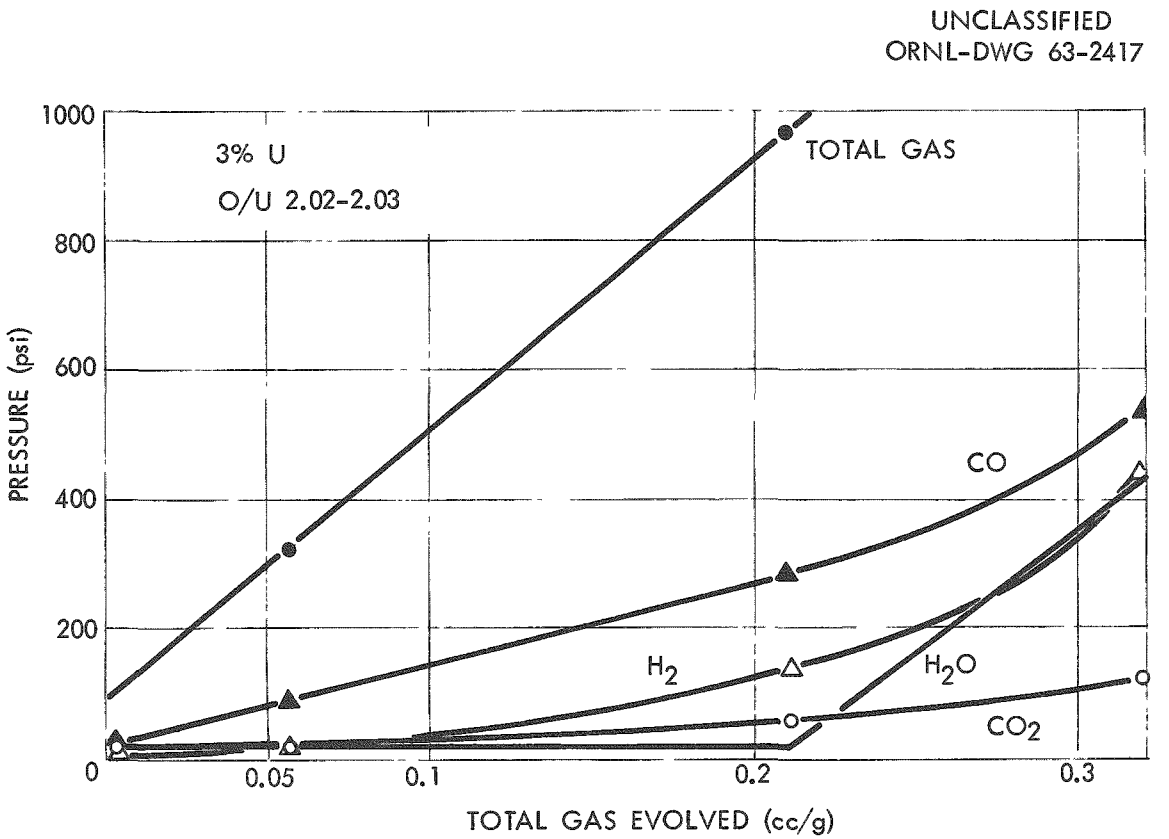

Fig. 3.19. Expected Gas Pressures Inside Kilorod Fuel Elements at 1670°F Mean Temperature, for Sol-Gel Oxides Calcined in 4% H_2--Ar.

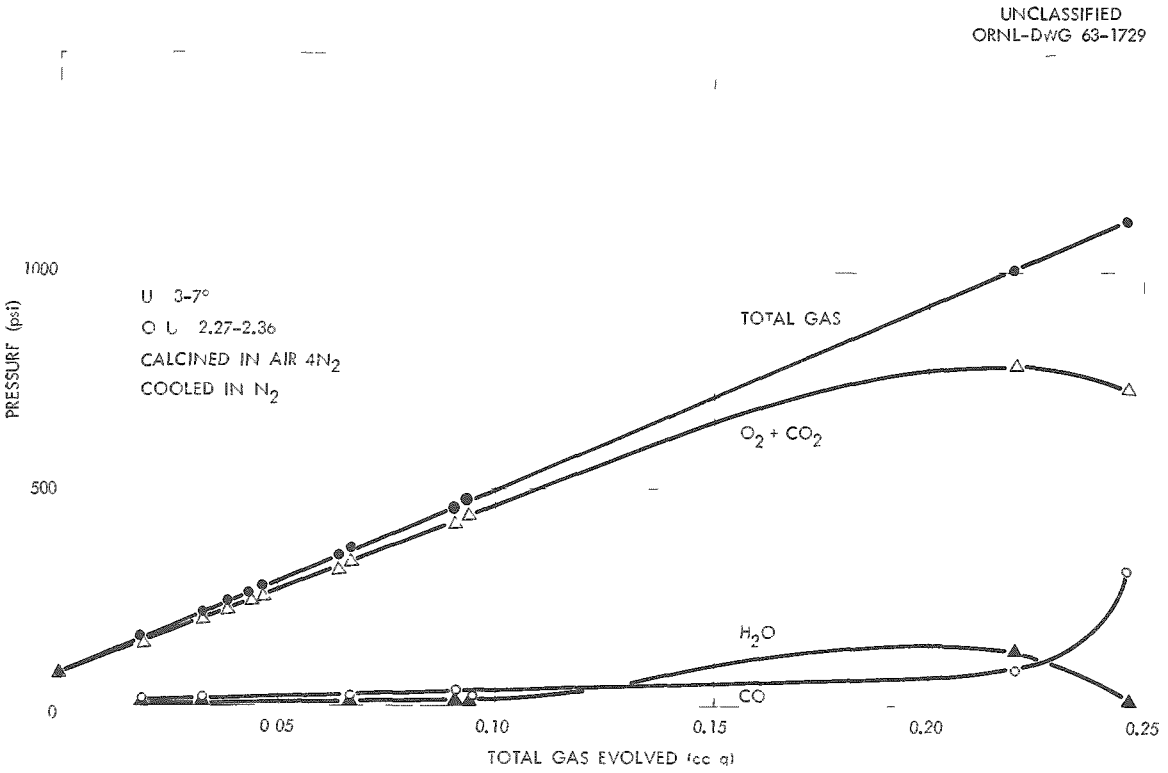

Fig. 3.20. Expected Gas Pressures Inside Kilorod Fuel Elements at 1670°F Mean Temperature, for Sol-Gel Oxides Calcined in Inert Atmosphere.

undertaken to determine whether the standard method of analysis of calcined oxide product is capable of detecting deviations of 0.03% U, which is the limit demanded by the Kilorod Program. This deviation represents 1% of the specified uranium concentration of 3%. A series of three sols was made up from a single ThO_2 powder, in which the U/Th atom ratio was increased progressively from sol to sol by 1%. Uranium analyses on the sols readily detected the increases, with little difference between results from analyses of starting materials and of sol products (Table 3.16). To detect differences in uranium uniformity to within the Kilorod

Table 3.16. Analysis of Sol-Gel Oxides

Analysis	Preparations Analyzed		
	10A	10B	10C
U/Th atomic ratio			
As charged in sol	0.02925	0.02954	0.02986
As analyzed in sol	0.02931	0.02959	0.02987
% difference	0.20	0.17	0.03
N/Th atomic ratio			
As charged in sol	0.1209	0.1218	0.1227
As analyzed in sol	0.1201	0.1212	0.1215
% difference	0.66	0.49	0.98
Percent scatter in analyses[a]			
U in sol	0.93	0.41	0.18
Th in sol	0.14	0.03	0.24
N in sol	4.53	3.02	4.15
U in calcined coarse (+16)	1.09	2.75	2.38
U in calcined fines (-200)	3.85	1.49	1.16
Th in calcined coarse (+16)	0.29	0.44	0.91
Th in calcined fines (-200)	0.22	0.25	0.41

[a]Based on triplicate analyses of each preparation ($\frac{\text{max difference}}{\text{mean}}$ x 100).

specification, the scatter in results between multiple samples should be no greater than 2%. For triplicate samples of the same sol preparations, all uranium results were within a scatter of less than 1%. However, in analysis of the calcined solids the scatter was greater than the 2% limit in three of six triplicates. An inspection of Tables A.5 and A.6 in the Appendix reveals considerable discrepancy between deviations of uranium percent from the average based on sol composition and those based on the weighted average of analyses of the solids. This suggests that either an error in the material balance in the sol makeup or in the analyses of the solids was made, or that samples were not representative. For the series shown in Table 3.16, grinding all solids to -200 mesh and reanalyzing greatly decreased the scatter, so that the U/Th ratio of the fired solids was within 1.02% of that of the sol. For the Kilorod Program it is recommended that samples for uranium analysis be taken of the calcined product mixture just prior to vibratory compaction and that the whole sample be ground to -200 mesh for the analysis. For other projects using the sol-gel process, the suggested sampling point is the dried gel, whose samples can be readily made into a sol for analysis.

APPENDIX A

Table A.4 presents complete data for the conditions of sol preparation for all batches prepared for development of the sol-gel process for the Kilorod Program. Columns 1 through 10 (through the "Sol pH") refer to conditions of the liquid sol. "Loss on Calcination (wt %)" refers to loss of volatile matter on conversion of the dried gel to calcined oxide product. Screen analyses and vibrated densities are properties of the final calcined product.

In Tables A.5 and A.6, conditions of sol preparation are related to uranium distribution in the final product for all batches of sol-gel product prepared in development for the Kilorod Project. The bases used in calculation of deviation of U/Th atom ratios from the average were (a) an average U/Th atom ratio based on the analyses of the uranium-bearing stream and the thoria product of the denitrator, and (b) a weighted average U/Th atom ratio of all sizes based on the analyses of samples of the individual size fractions. In the "as calcined" columns, the screened furnace product, size distribution was approximately 92% +6 mesh, 4-5% -6+35 mesh, and 3-4% -35 mesh. In the "as crushed and sized" columns the size distribution was 60% -6+16 mesh, 15% -50+100 mesh, and 25% -200 mesh. Weighted averages were calculated as a summation for all size fractions of U/Th atom ratios multiplied by weight fraction of size.

Table A.1. Rotary Denitrator Run Conditions and Objective for Ten Initial Runs

Charge: 30 kg of $Th(NO_3)_4 \cdot xH_2O$ or as noted

Run No.	Heater Program		Steam Program			Percent Thorium Carryover	Nondispersible Material Present	Purpose of Run, Other Conditions and Remarks
	Temp (°C)	No. of Hours	Flow Rate (lb/hr)	Inlet Temp (°C)	No. of Minutes			
1	400	6.66	22	-	450	-	Yes	Purpose: Initial run with system Other Conditions: Air at 1.33 SCFM for 3.00 hr used at end of run
	425	3.50						
2	425	8.00	40	350	480	9.75	Yes	Purpose: To increase heat flux into drum, and time of steam contact
3	425	7.17	48	350	130	0.94	Yes	Purpose: To study the effect of pulverizing the powder while in contact with steam Other Conditions: 19 kg of 5/8-in.-diam 316 stainless steel balls charged with $Th(NO_3)_4 \cdot xH_2O$
			22	325	260			
4	460	3.25	40	385	120	1.53	Yes	Purpose: To study the effect of an increasing heat flux into the drum
	475	0.58	22	350	70			
	485	2.50	11	255	195			
5	475	6.25	48	385	105	1.75	Yes	Purpose: To study the effect of a shorter run time
			22	350	75			
			9	225	170			
6	475	5.75	48	390	80	1.75	Yes	Purpose: To study the effect of a small charge, and higher denitrating rate Other Conditions: Charge was 10.59 kg of $Th(NO_3)_4 \cdot xH_2O$
			22	350	60			
			9	225	190			
7	500	6.00	45	375	120	1.77	Yes	Purpose: To study the effect of increased heater temperature with a similar steam program as run 4
			22	350	60			
			9	325	180			
8	500	10.00	45	375	60	0.82	Yes	Purpose: To study the effects of introducing air after denitrating to a low nitrate content, and a modified steam program's effect on the carryover Other Conditions: Air at 1.33 SCFM for 4.00 hr used at end of run
			22	350	120			
			9	325	180			
9	500	6.00	10-20	-	360	0.52	No	Purpose: To study the effect of an inlet steam baffle Other Conditions: Steam controlled manually due to diaphragm rupture
10	500	6.00	30	400	85	0.98	No	Purpose: Run 9 repeated to see if good product was reproducible
			16	340	275			

Table A.2. Rotary Denitrator Conditions for Runs to Demonstrate Consistent Operation

Charge: 30 kg of $Th(NO_3)_4 \cdot xH_2O$ or as noted

Run No.	Steam Program: Flow Rate (lb/hr)	Steam Program: Inlet Temp (°C)	Steam Program: No. of Minutes	Percent Thorium Carryover	Nondispersible Material Present	Purpose of Run, Other Conditions and Remarks
RDB-11	34 22	410 360	80 + 10[a] 280	0.78	Yes	To duplicate good product of run 10
RDB-12	29 17	400 340	78 + 15 285	0.80	No	To duplicate good product of run 10
RDB-13	28 16	400 340	112 + 15 249	0.74	Yes	To maintain the 30 lb/hr steam rate until reaching the second hold period
RDB-14	45 28 16	- 400 340	23 + 5 120 218	1.06	No	To test an initial steam rate of 40 lb/hr for a short time, then hold the 30 lb/hr rate until after the second hold period
RDB-15	41 28 16	- 400 340	25 + 5 113 225	1.08	No	To duplicate good product of run 14
RDB-16	41 28 16	425 400 340	35 + 5 112 215	0.85	Yes	To duplicate good product of runs 14 and 15
RDB-17	16 14	340 330	60 + 5 240	0.71	Yes	To utilize a low steam rate for the entire run
RDB-18	45 14	425 330	30 + 15 270	0.48	Yes	To test an initial steam rate of 40 lb/hr for a short time, then a low steam rate for the remainder of the run
RDB-19	41 17	425 340	90 125	0.46	Yes	To use run 18 conditions with the high steam rate prevailing until after the second hold period
RDB-20	19	350	330	0.63	No	Steam contact delayed until 180°C skin temperature was reached
RDB-21	19	350	240	0.46	No	To duplicate good product of run 20 and to shorten run time
RDB-22	19	350	240	0.60	No	To duplicate good product of run 21
RDB-23	19	350	240	0.51	No	To duplicate good products of runs 21 and 22
RDB-24	37 19	415 350	103 137	1.43	No	To test the effect of a high steam rate prevailing until after the second hold period with the delayed steam contact time
RDB-25	19	350	240	1.03	No	To repeat run 21 without the steam baffle in denitrator
RDB-26	30 19	405 350	142 248	1.23	No	To test the feasibility of a 45 kg $Th(NO_3)_4 \cdot xH_2O$ charge, with the steam contact time delayed
RD-27	19	350	360	1.04	No	To extend the time of run 21
RDB-28	30 19	405 350	127 + 15 158	1.14	No	To duplicate run 12 (for a shorter period) and thus confirm effect of early steam contact in producing creamy fraction
RDB-29	41 28 19	420 400 350	40 + 15 103 202	0.97	No	To duplicate run 14 to confirm effect of early steam contact in producing creamy fraction
RDB-30	30 19	405 350	120 600	0.96	No	To determine the effect of a long run time
RDB-31	30 19	405 350	120 270	1.38	No	To duplicate run 26
RDB-32	30 19	405 350	133 257	1.17	Yes	To duplicate run 26

[a] "+ 10" refers to time prior to zero run time.

Table A.3. Analysis of Products Produced in the 14-in.-diam Rotary Denitrator

Run No.	RD-1	RD-2	RD-3	RD-4	RD-5	RD-6	RD-7	RD-8	RDB-9[a]	RDB-10
Time in steam, min	445	465	420	385	360	330	360	360	360	360
Time in air, min	180	-	-	-	-	-	-	240	-	-
Product weight, kg	14.61	12.47	14.20	13.86	13.72	4.63	13.87	14.44	14.02	13.65
Thorium carryover, %	-	9.75	0.94	1.53	1.75	1.75	1.77	0.82	0.52	0.98
LOI (300-1000°C), %	4.68	3.45	4.39	2.79	2.36	2.25	1.95	1.58	1.57	2.74
Nitrogen, %	0.65	0.40	0.56	0.21	0.19	0.08	0.17	0.16	0.15	0.20
Thorium, %	84.73	84.85	84.09	85.76	86.28	86.39	86.49	86.88	86.63	86.29
N/Th, mole ratio	0.127	0.078	0.110	0.041	0.035	0.015	0.033	0.031	0.029	0.038
Crystallite size, A	59	66	65	77	67	78	78	80	70	73
Surface area, m^2/g	23.2	44.5	36.3	46.9	47.9	52.8	50.2	50.3	49.8	46.2
Nondispersible material present	Yes	Yes	Yes	Yes	Yes	Yes	Yes	Yes	No	No
Fe, ppm	215	54	145	22	50	53	45	-	-	-
Cr, ppm	25	30	35	35	50	50	50	-	-	-
Cu, ppm	50	70	75	75	50	50	50	-	-	-

	RDB-11[a]	RDB-12	RDB-13	RDB-14	RDB-15	RDB-16	RDB-17	RDB-18	RDB-19	RDB-20	RDB-21
Time in steam, min	360	360	360	360	360	360	300	300	210	330	240
Time in air, min	-	-	-	-	-	-	-	-	-	30	60
Product weight, kg	14.02	13.96	13.83	14.00	-[c]	-[c]	14.10	13.92	14.13	13.59	13.92
Thorium carryover, %	0.78	0.80	0.74	1.06	1.08[c]	-[c]	0.71	0.48	0.46	0.63	0.46
LOI (300-1000°C), %	1.63	1.98	2.16	2.20	2.08	2.14	1.96	1.97	2.45	1.92	2.27
Nitrogen, %	0.12	0.14	0.15	0.11	0.099	0.091	0.22	0.14	0.41	0.159	0.29
Thorium, %	86.55	86.53	86.40	85.23	84.96	86.09	84.62	85.34	85.54	86.34	85.38
N/Th, mole ratio	0.023	0.027	0.029	0.021	0.019	0.018	0.043	0.027	0.079	0.031	0.056
Crystallite size, A	77	74	76	72	75	82	76	76	72	69	69
Surface area, m^2/g	53.8	48.8	49.8	48.3	47.1	51.0	50.0	53.1	50.9	42.2	41.4
Nondispersible material present	Yes	No	Yes	No	No	Yes	Yes	Yes	Yes	No	No

	RDB-22[a]	RDB-23	RDB-24	RD-25	RDB-26[b]	RD-27	RDB-28	RDB-29	RDB-30[d]	RDB-31[b]	RDB-32[b]
Time in steam, min	240	240	240	240	390	360	300	360	600	390	390
Time in air, min	60	60	60	60	-	-	-	-	-	-	-
Product weight, kg	13.70	14.06	13.80	13.54	20.76	13.64	13.88	13.80	13.46	20.77	21.24
Thorium carryover, %	0.60	0.51	1.43	1.03	1.23	1.04	1.14	0.97	0.96	1.38	1.17
LOI (300-1000°C), %	2.54	2.95	-	-	-	-	-	-	-	-	-
Nitrogen, %	0.33	0.32	0.30	0.28	0.22	0.15	0.24	0.14	0.08	0.26	0.29
Thorium, %	84.98	84.64	84.94	85.50	85.34	86.11	85.49	86.47	84.25	85.16	85.87
N/Th, mole ratio	0.064	0.063	0.059	0.054	0.043	0.028	0.046	0.027	0.016	0.051	0.056
Crystallite size, A	67	70	62	68	71	70	64	68	73	66	64
Surface area, m^2/g	39.8	51.1	45.0	45.3	46.0	50.8	41.6	40.4	38.3	45.5	44.3
Nondispersible material present	No	No	No	No	No	No	No	No	No	No	Yes

[a] "B" signifies baffled steam inlet.

[b] A 45 kg charge of $Th(NO_3)_4 \cdot xH_2O$ crystals used for these runs.

[c] Product discharged directly in dispersing tank.

[d] 5-1/2 hr of denitration first day; shutdown overnight; and 6-1/2 hr of denitration on second day, 2 hr required to reach temperature on the second day not included in run time.

Table A.4. Tabulated Sol-Gel Data for Uranium-Thorium Oxide Preparations

ThO_2 slurry added to uranyl nitrate solution except as noted

Batch No.	Batch Size (g of ThO_2)	ThO_2 Powder Denitration Time (hr)	Th/U Atomic Ratio	NO_3^-/U Mole Ratio in UNH	NH_4OH/Th Mole Ratio	Added NO_3^-/Th Mole Ratio	Sol pH	Screen Analysis of Calcined Product, U.S. Mesh Size +16 (%)	16/35 (%)	-35 (%)	Vibrated Density of Product (g/cc)	Loss on Calcination (wt %)
7-A	3,000	4[a]	30	3.00	-	0.096	2.30	-	-	-	8.91	3.44
7-B	3,000	4[a]	30	3.00	0.041	0.096	2.95	-	-	-	8.94	3.86
7-C	3,000	4[a]	30	3.87	0.097	0.127	~4.00	-	-	-	8.85	4.68
8-A[b]	3,000	6-1/2	30	3.00	0.041	0.170	2.72	-	-	-	8.37	5.58
8-B[b]	3,000	6-1/2	30	3.00	0.052	0.170	3.04	-	-	-	8.42	5.77
8-C[b]	3,000	6-1/2	30	3.00	0.093	0.170	3.45	-	-	-	8.78	6.10
8-D[b]	1,965	6-1/2	28	2.40	0.082	0.159	3.42	-	-	-	8.75	6.18
8-E[b]	1,965	6-1/2	28	2.00	0.066	0.144	3.35	-	-	-	8.80	5.75
9-A	5,950	4[a]	30	3.00	-	0.096	2.87	-	-	-	-	4.91
9-B	5,490	4[a]	30	3.00	-	0.096	2.78	-	-	-	-	5.11
10-A	1,860	5	34	2.58	-	0.075	2.90	86.0	10.7	3.5	-	4.36
10-B	1,860	5	34	2.59	-	0.075	2.90	86.7	10.3	3.5	-	4.16
10-C	1,860	5	33	2.60	-	0.075	2.82	91.8	5.1	3.1	-	4.29
11-A[b]	2,630	4[a]	33	2.00	0.043	0.134	2.95	-	-	-	8.92	5.89
12-A	3,000	4[a]	33	3.00	0.035	0.090	3.15	-	-	-	8.80	5.24
12-B	3,000	4[a]	33	3.00	0.019	0.090	3.20	-	-	-	8.80	5.13
13-A	6,050	6	33	3.16	-	0.095	2.89	-	-	-	-	4.31
13-B	6,050	6	33	3.00	-	0.090	3.02	-	-	-	-	4.75
14-A	4,210	10	33	2.00	-	0.060	4.28	-	-	-	-	-
14-B	-	10	33	2.24	-	0.068	3.69	-	-	-	-	-
14-C	-	10	33	2.51	-	0.076	3.52	-	-	-	-	-
14-D	-	10	33	2.78	-	0.084	3.35	-	-	-	-	-
14-E	-	10	33	3.05	-	0.092	3.22	-	-	-	-	-
14-F	-	10	33	3.32	-	0.100	3.12	-	-	-	-	-
14-G	-	10	33	3.32	0.013	0.100	3.42	-	-	-	-	-
14-H	-	10	33	3.32	0.027	0.100	4.18	-	-	-	8.74	-
15-A	8,530	4[a]	33	2.56	0.007	0.077	3.13	-	-	-	8.76	5.05
15-B	6,930	4[a]	33	2.56	0.015	0.077	3.48	-	-	-	8.94	5.72
15-C	4,080	4[a]	33	2.56	0.030	0.077	3.76	-	-	-	8.94	5.62
15-D	2,760	4[a]	33	2.56	0.051	0.077	5.32	-	-	-	-	-
16[b]	9,190		33	2.40	0.072	0.144	3.32	-	-	-	-	-
17	8,640	5	33	2.23	-	0.067	3.32	-	-	-	-	2.33
18	8,880	5	33	2.23	-	0.067	3.28	-	-	-	-	4.85
19-4M	3,025	5	33	2.23	-	0.067	3.18	90.0	5.1	4.8	8.95	3.97
20-5M	4,540	5	33	2.23	-	0.067	3.31	92.9	3.6	3.5	9.06	3.91
21	2,935	6	26	2.22	-	0.086	2.90	94.5	3.1	2.3	8.96	4.30
22	2,935	6	24	2.24	-	0.093	2.90	95.0	2.8	2.2	8.60	4.32
23	6,160	6	33	2.32	-	0.070	3.05	94.3	3.4	2.3	9.00	5.67
24	2,940	5	33	2.32	-	0.070	2.97	93.9	3.5	2.6	9.10	4.89
25	7,000	-	33	2.33	-	0.070	-	-	-	-	-	-
27	5,000	6	33	2.50	0.015	0.075	3.70	94.96	2.75	2.29		4.02
28	5,000	6	33	2.52	0.020	0.077	3.92	93.62	3.87	2.51	8.94	4.22
29	5,000	5.5	33	2.71	0.025	0.083	4.1	93.22	3.98	2.80		3.97
30	7,640	5.5	33	2.67	0.023	0.080	3.75	92.39	4.16	3.46		3.47
31	6,750	6	33	2.67	0.023	0.080	3.80	93.90	3.86	2.24	8.78	3.88
32	5,850	6	33	2.82	0.025	0.085	3.65	92.94	4.30	2.96		-
26[c]	4,400	5	15.6	-	-	0.075	3.63	92.22	5.13	2.65	8.80	5.41
70[d]	2,500	5	12.6	2.56	0.017	0.077	3.85	93.70	-	-	8.82	-
71[e]	2,500	5	12.6	2.56	0.031	0.077	3.80	90.55	5.79	3.65	8.77	-

[a] Followed by 1 hr in air at 475°C.

[b] ThO_2 sol prepared by adding dilute HNO_3; uranyl nitrate solution added to sol.

[c] ThO_2 sol prepared by adding HNO_3; ADU added to sol.

[d] ThO_2 slurry added to uranyl nitrate solution to 3 atom % U. Remainder of U added as ADU.

[e] ThO_2 slurry added to uranyl nitrate solution to 3 atom % U. Remainder of U added as $UO_3 \cdot H_2O$.

Table A.5. Sol Preparation Conditions and Uniformity of Uranium Distribution

ThO_2-H_2O slurry added to dilute uranyl nitrate solution except as noted

Batch No.	Added NO_3/Th Mole Ratio	Added NH_4OH/Th Mole Ratio	Sol pH	Screen Size (U.S. Std)	Percent Deviation of U/Th Atom Ratio from Average: As Calcined, Basis, Avg U/Th in Sol Preparation	As Calcined, Basis, Weighted[a] Avg U/Th in Product	As Crushed and Sized, Basis, Avg U/Th in Sol Preparation	As Crushed and Sized, Basis, Weighted[a] Avg U/Th in Product
8-C[b]	0.170	0.093	3.45	6/16	-	-	-0.67	-2.94
8-C				-200	-	-	+12.1	+9.49
8-D[b]	0.159	0.082	3.42	6/16	-	-	-3.30	-3.30
8-D				-200	-	-	+12.9	+12.9
8-E[b]	0.144	0.066	3.35	6/16	-	-	-1.33	-2.16
8-E				-200	-	-	+9.64	+8.63
9-B	0.090	0.0	2.32	6/16	-	-	-2.71	-4.37
9-D				50/140	-	-	+5.69	+6.58
9-F				-200	-	-	+5.72	+6.56
10-A	0.075	0.0	2.90	+16	6.96	-0.51	-	-
10-A				-35	+22.4	+13.9	-	-
10-A				-200	-	-	+1.02	-
10-B	0.074	0.0	2.90	16	-1.35	-1.12	7.24	+3.06
10-B				16/35	-	-	+0.0	+3.90
10-B				-35	+30.8	+30.5	-1.18	-5.01
10-C	0.078	0.0	2.82	+16	-4.98	-1.22	+4.96	+1.92
10-C				16/35	-	-	+0.47	-2.44
10-C				-35	+32.6	37.9	-0.20	-3.09
12-A[b]	0.095	0.035	3.15	+16	+0.36	-	-	-
12-A				-35	+3.45	-	-	-
12-B[b]	0.09	0.019	3.20	+16	-4.58	-	-	-
12-B				-35	+15.2	-	-	-
14-C	0.070	0.0	3.52	+6	+1.73	-0.85	-	-
14-C				6/35	+4.04	+1.41	-	-
14-C				-35	+7.46	+4.74	-	-
14-F	0.100	0.0	3.12	+6	-6.30	-5.21	-	-
14-F				6/35	+14.4	+15.6	-	-
14-F				-35	+23.6	+25.0	-	-
14-G[b]	0.100	0.013	3.42	-6	+1.66	-1.13	-	-
14-G				6/35	+3.65	+0.80	-	-
14-G				-35	+10.2	+7.13	-	-
14-H[b]	0.100	0.027	4.18	+6	+2.19	-0.04	-0.53	-0.70
14-H				6/35	+2.69	+0.95	+2.02	+1.92
14-H				-35	+4.34	+2.56	+0.63	+0.46
13-A	0.067	0.0	3.28	+16	-0.43	-	-	-
13-A				-35	+14.6	-	-	-
19-4M	0.067	0.0	3.18	+16	-2.65	-1.34	-0.29	-2.27
19-4M				16/35	+9.79	+11.3	+6.54	+4.35
19-4M				-35	+12.2	+13.7	+4.31	+2.76
20-5M	0.067	0.0	3.31	+16	-1.03	-0.81	+0.76	-1.62
20-5M				16/35	+9.59	+7.59	+6.27	+3.76
20-5M				-35	+14.2	+12.1	+4.21	+1.75
21	0.086	0.0	2.90	+16	-7.62	-1.99	-	-
21				16/35	+27.3	+35.1	-	-
21				-35	+27.0	+34.7	-	-
22	0.093	0.0	2.90	+16	-2.65	-1.51	-	-
22				16/35	+26.9	+28.4	-	-
22				-35	+27.4	+28.9	-	-
23	0.070	0.0	3.05	+16	+0.93	-0.52	-0.60	-1.61
23				16/35	+7.30	+5.41	+4.28	+3.22
23				-35	+10.8	+8.90	+2.95	+1.91
24	0.070	0.0	2.97	+16	+0.53	-0.53	-0.80	-2.10
24				16/35	+7.54	+6.41	+5.12	+3.74
24				-35	+12.0	+10.8	+4.02	+2.66

[a] $\sum_{-200}^{+16}$ (U/Th analysis for size x weight fraction of size).

[b] Low sol pH adjusted upward by addition of ammonia and further agitation.

Table A.6. Sol Preparation Conditions and Uniformity of Uranium Distribution

ThO_2-H_2O slurry added to uranyl nitrate solution except as noted

Batch No.	Added NO_3^-/ThO_2 Mole Ratio	Added NH_4OH/ThO_2 Mole Ratio	Sol pH	Percent Deviation of U/Th Atom Ratio from Average: As Calcined — Screen Size (U.S. Std)	As Calcined — Basis, Avg U/Th in Sol Preparation	As Calcined — Basis Weighted[a] Avg U/Th in Product	As Crushed and Sized — Screen Size (U.S. Std)	As Crushed and Sized — Basis, Avg U/Th in Sol Preparation	As Crushed and Sized — Basis, Weighted[a] Avg U/Th in Product
27	0.075	0.015	3.70	+16	+12.97	+0.09	6/16	+1.49	+0.20
27				16/35	+11.77	-0.97	50/100	+1.71	+1.31
27				-35	+5.74	-6.82	-200	-0.92	-1.31
28	0.077	0.017	3.92	+16	+0.54	-0.10	6/16	-1.04	+0.03
28				16/35	+3.65	+2.26	50/100	-1.28	+1.18
28				-35	+1.16	.0.49	-200	-1.04	-0.03
29	0.083	0.026	4.10	+16	+3.88	+0.85	6/16	-1.08	-0.10
29				16/35	-0.65	-4.08	50/100	+1.71	+1.81
29				-35	-2.51	-2.68	-200	-0.92	-0.82
30	0.80	0.023	3.75	+16	+0.63	0.0	-	-	-
30				16/35	+1.72	+1.09	-	-	-
30				-35	+2.02	-1.98	-	-	-
31	0.080	0.023	3.80	+16	+3.28	+0.17	-	-	-
31				16/35	+0.07	-2.03	-	-	-
31				-35	+2.02	-1.09	-	-	-
32	0.085	0.028	3.65	+16	+1.00	-0.07	6/16	-0.40	+0.69
32				16/35	+2.39	+1.37	50/140	+1.09	+0.74
32				-35	+0.30	-0.69	-200	+1.56	+1.26
26[b]	0.075	-	3.63	+16	+2.41	-0.43	6/16	-0.28	-1.45
26				16/35	+5.01	+1.81	50/140	+3.41	+2.19
26				-35	+13.54	+10.4	-200	+3.42	+2.21
70[c]	0.077	0.017	3.85	+16	+0.47	-	6/16	-2.43	-2.03
70				16/35	+4.09	-	50/140	+2.61	+3.02
70				-35	+11.37	-	-200	+2.76	+3.18
71[d]	0.077	0.031	3.80	+16	-0.13	-0.40	6/16	-0.04	-1.19
71				16/35	+3.96	+3.10	50/140	+2.96	+1.78
71				-35	+6.15	+5.27	-200	+2.97	-1.79

[a] $\sum_{-200}^{16}$ (U/Th analysis for size x weight fraction of size).

[b] ThO_2 sol prepared by adding powder to dilute HNO_3; 93% enriched U (6%) added as ADU.

[c] ThO_2-H_2O slurry added to uranyl nitrate solution to 3% U. 4-1/2% U added as ADU.

[d] Same as c, except 4-1/2% U added as $UO_3 \cdot H_2O$.

Table A.7. Summary: Gases Evolved from Sol-Gel Uranium-Thorium Oxide by Heating

Samples heated to 1200°C in vacuum; held at 1200°C until pressure became constant

		Gases Released, std cc/g and percent of total gas released									
		Hydrogen		H_2O		CO + N_2		Oxygen		CO_2	
Oxide	Total	cc/g	Vol %	cc/g	Vol %	cc/g	Vol %	cc/g	Vol %	cc/g	Vol %
D	0.012	0.00316	26.3	0.00077	6.4	0.00633	52.7	Hydrocarbon 0.00011	Hydrocarbon 0.9	0.00163	13.5
E	0.027	0.00869	31.8	0.00066	2.4	0.01244	45.5	0	0	0.00551	20.1
32C[a]	0.033	0	0	0.000364	1.1	0.00102	3.1	0.0251	76.3	0.00638	19.3
32F	0.067	0	0	0.00067	1.0	0.00261	3.9	0.0403	60.0	0.0224	33.4
70C	0.044	0	0	0.00051	1.16	0.00113	2.57	0.0412	93.5	0.00107	2.44
70M	0.047	0	0	0.000564	1.2	0.00111	2.37	0.0424	90.2	0.00281	6.0
70F	0.039	0	0	0.000612	1.57	0.00267	6.84	0.0190	48.7	0.0166	42.6
101F	0.160	0	0	0.00134	0.83	0.00472	2.95	0.111	69.5	0.0428	26.8
28Cg	0.017	0.000017	0.1	0.000273	1.60	0.00041	2.4	0.01370	80.6	0.00267	15.7
28Mg	0.041	0.00041	1.0	0.00620	15.3	0.0007	1.7	0.00016	0.39	0.0336	81.8
70Cg	0.094	0	0	0.00106	1.3	0.00243	2.60	0.0882	93.7	0.0021	2.2
70Mg	0.091	0	0	0.00104	1.14	0.00708	8.55	0.0216	23.7	0.0609	67.0
70Fg	0.220	0	0	0.02737	12.4	0.01830	8.34	0.00024	0.11	0.1731	78.7
71Cg	0.061	0	0	0.00103	1.7	0.00196	3.2	0.05732	94.0	0.00064	1.1
27Cg	0.003	0.000072	2.4	0.00082	27.0	0.00039	13.0	0	0	0.00162	54.1
27Mg	0.057	0.00188	3.3	0.00188	3.3	0.0156	27.4	0	0	0.0375	65.7
27Fg	0.210	0.0303	13.3	0.00168	0.8	0.0643	30.7	0	0	0.1134	54.0
30Fg	0.320	0.0941	29.4	0.0170	5.3	0.113	37.0	0	0	0.0917	28.6
26Cg	0.012	-	-	-	-	-	-	-	-	-	-
26Mg	0.062	-	-	-	-	-	-	-	-	-	-
26Fg	0.206[c]	0.100[c]	48.5[c]	0.003	1.5[c]	0.083[c]	40.2[c]	0.001[c]	0.49[c]	0.011[c]	5.3[c]
Ag	0.125	0.05023	40.3	0.01863	14.9	0.03169	25.4	Hydrocarbon 0.00250	Hydrocarbon 2.0	0.02171	17.4
Bg	0.151	0.05550	36.0	0.02709	17.5	0.03772	24.4	Hydrocarbon 0.00334	Hydrocarbon 2.1	0.03029	19.6
Cg	0.055	0.0188	34.2	0.00324	5.9	0.03110	56.6	-	-	0.00149	2.7
29Cg	0.021	0	0	0.00031	1.5	0.00061	2.9	Oxygen 0.01740	82.7	0.00270	12.9
71C	0.023	0	0	0.00029	1.23	0.00073	3.15	0.01950	84.7	0.00245	10.7
71M	0.033	0	0	0.00030	0.91	0.00091	2.76	0.02720	82.4	0.00453	13.7
71Mg	0.091	0	0	0.00104	0.86	0.00703	8.04	0.02160	27.9	0.06090	63.2
31Cg	0.019	0	0	0.00030	1.6	0.00063	3.3	0.01510	79.5	0.00300	15.5
31Fg	0.246	0	0	0.00394	1.6	0.07060	28.7	0.00037	0.2	0.16160	65.7

[a]Caps after numbers: C = coarse fraction, 90 wt %; M = medium fraction, 6 wt %; F = fine fraction, 4 wt %; all as fired; Cg = coarse sized fraction, 60 wt %; Mg = medium, 15 wt %; Fg = fine, sized, 25 wt %.

[b]BET (N_2) measurement. All others estimated from particle size.

[c]Data collected on blended sample containing all sizes.

Table A.7. (Continued)

Oxide	U (wt %)	O/U Atom Ratio	Surface Area (m^2/g)	1150°C Firing Conditions: Calcining Blanket Gas	1150°C Firing Conditions: Cooling Blanket Gas	Total Carbon Content (Analysis) (ppm)	Log Mean Particle Size (microns)	U.S. Sieve Size Range, Mesh
D	2.43	2.01	0.008[b]	100% H_2	Argon	40	-	-10, +100
E	4.21	2.02	0.015[b]	100% H_2	Argon	130	-	-10, +100
32C[a]	3.0	-	0.002	100% argon	Nitrogen	-	2100	-6, +16
32F	3.0	-	0.014	100% argon	Nitrogen	-	290	-35, +100
70C	6.62	2.29	0.002	100% nitrogen	Nitrogen	-	2100	-6, +16
70M	6.85	2.325	0.005	100% nitrogen	Nitrogen	-	795	-16, +35
70F	7.29	2.360	0.014	100% nitrogen	Nitrogen	-	290	-35, +100
101F	9.77	2.429	0.014	100% argon	Argon	-	290	-35, +100
28Cg	3.0	-	0.002[b]	100% nitrogen	Nitrogen	-	2100	-6, +16
28Mg	3.0	-	0.010[b]	100% nitrogen	Nitrogen	-	185	-50, +140
70Cg	6.62	2.266	0.002	100% nitrogen	Nitrogen	-	2100	-6, +16
70Mg	6.85	2.319	0.022	100% nitrogen	Nitrogen	-	185	-50, +140
70Fg	7.29	2.360	0.077	100% nitrogen	Nitrogen	-	54	-200, +325
71Cg	6.60	2.244	0.002	100% nitrogen	Nitrogen	-	2100	-6, +16
27Cg		-	0.002	4% H_2-argon	Argon	-	2100	-6, +16
27Mg		-	0.022	4% H_2-argon	Argon	-	185	-50, +140
27Fg		-	0.077	4% H_2-argon	Argon	-	54	-200, +325
30Fg		-	0.077	4% H_2-argon	Argon	-	54	-200, +325
26Cg	5.50	2.026	0.015[b]	4% H_2-argon	Argon	-	2100	-6, +16
26Mg	5.62	2.027	0.065[b]	4% H_2-argon	Argon	-	185	-50, +140
26Fg	6.65[c]	2.025[c]	0.047[b]	4% H_2-argon	Argon	-	54	-200, +325
Ag	4.31	2.005	0.20[b]	100% hydrogen	Argon	110	-	-10, +325
Bg	4.39	2.005	0.26[b]	100% hydrogen	Argon	100	-	-10, +325
Cg	4.01	2.035	0.03[b]	100% hydrogen	Argon	60	-	-10, +16
29Cg		-	0.002	100% argon	Argon	-	-	-6, +16
71C	6.60	2.244	0.002	100% nitrogen	Nitrogen	-	-	-6, +16
71M	6.64	2.285	0.005	100% nitrogen	Nitrogen	-	-	-16, +35
71Mg	6.64	2.319	0.022	100% nitrogen	Nitrogen	-	-	-50, +140
31Cg		-	0.002	100% argon	Nitrogen	-	2100	-6, +16
31Fg		-	0.077	100% argon	Nitrogen	-	54	-200, +325

[a]Caps after numbers: C = coarse fraction, 90 wt %; M = medium fraction, 6 wt %; F = fine fraction, 4 wt %; all as fired; Cg = coarse sized fraction, 60 wt %; Mg = medium, 15 wt %; Fg = fine, sized, ≥5 wt %.

[b]BET (N_2) measurement. All others estimated from particle size.

[c]Data collected on blended sample containing all sizes.

Table A.7. (Continued)

Oxide	Adsorbed CO_2 cc/g	Adsorbed CO_2 Vol % of Total $CO + CO_2$ Evolved	Carbon from Bulk of Oxide in Evolved Gases (ppm)	Evolved $\frac{CO}{CO + CO_2}$	Excess Oxygen Evolved, Fraction of Available Excess	Evolved $\frac{CO + CO_2}{\text{Surface Area}}$ (cc/m^2)	Volume Ratio, $\frac{\text{Oxidizing Gases}}{\text{Total Gas}}$	Volume Ratio, $\frac{\text{Reducing Gases}}{\text{Total Gas}}$	Excess Oxygen Above UO_2 in $UO_2 + x$ (cc/g)
D	0.001085	13.6	3.68	0.795	0	1.00	0.135	0.865	0
E	0.00204	11.4	8.54	0.692	0	1.20	0.201	0.799	0
32C[a]	0.000272	2.87	3.8	0.109	-	3.70	0.956	0.044	-
32F	0.0019	7.6	12.4	0.104	-	1.79	0.934	0.066	-
70C	0.000272	22.7	1.04	0.512	0.0456	1.10	0.959	0.041	0.9034
70M	0.00068	17.3	1.74	0.283	0.0406	0.79	0.962	0.038	1.044
70F	0.0019	9.9	9.3	0.139	0.0153	1.38	0.913	0.087	1.235
101F	0.0019	4.0	24.3	0.099	0.0562	3.41	0.963	0.037	1.972
28Cg	0.000272	8.8	15.0	0.132	-	1.54	0.963	0.037	-
28Mg	0.003	8.8	16.7	0.02	-	1.81	0.822	0.178	-
70Cg	0.000272	6.0	2.3	0.535	0.106	2.26	0.959	0.041	0.830
70Mg	0.003	4.43	34.7	0.104	0.021	2.80	0.907	0.093	1.03
70Fg	0.0105	5.47	100	0.0956	0.00019	2.48	0.788	0.212	1.24
71Cg	0.00027	10.4	1.25	0.755	0.077	1.30	0.951	0.049	0.758
27Cg	0.00027	13.4	0.93	0.193	-	1.01	0.541	0.459	-
27Mg	0.003	5.65	26.9	0.363	-	2.42	0.657	0.343	-
27Fg	0.0105	5.91	89.4	0.362	-	2.31	0.540	0.460	-
30Fg	0.0105	7.8	106.7	0.563	-	2.72	0.286	0.714	-
26Cg	-	-	-	-	-	-	-	-	0.0683
26Mg	-	-	-	-	-	-	-	-	0.0724
26Fg	0.0064	6.8	50.4	0.882	0.0075	2.00	0.073	0.889	0.0547
Ag	0.02720	51.0	14.0	0.593	0	2.66	0.174	0.826	0.0103
Bg	0.03540	61.0	17.5	0.554	0	2.62	0.196	0.804	0.0105
Cg	0.00408	12.5	15.3	0.956	0	1.08	0.027	0.973	0.0300
29Cg	0.00027	8.1	1.6	0.225	-	1.65	0.956	0.044	-
71C	0.00027	8.5	1.6	0.220	0.026	1.59	0.954	0.046	0.758
71M	0.00027	5.0	2.8	0.167	0.0303	1.08	0.961	0.039	0.893
71Mg	0.003	4.4	34.7	0.104	0.0216	3.09	0.911	0.889	1.00
31Cg	0.00027	7.4	1.8	0.174	-	1.82	0.950	0.050	-
31Fg	0.0105	4.5	118.3	0.304	-	3.01	0.659	0.341	-

[a]Caps after numbers: C = coarse fraction, 90 wt %; M = medium fraction, 6 wt %; F = fine fraction, 4 wt %; all as fired; Cg = coarse sized fraction, 60 wt %; Mg = medium, 15 wt %; Fg = fine, sized, 25 wt %.

Table A.3. Total Gases Evolved from Large Batches of Calcined Sol-Gel Products

Batch size: 2-7 kg

Composition: 3 at. % U-ThO_2

Firing procedure: air, 300°/hr to 1150°C, at 1150°C, 1 hr; argon--4% H_2, 4 hr at 1150°C; cooled in argon to <100°C (except as noted)

Batch No.	Total Gases Released at 1200°C in Vacuum, st cc/g							
	After Calcination				After Grinding to Size			
	Unscreened	+16 Mesh	16/35 Mesh	-35 Mesh	6/16 Mesh	50/140 Mesh	-200 Mesh	Composite[a]
10A	-	0.024	-	0.130	-	-	-	-
14H	-	-	-	-	0.006	0.044	0.150	0.048
17A	0.005	-	-	-	-	-	-	-
17F	0.004	-	-	-	-	-	-	-
18A	0.160	-	-	-	-	-	-	-
19	0.005	-	-	-	0.005	0.160	0.190	0.075
20	0.003	-	-	-	0.007	0.081	0.270	0.084
21	0.002	-	-	-	-	-	-	-
22	0.02	-	-	-	-	-	-	-
23	0.009	-	-	-	0.014	0.055	0.190	0.066
24	0.065	-	-	-	0.006	0.054	0.170	0.054
25A[b]	0.034	-	-	-	-	-	-	-
25N[c]	0.074	-	-	-	-	-	-	-
26	-	0.004	0.004	0.067	0.012	0.062	0.170	0.059
27	-	0.003	0.006	0.088	0.003	0.057	0.210	0.063
28N[c]	-	0.013	0.055	0.120	0.017	0.044	0.320	0.096
29A[b]	-	0.015	0.040	0.130	0.021	0.057	0.210	0.074
30	-	0.009	0.012	0.049	-	-	-	-
31AN[d]	-	0.030	0.047	0.050	-	-	-	-

[a]Composite, calculated with 60 wt % 6/16, 15 wt % 50/140, and 25% of -200 mesh.

[b]Firing procedure: reduced with argon, no H_2, 1150°C, 4 hr; cooled under argon to < 100°C.

[c]Firing procedure: reduced with nitrogen, no H_2, 1150°C, 4 hr; cooled under nitrogen to <100°C.

[d]Firing procedure: reduced with argon, no H_2, 1150°C, 4 hr; cooled under nitrogen to <100°C.

Table A.9. Gases Evolved from Sol-Gel Uranium-Thorium Oxides at Various Temperatures

Calcined in air, then H_2 at 1150°C; cooled in argon

Samples heated in vacuum, gases collected, measured, analyzed by mass spectrography

Properties	A	B	C	D	E	26[b]
Surface area (BET, N_2), m^2/g	0.20	0.26	0.03	0.006	0.015	0.047
O/U ratio	2.005	2.005	2.035	2.035	2.010	2.025
Total gases released, cc/g[a]	0.125	0.151	0.055	0.012	0.027	0.206
	Gases Released at 25-300°C, std cc/g			Gases Released at 25-750°C, std cc/g		
Total	0.022	0.026	-	0.0050	0.0210	0.1400
Hydrogen	0.00042	0.00083	0.0180[a]	0.00044	0.00585	0.0750
Hydrocarbons	-	-	-	0.00011	-	0.0039
Water	0.01100	0.01500	0.00324[a]	0.00057	0.00051	0.0014
N_2 + CO	0.00130	0.00066	0.0311[a]	0.00255	0.00956	0.0511
CO_2 + N_2O	0.00900	0.00950	0.00149[a]	0.00133	0.00516	0.0081
	Gases Released at 300-500°C, std cc/g			Gases Released at 750-1000°C, std cc/g		
Total	0.032	0.039	-	0.0050	0.004	0.0500
Hydrogen	0.00538	0.00522	-	0.00151	0.00172	0.0200
Hydrocarbons	0.00173	0.00187	-	-	-	-
Water	0.00622	0.00362	-	0.00014	0.00014	0.0007
N_2 + CO	0.00749	0.00758	-	0.00309	0.00187	0.0271
CO_2 + N_2O	0.0112	0.0153	-	0.00026	0.000256	0.0020
	Gases Released at 500-750°C, std cc/g			Gases Released at 1000-1200°C, std cc/g		
Total	0.050	0.066	-	0.002	0.002	0.0160
Hydrogen	0.0361	0.0357	-	0.00121	0.00112	0.0050
Hydrocarbons	0.00075	0.00145	-	-	-	-
Water	0.0012	0.00225	-	0.00006	0.000011	0.0004
N_2 + CO	0.0105	0.0220	-	0.0007	0.0007	0.0048
N_2O + CO_2	0.00145	0.00491	-	0.00004	0.0001	0.0009
	Gases Released at 750-1010°C, std cc/g					
Total	0.021	0.020	-			
Hydrogen	0.00833	0.0137	-			
Hydrocarbons	0.00002	0.00002	-			
Water	0.00021	0.00056	-			
N_2 + CO	0.0124	0.00748	-			
N_2O + CO_2	0.00006	0.00058	-			

[a]Gas released when heated 25-1200°C.

[b]Calcined in 4% H_2-argon; cooled in argon.

Table A.10. Effects of Particle Size, Calcination Atmosphere, and Grinding in Air on Amounts and Species of Gases Evolved from Sol-Gel Oxides on Heating to 1200°C in Vacuum

Oxide No.[a]	Particle Size, U.S. Mesh	Calcination Furnace Atmosphere: Calcination	Calcination Furnace Atmosphere: Cooling	O/U Atomic Ratio	Surface Area[b] (m^2/g)	CO_2[c] Adsorbed (μmoles/g)	Gases Evolved on Heating to 1200°C, in Vacuum (μmoles/g): Total	H_2	H_2O	CO . N_2	CO_2	O_2
32C	6/16	Argon	N_2	-	0.002	0.0121	1.47	0	0.016	0.046	0.284	1.128
31C-g	6/16	Argon	N_2	-	0.002	0.0121	0.85	0	0.014	0.028	0.132	0.677
32F	-35	Argon	N_2	-	0.014	0.085	2.98	0	0.030	0.117	1.125	1.790
31F-g	-200	Argon	N_2	-	0.077	0.47	11.00	0	0.176	3.150	7.220	0.022
70C	6/16	N_2	N_2	2.290	0.002	0.0121	1.96	0	0.024	0.051	0.047	1.835
70Cg	6/16	N_2	N_2	2.266	0.002	0.0121	4.20	0	0.055	0.109	0.093	3.940
70M	16/35	N_2	N_2	2.325	0.005	0.0304	2.10	0	0.025	0.051	0.126	1.900
70M-g	50/140	N_2	N_2	2.319	0.022	0.134	4.06	0	0.045	0.350	2.720	0.965
70F	-35	N_2	N_2	2.360	0.014	0.085	1.74	0	0.028	0.118	0.740	0.848
70F-g	-200	N_2	N_2	2.307	0.077	0.47	9.83	0	1.220	0.815	7.680	0.010
E	6/100	H_2	Argon	2.02	0.015	0.091	1.20	0.383	0.029	0.548	0.210	0.0
A-g	+10 to 325	H_2	Argon	2.01	0.20	1.21	5.58	2.255	0.833	1.420	0.974	0.0
26[d]	-6 to -200	4% H_2-A	Argon	2.025	0.047	0.285	9.20	4.46	0.134	3.700	0.492	0.045
27C-g	6/16	4% H_2-A	Argon	-	0.002	0.012	0.134	0.003	0.037	0.017	0.072	0.0
27F-g	-200	4% H_2-A	Argon	-	0.077	0.47	9.38	1.352	0.075	2.87	5.070	0.0

[a] Letters after oxide numbers refer to coarse, medium, and fine fractions; subscript g indicates "ground."

[b] Numbers with asterisks are estimated surface areas from measured areas of similar preparations.

[c] Based on surface areas and M. E. Wadsworth's work on adsorption of CO_2 on thoria.[7]

[d] Sample composite of sizes, all ground.

[7] C. H. Pitt and M. E. Wadsworth, "Carbon Dioxide Adsorption on Thoria," Technical Report No. 1, p. 1, Univ. of Utah (1958).

4.0 FABRICATION AND MATERIAL DEVELOPMENT

(D. A. Douglas)

Work in the Metals and Ceramics Division can be broadly separated into three categories. One area (Sections 4.1, 4.2, and 4.3) involves the development of equipment and process schemes for the remote fabrication of fuel elements containing thorium. Much of this work in the past year has been directed toward solving specific problems involved in the production of fueled rods for the Brookhaven National Laboratory criticality experiments. A second area (Section 4.4) is the study of the irradiation characteristics of thorium-base fuels produced through chemical extraction and separation of fissionable and fertile material from irradiated fuels. Experiments to characterize mixed oxides of thorium and uranium processed by the sol-gel technique have been conducted in the Materials Testing Reactor, MTR, Chalk River Reactor, NRX, and Oak Ridge Research Reactor, ORR, test reactors. The third area (Section 4.5) concerns the development of advanced thorium-base fuels both ceramic and metallic in nature. Work on the development of thoria pellets suitable for fluidized blanket systems was brought to a conclusion. Research to improve the irradiation resistance of thorium metal is continuing.

4.1 Kilorod Program (J. D. Sease, A. L. Lotts)

To extend thorium fuel cycle technology, a facility which provides space and equipment for performing the chemical processing and fabrication operations involving U^{233} and thorium was designed and constructed. Process equipment was constructed, and it is now being installed. Although this facility, known as the Kilorod Facility, has sufficient flexibility to accommodate a variety of work, it was specifically designed for making fuel rods that are to be used in criticality, zero power experiments at Brookhaven National Laboratory, BNL.

The design of the BNL fuel rod is shown in Fig. 4.1. Each of the Zircaloy-2 tubes contains 890 g of oxide (3 wt % U^{233}–97 wt % Th). The U^{233} to be used contains nominally 40 ppm U^{232}. The cone-shaped bottom

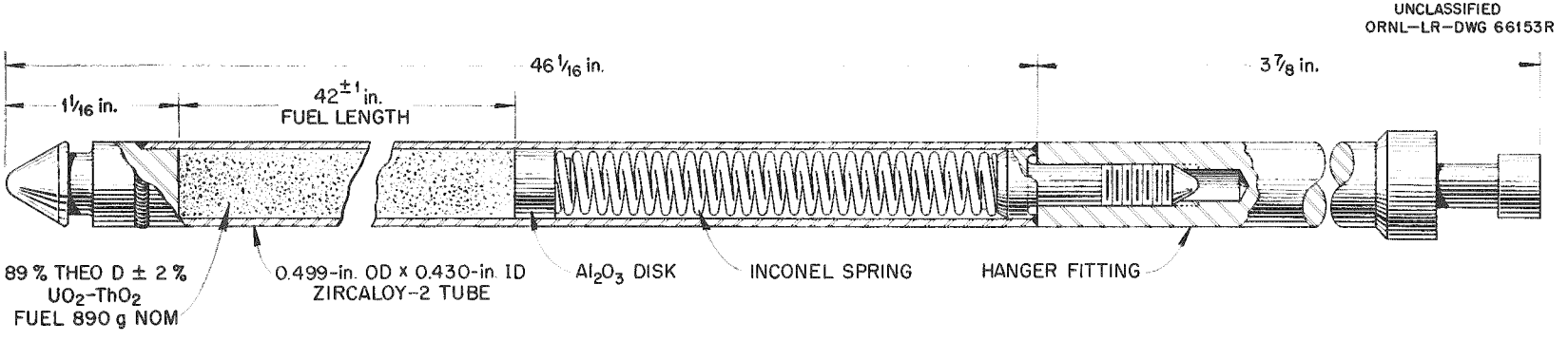

Fig. 4.1. Design Features of the BNL Fuel Rod.

fitting serves to locate the rods in the critical lattice, and the top end fitting supports the rods in the lattice and provides a lifting lug by which the rods may be handled. The compression spring and ceramic spacer, shown in the void volume at the top of the fuel column, prevents fuel redistribution if the rods are inverted in handling. In addition to these 46-in.-long rods, 18-in.-long fuel rods, otherwise identical in design, will be fabricated. In all, some 900 rods, each containing 890 g of oxide and about 200 rods containing 310 g of oxide will be manufactured.

The Kilorod Program encompasses the solvent extraction purification of U^{232} decay products from U^{233}, production of bulk oxide by the sol-gel process, and the fabrication of rods using the bulk oxide. This section describes the rod fabrication portion of the Kilorod Program and is divided into three parts: a discussion of the process, the facility, and the fabrication process equipment. Information pertaining to the sol-gel and solvent extraction portions of the Kilorod Program may be reviewed in another section.

4.1.1 The Process

The procedures employed to fabricate the BNL fuel rods include: (1) sizing the UO_2-ThO_2 received from the solids preparation facility into an optimum particle-size distribution for vibratory compaction; (2) vibratory compaction; (3) welding of the final end closure; (4) fuel rod decontamination; and (5) fuel rod inspection.

The optimum-size distribution for UO_2-ThO_2 produced by the sol-gel process consists of a mixture of three size fractions: a coarse fraction, a fine fraction, and an intermediate fraction. As seen in the flow diagram (Fig. 4.2), these fractions are produced from the as-received oxide by a system of crushing, classifying, and ball milling. Following comminution and classification of the bulk fuel into the three working fractions, quantities of each fraction appropriate to one fuel rod loading will be apportioned and blended together.

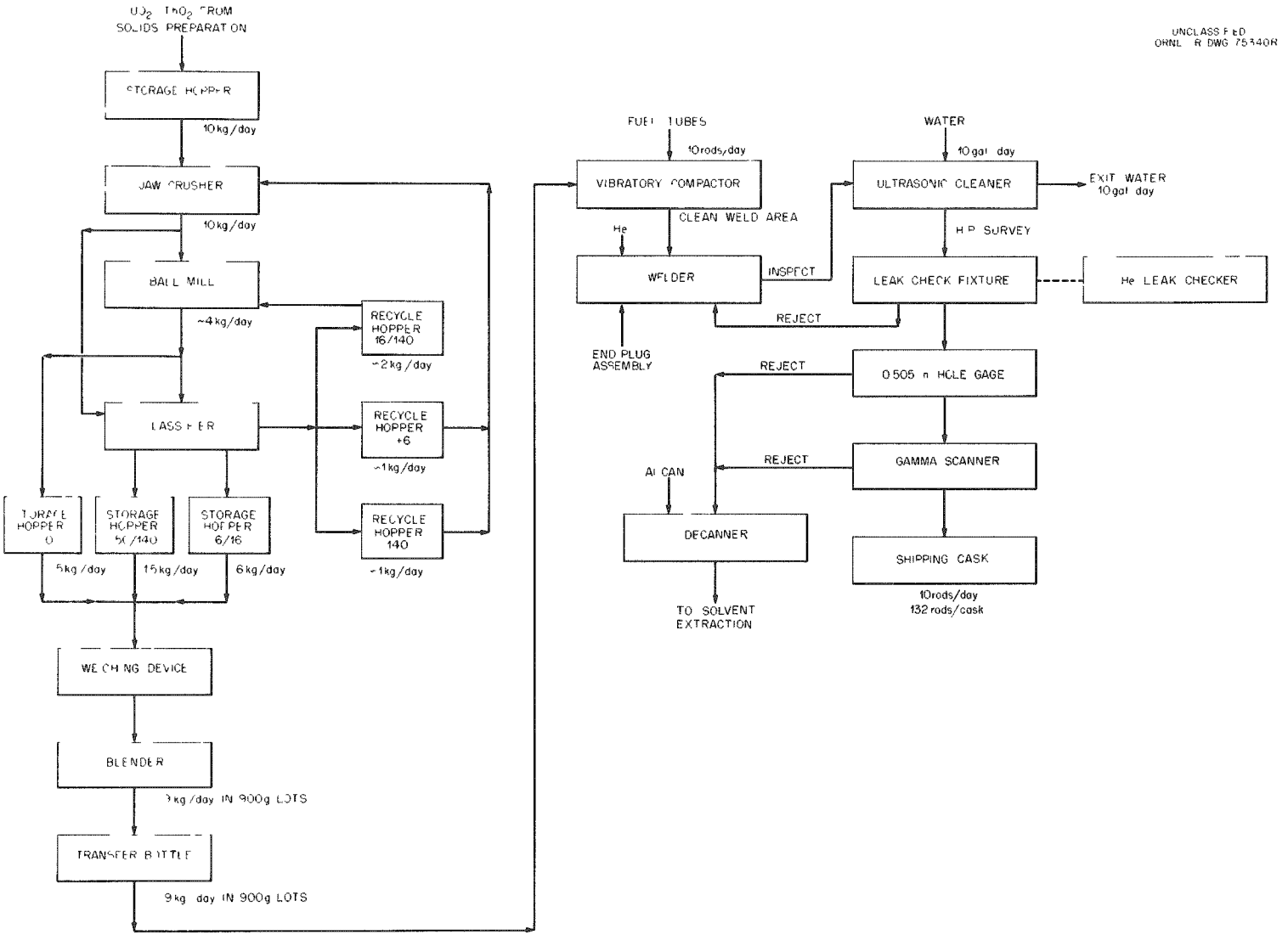

Fig. 4.2. Rod Fabrication Process Flow Diagram.

In the vibratory-compaction operation, the blended aliquot of fuel is loaded into a fuel tube, which contains one end plug, and vibrated to the specified density. This loaded fuel tube is transferred to a welding fixture where the final end-closure weld is made and visually inspected.

At this juncture, the loaded and sealed fuel rod is decontaminated by ultrasonic cleaning in water and smeared to check the level of surface contamination. The integrity of the end-closure weld is evaluated by helium leak checking, and the density of the fuel is determined with a gamma-absorption scanning device. Finally, the hanger fitting is attached prior to loading into a shipping cask.

4.1.2 Facility

The oxide preparation and rod fabrication steps will be accomplished in shielded, alpha-tight cubicles which are shown in Fig. 4.3. The cubicles were designed around the process and are installed in a 20-ft-long x 19-ft-wide x 27-ft-high chemical processing cell which is being used for secondary containment of radioactivity which might escape from the cubicle.

The cubicles for performing the rod fabrication occupy the first and second levels of this cell. Located on one corner of the first level and extending to the top of the second level is the 4- x 7-ft powder preparation shaft. Directly adjacent to this shaft on the first level are three fabrication cubicles that extend along two walls. The first of these cubicles is used for vibratory compaction and welding, the second for decontamination, and the third for inspection. A glove repair box is located on the second level adjacent to the powder preparation shaft and directly above the vibratory-compaction welding cubicle and the decontamination cubicle. The box is equipped with a large bag-out port air lock and a monorail crane that will run the length of the glove box and will be used to lift and convey equipment. Access to the powder preparation shaft is through a door in the rear of the shaft, while access to the fabrication cubicles will be through shield-access ports in the floor of the box.

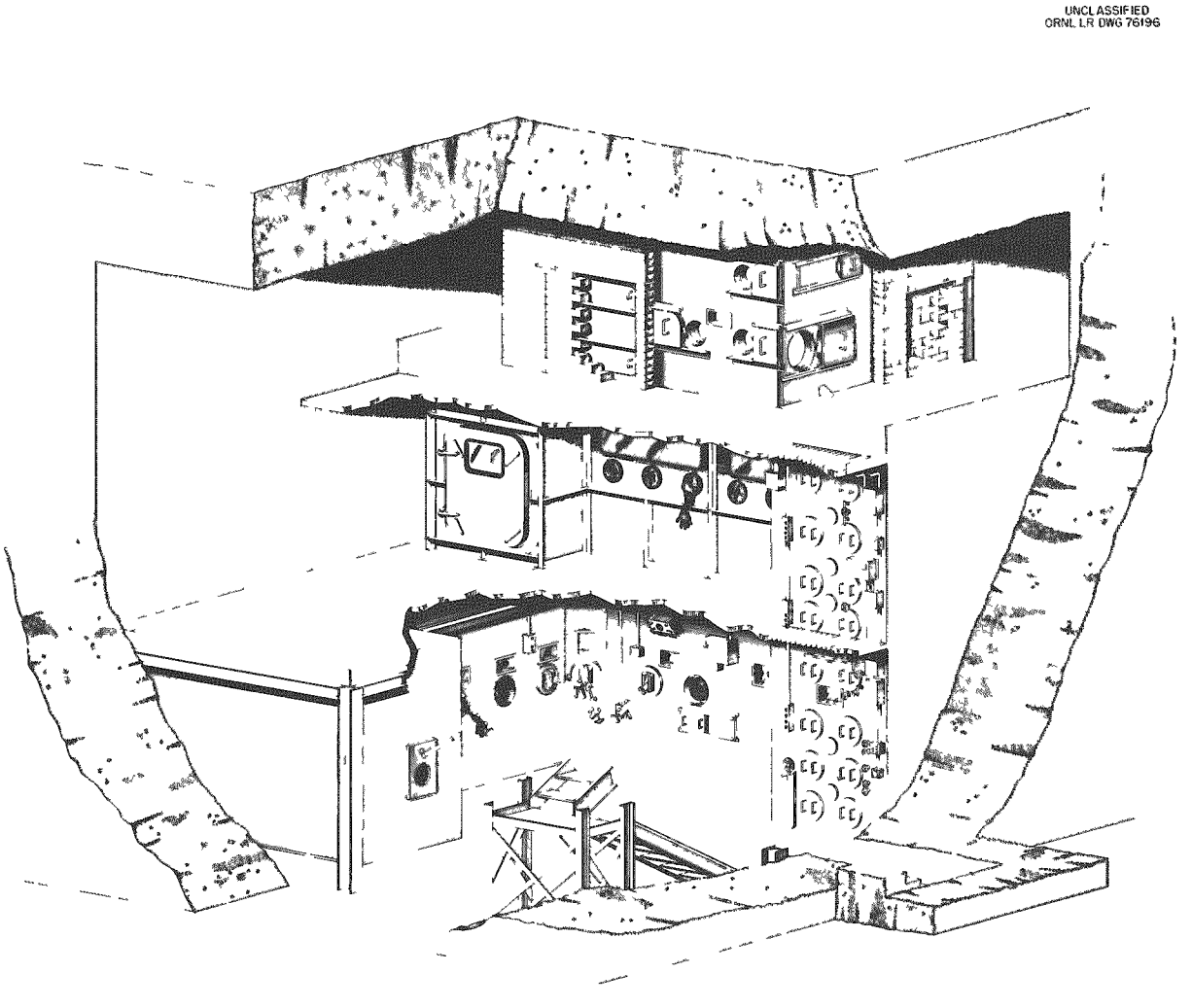

Fig. 4.3. Kilorod Solids Preparation and Rod Fabrication Facility.

Primary alpha containment for the cubicles is provided by an 11-gage mild-steel liner. Gamma shielding is provided by 4 1/4-in.-thick armor plate placed on the top and operating face of the cubicles. The facility was designed to be constructed as an integral unit structurally independent of the cell proper. Attachment to the chemical processing cell and penetration of the cell wall were held to an absolute minimum due to the health physics problem associated with spreading contamination that is residually contained in the walls.

The facility ventilation system is designed so that cubicles will be maintained at pressures below atmospheric, through the use of existing ventilation systems in the vicinity of the cell. The cell will be maintained at -0.3-in. water gage with respect to ambient, and the cubicles will be maintained at -0.3-in. water gage with respect to the cell. All air entering or leaving the cell and cubicles will be filtered with high efficiency filters. Cubicle and cell pressures are controlled by manually operated dampers and safeguarded with backflow preventers and differential pressure alarms and indicators.

The fabrication cubicles have a total of twenty windows. Thirty-one ports are provided which will allow outfitting with either gloves or manipulator tongs and allow interchange of gloves and tongs without loss of containment of radioactive material. Plans are to operate the rod fabrication process with nine tongs and two glove ports. The remaining twenty will be used for maintenance.

4.1.3 Equipment

As with any new type of equipment, the rod fabrication equipment, as built, was not in a sufficient stage of development to be installed directly into the cell facility. It was necessary, therefore, to test and evaluate the pieces of equipment under simulated conditions. The powder preparation equipment, due to its complexity, was tested in a mockup using (Th–3 wt % U^{238})O_2 produced by the sol-gel process. The other pieces of equipment were evaluated under similar test conditions, but without the use of the oxide. A number of flaws in the equipment were

obviated by the mockup experiments. These were corrected, and the discussion on equipment which follows is for the equipment as revised from the mockup experience.

The powder preparation equipment was designed to afford maximum dust confinement and to utilize gravity feed for transporting the fuel through pipes from one equipment unit to the next. All of the equipment in the powder preparation shaft (shown in Fig. 4.4) is remotely controlled either electrically or by flexible shafts. Minor repairs to the equipment can be made in place through glove access ports. For major repairs, the equipment is mounted on movable racks in the front half of the shaft, and the offending piece of equipment can be removed by pushing the equipment rack to the rear and lifting the piece with a hoist to the glove maintenance area.

Located on the top rack of the shaft is the jaw crusher and ball mill. Directly above the jaw crusher is a feeder valve which is used to control the rate of feed to the jaw crusher. The classifier, located directly below the jaw crusher and ball mill, continuously classifies the feed material into dispensing hoppers. The rate of feed to the classifier is controlled either by the feeder valve controlling the feed to the jaw crusher or by another feeder valve controlling the feed rate from the ball mill. Six transparent glass storage hoppers, three for the working fractions and three for the recycle fractions, are located around the base of the classifier. The three recycle hoppers are connected directly to a recycle manifold. The recycle manifold empties into a recycle hopper which is used to convey material to the jaw crusher or the ball mill for recycling.

Directly below the classifier is a remote weigher where exact quantities of each of the working fractions are weighed out. As each fraction is weighed, it is dumped directly into the blender located below the weigher.

Each major piece of equipment in the powder preparation shaft is discussed in the paragraphs that follow.

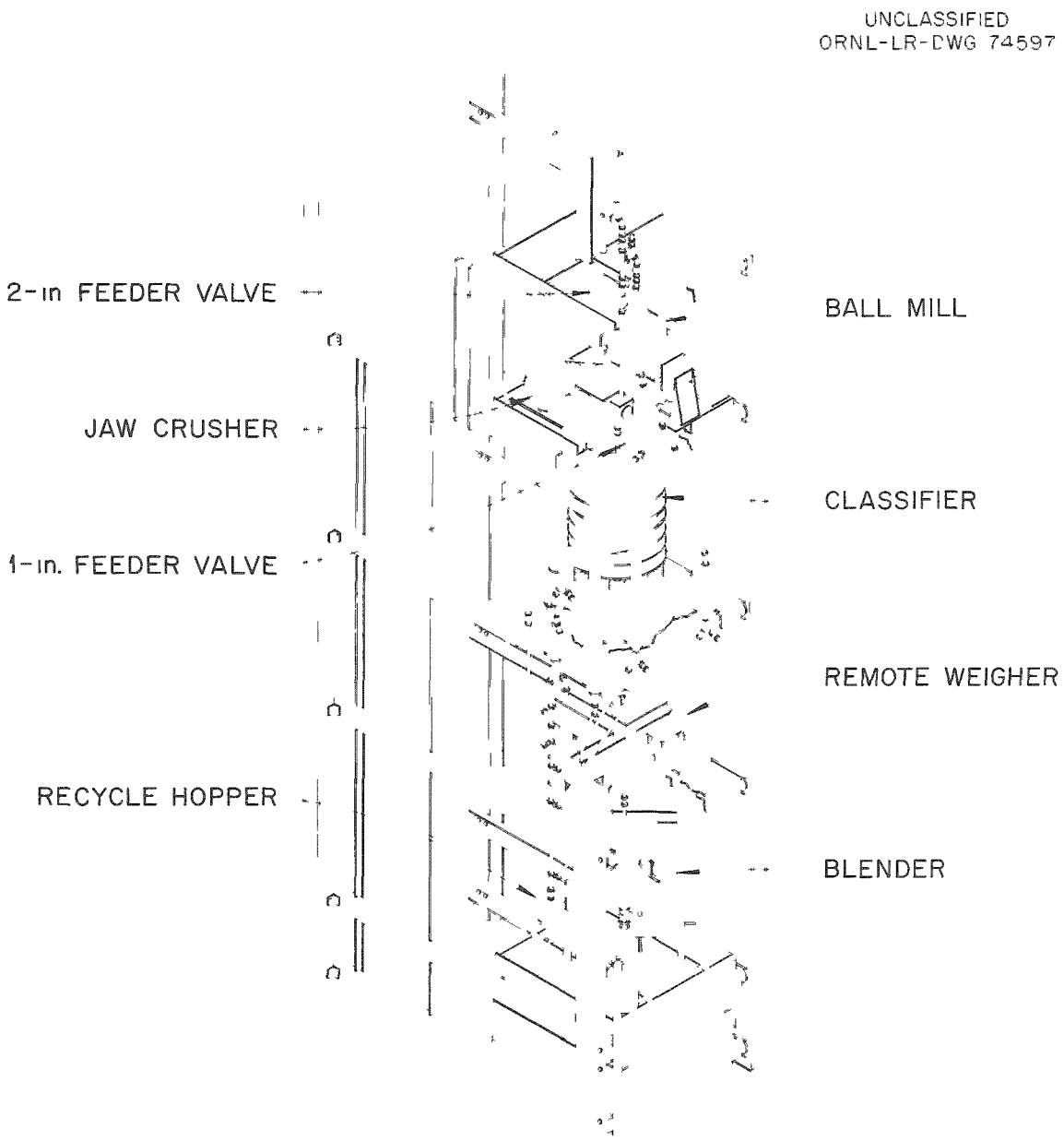

Fig. 4.4. Powder Preparation Shaft.

Jaw Crusher. Sufficient crushing capacities and yields are obtained by employing a standard laboratory-size jaw crusher. The crusher was modified to allow continuous feeding and discharging and to effect maximum dust confinement. The major limitation to the jaw crushers use in the remote facility is its tendency to jam under an excessive feed rate; however, by closely controlling the feed rate, this drawback appears to be eliminated.

Ball Mill. A ball mill was necessary for sizing the fine and intermediate fractions for vibratory compaction. The mill, however, had to be capable of performing the tasks of being filled, grinding, and being discharged while maintaining a seal from the cubicle atmosphere. The mill used in the facility incorporates a standard alumina grinding jar and a single roll mill in a device that allows the grinding jar to be rotated on two separate axes simultaneously. In the mill, the large outer ring acts as a valve seat while the grinding jar opening is employed as the valve stem.

Classifier. An 18-in., five-deck, vibra-energy separator is employed for classifying the crushed and ground material into its different size fractions. The classifier used in the facility is essentially a commercial unit that has been modified to minimize dust and material holdup. The major limitation to the use of a classifier in the remote facility is the tendency of screens to blind; however, this problem is prevalent with any screen classification system. During trial runs, the blinding of the screens did not appear to be of any consequence.

Recycle Hopper. In order to lift material for recycling to the jaw crusher or ball mill, the recycle hopper was designed. The apparatus consists of a hopper that is mounted on a vertical track that runs the height of the cubicle and a cam mechanism for swinging the hopper into and out of position.

Weigher. The remote weigher consists of one scale and three individually controlled feeders containing the three size fractions. The weigher uses a one-to-one ratio scale with an "over-under" weight type indicator, precision cut-off controls, and an impact-free dumping mechanism. The feeders are electrically linked to weights that correspond to the desired weight distribution of the three fractions. The feeders and scale pan are contained in a Plexiglas cover to reduce dust spread.

Blender. The blender is a 4-qt, twin-shell type that employs a cam actuated seating mechanism for connecting and disconnecting the blender from the powder lines while maintaining a dust-tight seal. After blending, the powder is emptied into a bottle for transfer to the vibratory-compaction apparatus.

4.1.4 Vibratory-Compaction Apparatus

The uniformity with which a fuel tube is loaded and the rigidity with which the tube is held during vibration are the two important considerations in the design of a vibratory-compaction rig. The vibratory-compaction apparatus (shown in Fig. 4.5) consists of two main components, the tube-filling assembly and the chuck assembly. The tube-filling assembly is located in the powder preparation shaft at the upper right corner of the vibratory-compaction welder cubicle, but is separated from it by a nylon iris valve. The fuel tube is inserted through the iris and into the filler mechanism.

The tube-filling assembly consists of a hopper into which blended fuel is received and a "Syntron" vibratory feeder which enables close control of the fuel feeding. Also included in this assembly is a funnel for directing the fuel into the tube without spread of dust, and a mechanism for applying a static load to the fuel column during vibration. The static load mechanism consists of a rack gear connected directly to a load and disengageable pinion gear that enables the lowering of the static load onto the fuel column. The rack gear also serves as a direct means of measuring the height of the fuel column in the tube.

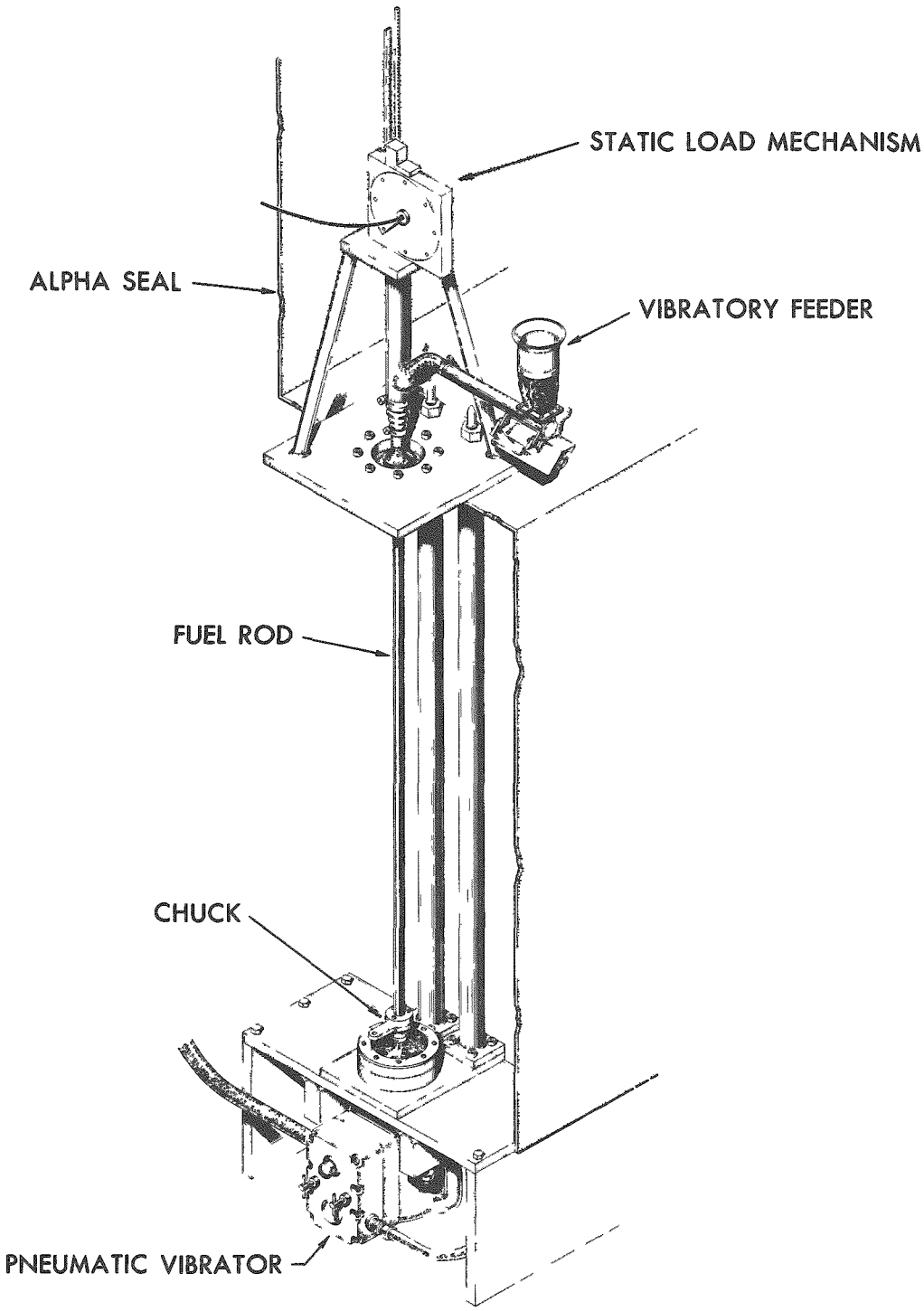

Fig. 4.5. Vibratory Compaction Assembly.

The vibratory-chuck assembly consists of an anvil, to which the chuck is attached and through which the vibrational energy is transmitted, and a Branford Variable Impact Vibrator. The chuck, which is the most critical single piece of rod fabrication equipment, employs the use of cam actuated sliding tapered jaws. When the chuck is closed on the fuel rod, the tapered jaws engage in the matching taper of the rod end plug effecting a rigid connection. The chuck and anvil are placed inside the cubicle, and, to allow convenient servicing, the vibrator is located outside the cubicle. The vibrator is sealed from the cubicle by a neoprene diaphragm.

4.1.5 End-Cap Welding Machine

The vertical end-cap welding machine (Fig. 4.6) was specifically designed to weld the top end plug onto the fuel rod by a fusion lip weld. The unit is also equipped with a press for seating the top end plug on the fuel rod immediately after the rod has been evacuated and backfilled with helium. The welding machine is composed of two main components, an elevation mechanism and the welding chamber.

The elevation mechanism employs a synchronous drive motor and a lead screw arrangement for inserting the fuel rod into the welding chamber. The elevator also actuates a vacuum seal around the fuel rod as it is seated in the welding chamber.

In the welding chamber are located the helium-arc torch and the end plug press. The press uses a lead screw and a synchronous drive motor for inserting the end plugs. The torch is positioned by two high-ratio, lead screw motor arrangements. During welding, the rod is rotated by a constant speed drive motor.

4.1.6 Decontamination Equipment

A 1-kw ultrasonic cleaner is used to decontaminate, one at a time, the completed fuel rods. The cleaner is equipped with a remote cover which embodies a mechanism for holding and rotating the rods during cleaning

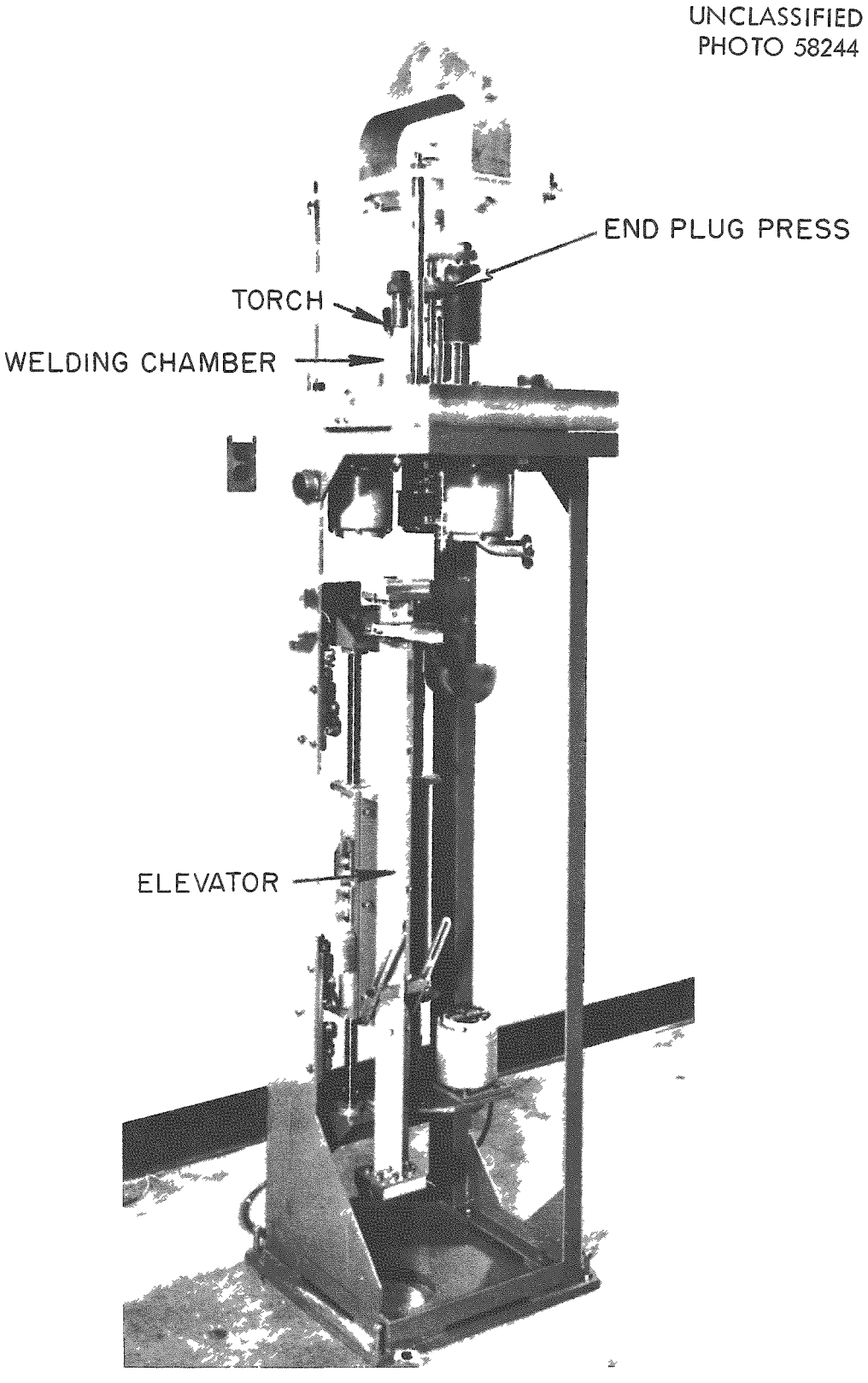

Fig. 4.6. End-Cap Welding Machine.

operations. The cleaning cycle, which is manually controlled, consists of filling, cleaning, emptying, spray rinsing, and drying.

4.1.7 Helium-Leak Checking System

The welded and decontaminated rod will be checked for leak-tightness with a mass spectrometer helium-leak detector. The system includes a chamber in which the end of the fuel rod is sealed, a standard leak, the leak detector, and a roughing vacuum pump station. Particle filters are used to isolate the rod vacuum chamber from the pumping and detection station.

4.1.8 Density Scanner

The density of each rod is determined by means of a gamma-absorption device which is shown in Fig. 4.7. The scanner consists of a one-curie Co^{60} source, collimated through a 1/8- x 3/8-in. longitudinal slot, and a detecting crystal with its associated power supply, amplifier, and recorder. A trolley is provided to drive the fuel rod through the collimated beam at a constant rate.

4.1.9 Shipping Cask

The shipping cask, which is designed to hold 132 rods, is loaded in the horizontal position in the facility, and discharged vertically at BNL. For loading, the cask is held on a dolly in the horizontal position and secured to the cubicle door with turnbuckles. The lattice structure which is provided in the cask to position the rods is partially inserted into the loading cubicles to facilitate loading by tongs. After loading, the lattice is retracted into the cask, the top secured, and the cask removed by means of an overhead crane. During production, two casks are to be shuttled between the facility and BNL.

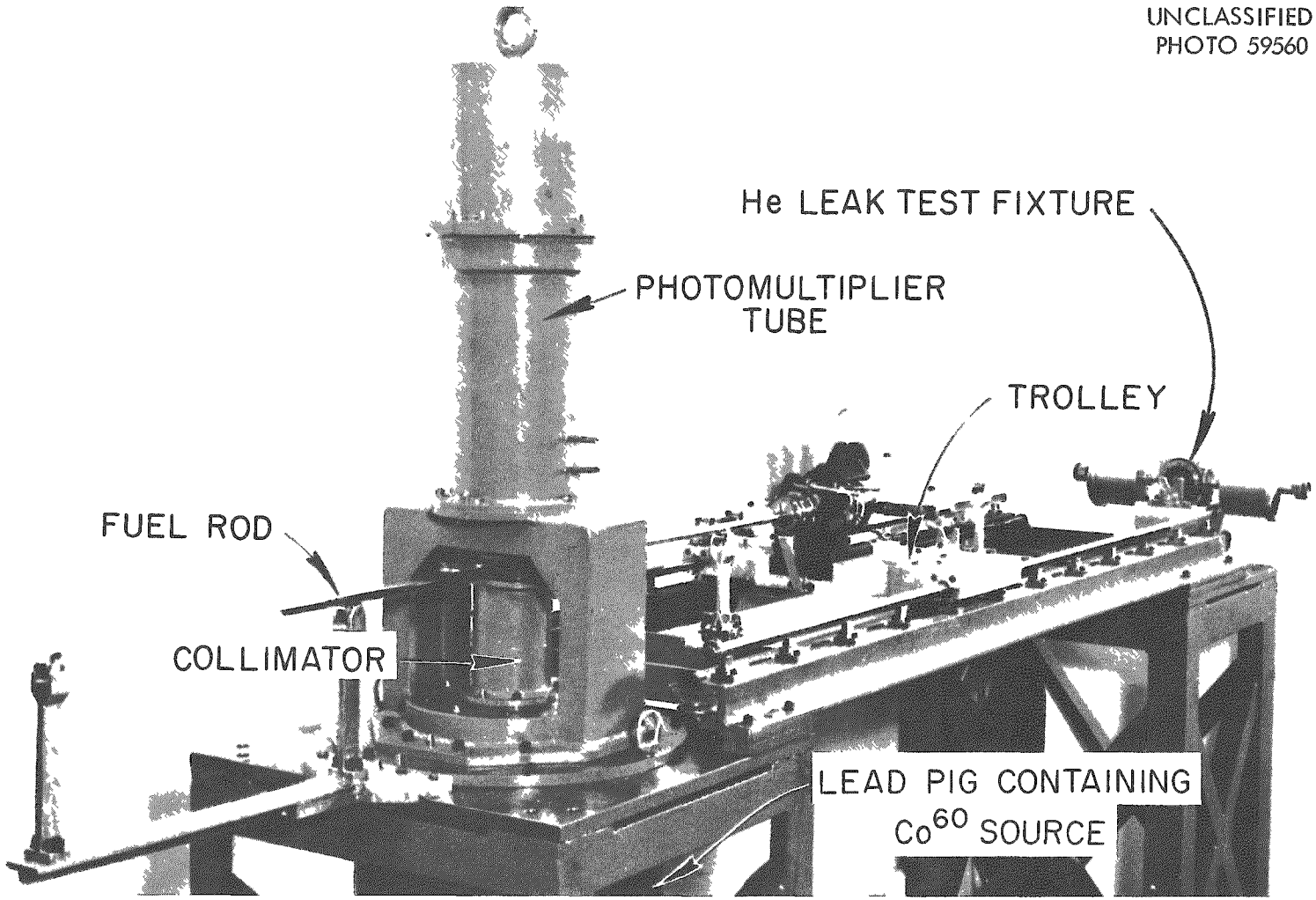

Fig. 4.7. Gamma Scanner.

4.1.10 Summary

The construction of the cell facility is complete, and equipment is now being installed. Hot operation of the facility will begin early in 1963.

The process equipment has operated satisfactorily under mockup conditions; however, the adaptability of the process and equipment can be proved only by operation of the integrated facility. As the process involves operations never before performed, a number of the features of the facility, equipment, and procedure were selected by personal intuition and judgment. Operation of the facility will test the design philosophy and will give invaluable experience in determining the manner in which future facilities and equipment for similar operations should be designed.

4.2 Welding Research (J. W. Tackett)

During 1963, the Remote Fabrication Group of the Metals and Ceramics Division at the Oak Ridge National Laboratory will fabricate 1100 fuel rods containing $(U^{233}\text{-Th})O_2$ for BNL. The proposed manufacturing procedures (described in detail in Section 4.1) consist essentially of the following steps: (1) a Zircaloy-2 bottom end plug is attached to a Zircaloy-2 tube (0.500-in. o.d. x 0.035-in. wall x 45 1/2 in. long) by a circumferential fusion weld, as shown in Fig. 4.1; (2) the oxide is loaded into the tube and densified by vibratory compaction; and (3) the second end of the fuel rod is then closed by a Zircaloy-2 top end plug, also welded as shown in Fig. 4.1. The Welding and Brazing Group of the Metals and Ceramics Division have assisted the Remote Fabrication Group in developing techniques and procedures for producing the high integrity end-closure welds required for the BNL fuel rods.

Early in the development program, techniques and procedures were worked out for producing such welds using short lengths of tubing with conventional, vacuum-purged, inert-atmosphere dry box equipment and appropriate copper chill rings. Vacuum equipment is usually

required to obtain an atmosphere suitable for welding Zircaloy-2. Massive copper chill rings are usually positioned below the weld to provide a "heat sink" for additional cooling of the tubing during welding. The copper chill ring prevents significant temperature buildup in the base metal, reduces the time at which the weld bead is at high temperature (both very important in preventing undesirable surface oxidation and weld contamination), and, in the case of the top end plug weld, minimizes the problem of "rollover."

Some difficulty was experienced in axially aligning the tungsten electrode directly above the joint between the tube end and the bottom end plug. The alignment of the welding electrode in both radial (arc gap) and axial directions is doubly complicated by (a) the limited visibility imposed by the dry box and by (b) the obscuring of the visible interface line between the tube end and end plug during precleaning of the joint components by wire brushing (usual method). This situation is considered very serious for three reasons: (1) a misalignment of only 0.030 in. in the axial direction can seriously affect the integrity of the welded joint, (2) a misalignment of 0.010 in. in the radial direction can seriously affect the weld width-to-penetration ratio, and (3) no satisfactory nondestructive inspection method is available to evaluate this particular weld joint.

In view of the shock wave (the Branford Variable Impact Vibrator is rated at 20,000 to 100,000 g) which may be transmitted through the bottom end plug weld during the fuel compaction step, the integrity requirement for this weld joint becomes doubly important. The joint integrity of the weld is measured in terms of (a) weld penetration — the penetration should be at least equal to the thickness of the tube wall; (b) weld imperfections — root cracks, for example, would be highly undesirable; (c) weld contamination — oxygen contamination of the weld might affect the corrosion resistance and mechanical properties of the weld. It is apparent that each of these parameters is determined by destructive examination.

In view of the large number of fuel rods to be fabricated (1100 total), some consideration has been given to making the bottom welds outside a

dry box, concentrating on improved inert-gas shielding and joint area chilling. Making the welds outside a dry box would not only greatly reduce the total time required, but would also help to eliminate the electrode alignment problem (described above). Satisfactory welds have been made outside the dry box (Fig. 4.8 is typical of a good weld), and the technique is currently being refined such that this particular fabrication step can be performed by Engineering and Mechanical Division shop personnel.

The top end plug will be installed and the closure weld will be made remotely inside the contamination zone cubicle. The special equipment designed and constructed for this particular step in the fuel rod manufacturing sequence is described in Section 4.1.5 (Fig. 4.6). In the design of this equipment, no provisions were made for weld chill rings, and, in order to determine their importance, test welds were made using a conventional "square" edge weld joint design (shown in Fig. 4.9a). Welds made with a 1-T penetration resulted in excessive "rollover." This condition would make it difficult to remove the fuel rod from the welding jig and could prevent its insertion into the scanner for inspection. In an effort to circumvent this problem, the edge weld joint design was changed from a "square" edge to a "V groove" edge as illustrated in Fig. 4.9b. Test welds made using the new "V groove" configuration (made without chill rings) resulted in adequate weld penetration without "rollover." Some visible surface oxidation occurred in the case of each weld made without chill rings. Investigations are under way to determine if this discoloration is undesirable. Figure 4.10 is typical of the "V groove" edge welds made without chill rings.

4.3 Vibratory-Compaction Research and Development (W. S. Ernst)

Some experimental studies in vibratory compaction of Th-U oxide made by the sol-gel process were performed for general development of the art. However, direct support of the BNL Kilorod Program and service support for other phases of the Fuel Cycle Program demanded most of the effort.

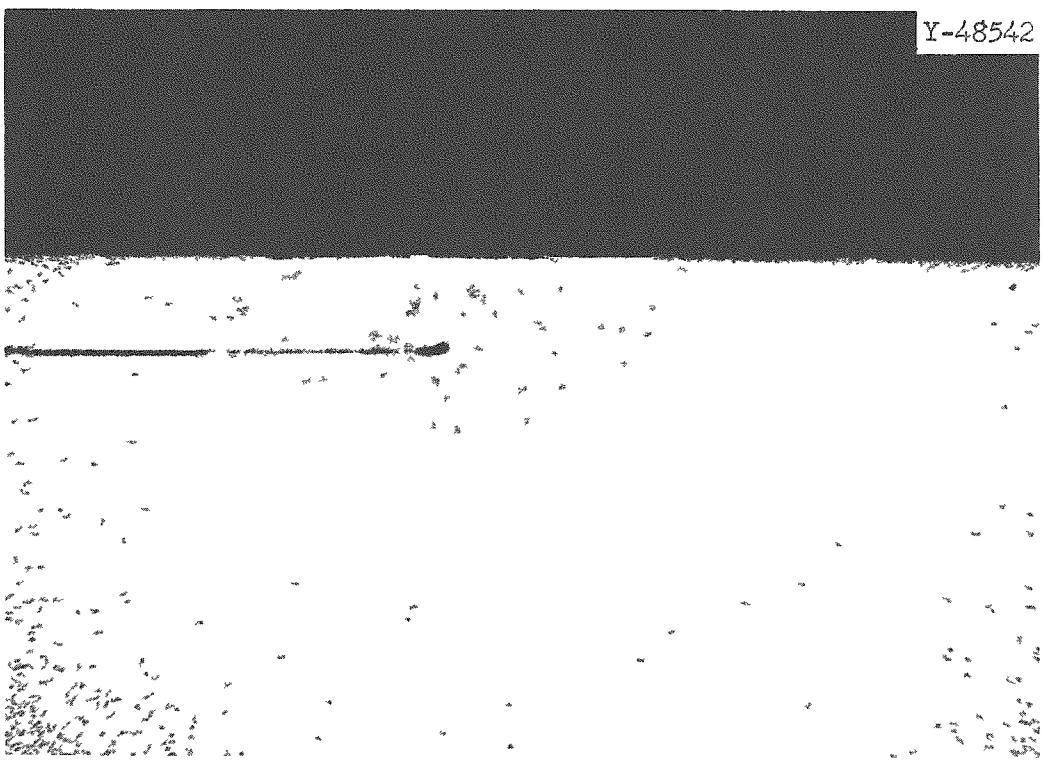

Fig. 4.8. Cross Section of Bottom End Plug Well. Etchant: 50 lactic, 50 HNO_3, 4 HF. 15X.

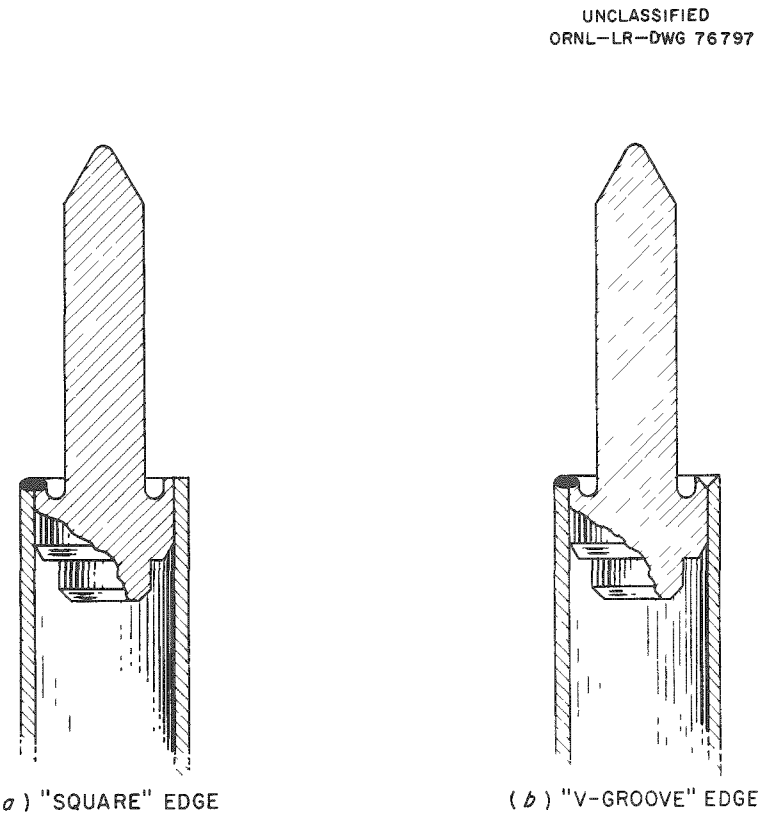

Fig. 4.9. Top End Plug Assembly – Illustrating the "Square" Edge and the "V Groove" Edge Joint Preparation.

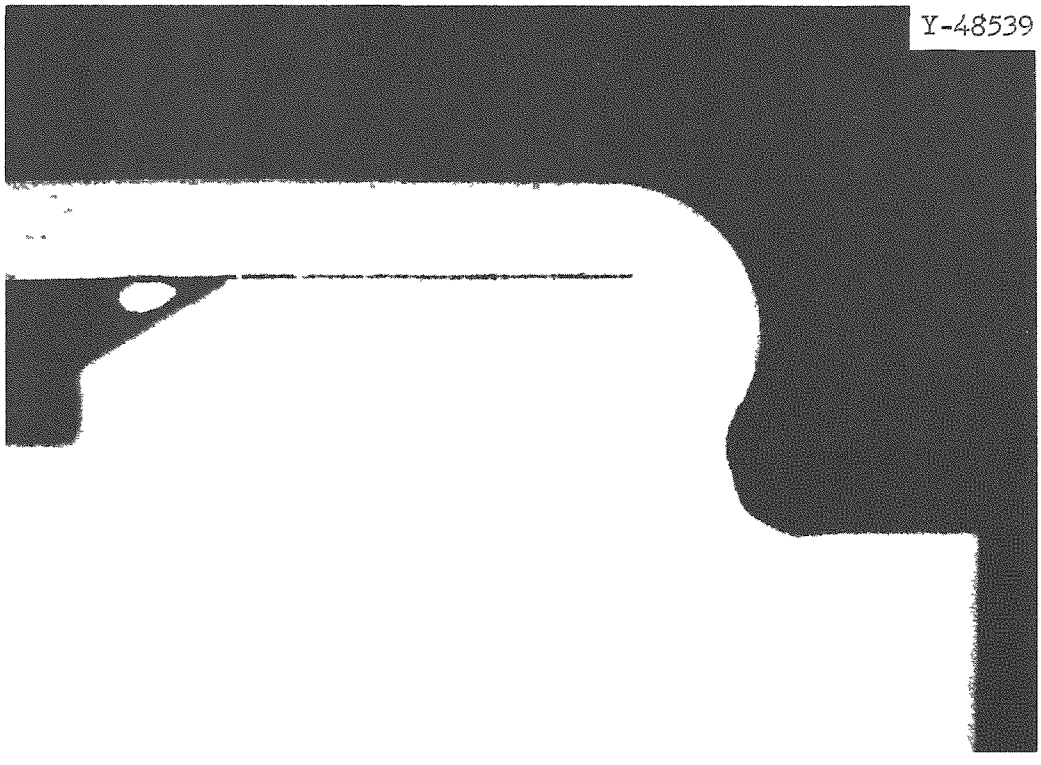

Fig. 4.10. Cross Section of Top End Plug Weld. Etchant: 50 lactic, 50 HNO_3, 4 HF. 15X.

4.3.1 Particle-Size Distribution

Studies that relate bulk density with particle-size distributions were initiated to gain insight into packing phenomenon. Several systems of the ternary and binary classes are being investigated and some of the results obtained are discussed below. In these experiments, vibration energy generated by the Branford Variable Impact Vibrator was used to compact Th-U oxides into type 304 stainless steel tubes 45 in. long x 1/2-in. o.d. x 0.035 in. wall.

The Particle-Size System (-6 +16, -50 +140, -200 mesh). This ternary system is of considerable practical interest because a sufficient yield of the coarse fraction (-6 +16) can be readily obtained from the crude sol-gel Th-U oxides. In addition, this system also readily fits into a 1/2-in.-diam tube. A trilinear plot (Fig. 4.11) shows the relationship between particle-size distribution of this system and bulk density obtained for UNOP Batches 20, 23, and 24 combined into one large one. Isorithms (lines of constant density) have been drawn for 8.8 and 8.9 g/cm^3. These isorithms are based on the results obtained from 35 different distributions in this general area. Distributions lying inside either of these lines yielded bulk densities that are equal to or greater than the value of the enclosing line.

Because the degradation characteristic of the coarse fraction has an effect on the vibrated bulk density, a meaningful plot can be obtained only by requiring each distribution be made of material whose chemical and physical histories are identical. Practically, this requirement means the material can be vibratory compacted only once because other studies have shown that degradation of the coarse fraction is dependent upon the total time that the material has been vibrated. As a consequence of this requirement a large amount of material is needed to obtain a plot. Because large batches of material have not been available, the isorithms shown in Fig. 4.11 are to be regarded as only approximate since the values of bulk density are based on a single value for each distribution. Furthermore, they can be expected to shift or even disappear with changes

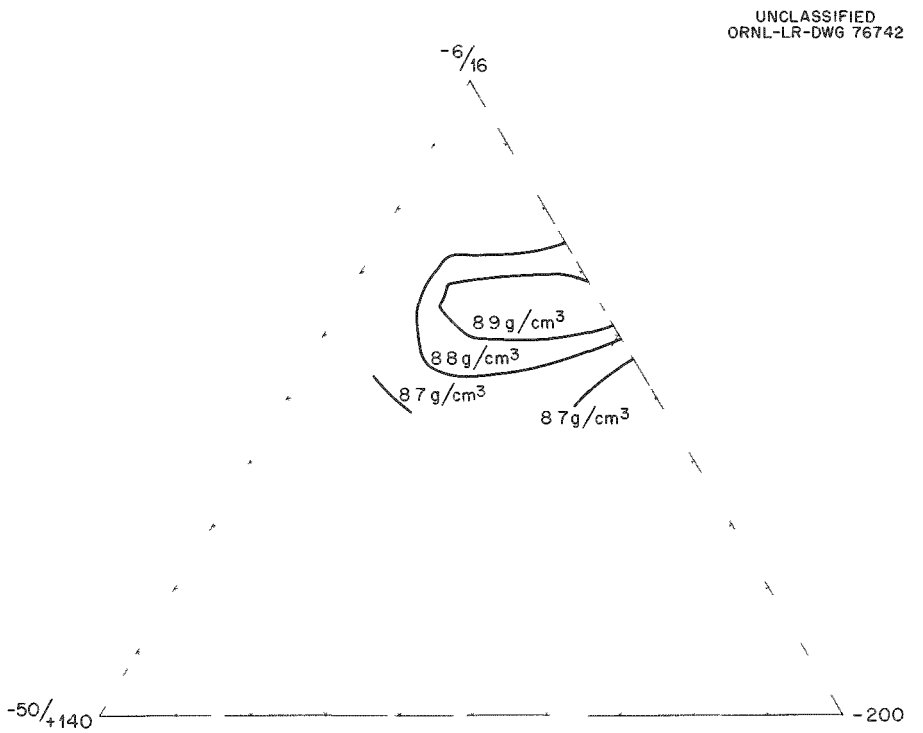

Fig. 4.11. Effect of Particle-Size Distribution on Vibrated Density of Ternary Mixtures. Isorithmic lines for 8.9, 8.8, and 8.7 g/cm^3 are shown.

in the chemical history of the oxides. For example, some of the oxides made by the sol-gel process have yielded densities greater than 9.0 g/cm^3 for a distribution that yielded only 8.9 g/cm^3 in this experiment.

Figure 4.11 shows that there is a range of distributions with which bulk densities of greater than 8.9 g/cm^3 can be obtained and an even larger range of distributions for 8.8 g/cm^3.

Other Ternary Systems. By increasing the range in size of the coarse fraction to -4 +16 mesh, another system of practical interest is obtained since this size fraction can be obtained more readily than the -6 +16 mesh size fraction. Bulk densities greater than 9.0 g/cm^3 have been obtained for a distribution of 60 wt % -4 +16, 15 wt % -50 +140, and 25 wt % -200 mesh. This system is not entirely satisfactory for 1/2-in.-diam tubes because the large particles occasionally bridge in the tube and cause a low density region to form. The small amounts of available material have not permitted a trilinear plot such as Fig. 4.11 to be obtained for this system.

The system -6 +10, -35 +50, -200 yielded bulk densities about 1% higher than did the -6 +16, -50 +140, -200 system for the same material. For a distribution composed of 60 wt % -6 +10, 15 wt % -35 +50, and 25 wt % -200 mesh bulk densities of 9.1 g/cm^3 were obtained. This system requires a laborious procedure for obtaining yields of the coarse fraction in sufficient quantities that are useful.

Binary Systems. The binary systems -6 +16, -200 and -4 +16, -200 are particularly interesting because the troublesome medium size fraction is eliminated. The relationship between bulk density and the amount of coarse material in a distribution is shown in Fig. 4.12. The data for these plots were obtained with a mixture of materials from UNOP Batches 20, 23, and 24, and, therefore, these data apply for this mixture only. However, similar relationships can be expected, in general, to hold for other Th-U oxides with slightly different chemical histories although the maximum density can be expected to shift in value and with respect to the distribution.

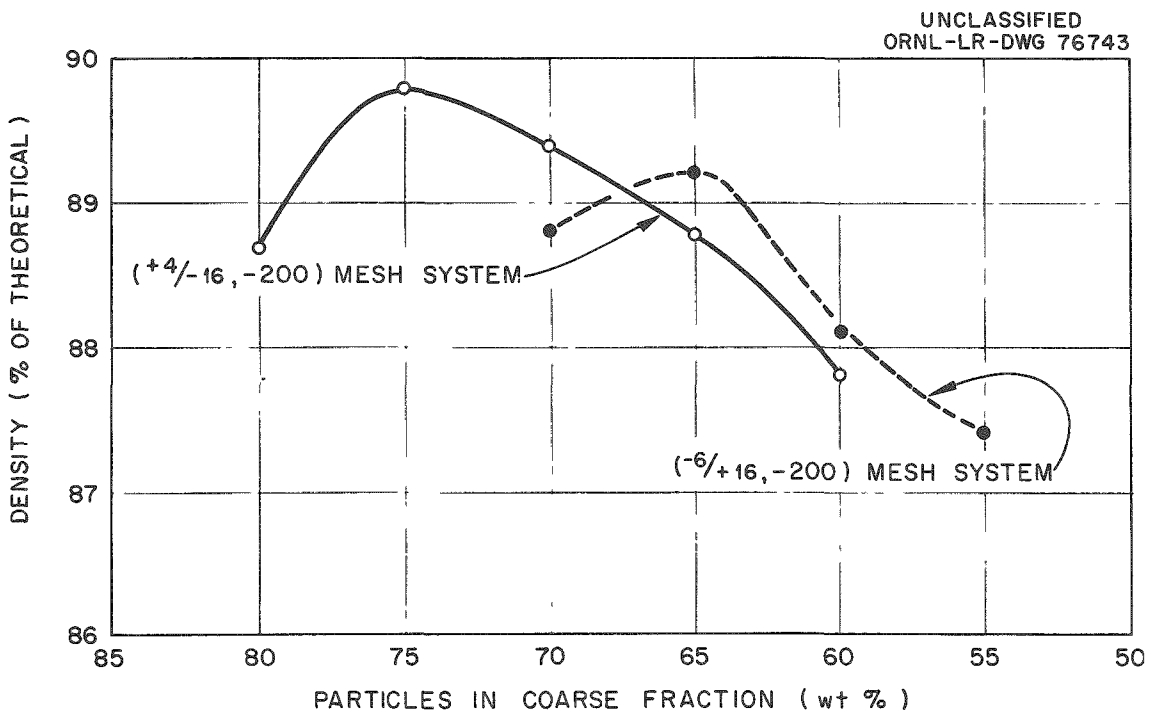

Fig. 4.12. Effect of Particle-Size Distribution on Vibrated Density of Binary Mixture. Theoretical density of the mixed oxides taken as 10.0 g/cm^3.

Screen analyses of the distributions after completing the compaction process were obtained for these binary systems. In general, it appears that a ternary system is generated from the -4 +16, -200 system and that the -6 +16, -200 system remains nearly a binary. This may explain why a slightly higher density is obtained with about 10 wt % more coarse material in the -4 +16, -200 system than is the case for the -6 +16, -200 system.

4.3.2 Vibrators

The Branford Variable Impact Vibrator with an external mechanical wave guide shown in Fig. 4.13 has been used for most of the experimental studies in support of the BNL Program. The use of mechanical wave guide makes an effective alpha seal practicable for remote operation. This system produces acceleration pulses having peak values between 20,000 to 100,000 times that due to gravity. The pulse width is about 15 μsec. Because of the very high acceleration levels, measurements have been very difficult and unreliable but the order of magnitude is believed to be accurate. For compacting fuel, a rate of about six pulses per second has usually been employed.

Although the NAVCO Bin Hopper type vibrators are satisfactory for compacting fuels, they are not entirely satisfactory, from an operation point of view, for remote operation. Additional engineering design is needed to solve the alpha seal problem and the fatigue problem associated with the relatively large amplitudes and frequencies.

4.3.3 BNL Kilorod Support

Those experiments deemed necessary were performed to determine the types of equipment suitable for meeting the requirements of this program. Furthermore, experiments were also performed to determine the overall process and materials preparation methods. From these experiments, the basic guides for engineering a remote operating system were obtained. Among the important guides determined were:

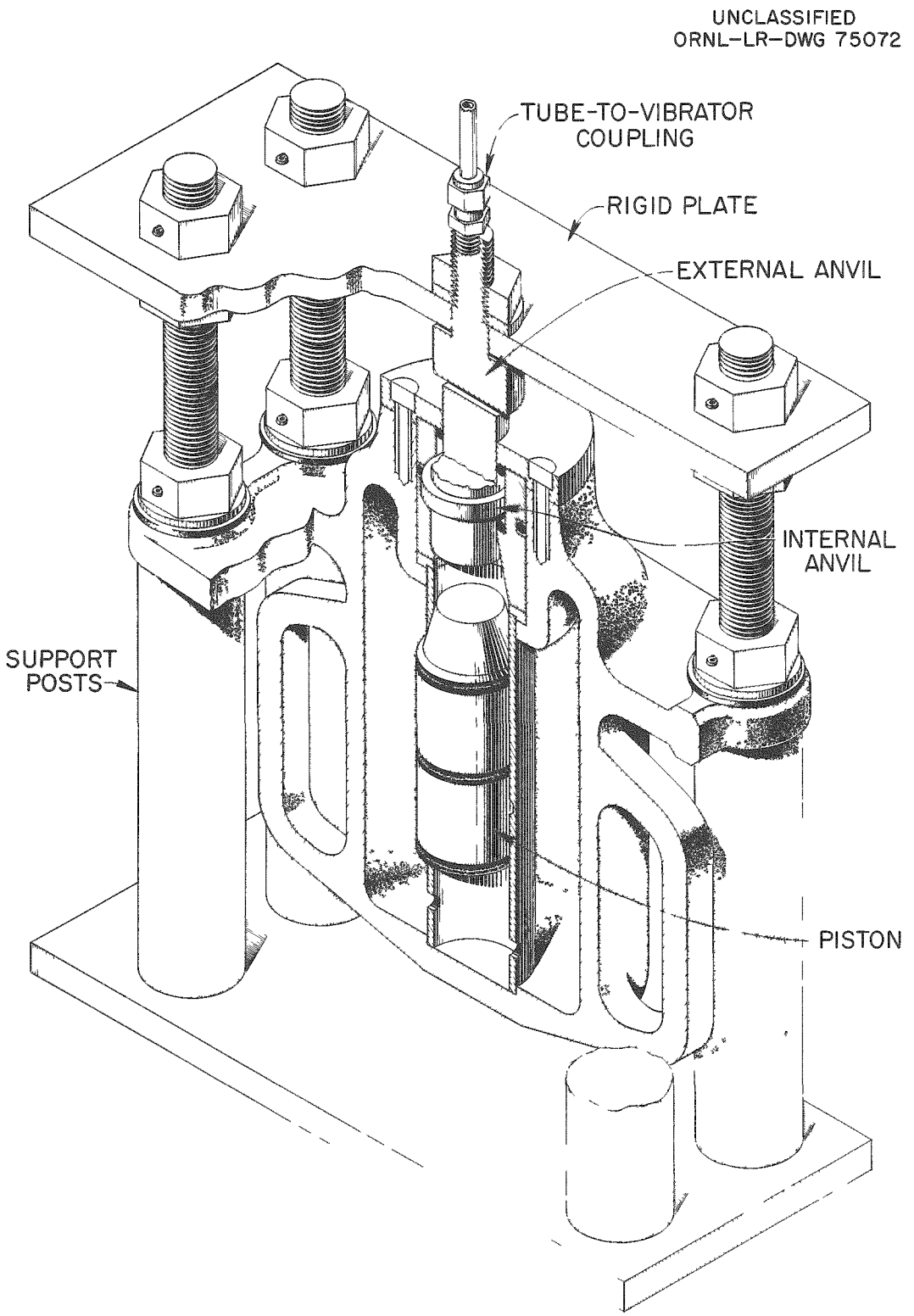

Fig. 4.13. Branford Variable Impact Vibrator Mounted for Fuel Compaction.

1. A jaw crusher would be suitable for crude comminution.
2. A ball mill would be necessary for generating both the medium size fraction and the fine fraction.
3. A means to recycle oversize material through either the jaw crusher or ball mill should be provided.
4. Each size fraction for each fuel rod would have to be weighed.
5. The blended material should be loaded in such a fashion that the particle-size distribution is distributed uniformly in the tube.
6. The Branford Variable Impact Vibrator with a mechanical wave guide was the preferred system.

Although a particle-size distribution (60 wt % -6 +16, 15 wt % -50 +140, and 25 wt % -200 mesh) was selected as a reference for engineering design and development studies, the process flow path and equipment were selected such that a flexible system was obtained. This will permit a range of other ternary systems or binary systems to be used. The final selections will be made on the basis of meeting the density requirement and the yield requirement.

The results of many fuel rods fabricated for determining the axial fuel distribution are questionable. To date, it is not known if the axial fuel distribution meets the requirements for the BNL Kilorod Program because the measuring device has not been absolutely nor accurately calibrated. A study of the axial fuel distribution was carried out by cutting fuel rods into several sections. The data obtained suggested that the fuel distribution might be directly dependent upon the initial distribution as loaded into the tube. Experiments have shown that a vibrating trough will, in fact, uniformly transport the blended materials. Tubes loaded by means of such systems appear to be better in this respect. Work is still in progress to resolve this problem.

A considerable portion of the effort during the past year falls in the category of performing service for others. Over 50 different batches of sol-gel oxide were crushed, screened, and vibratorily compacted into tubes for the Chemical Technology Division. The study of bulk density

as affected by the chemical history of the oxide is discussed in their portion of this report. In addition, most of the capsules for the irradiation program were prepared in this group.

4.4 Irradiation Studies of Mixed Oxides of Thoria and Urania (S. A. Rabin)

In support of the Thorium Fuel Cycle Program, irradiation experiments are being conducted to evaluate the in-pile behavior of thoria-base fuels.

4.4.1 General Scope of the Study

The materials currently under investigation include oxide powders made by either the arc-fusion or sol-gel routes. Properties of the oxides incorporated in the irradiation specimens are summarized in Table 4.1. Representative photomicrographs are depicted in Figs. 4.14 and 4.15. The most widely used particle-size distribution was 60 wt % -10 +16, 15 wt % -70 +100, and 25 wt % -200 mesh.

All of the ThO_2-UO_2 bearing rods were fabricated by vibratory compaction, as described in the previous section of this report. The rods containing ThO_2-PuO_2 were simply tamp packed. End closures were made using conventional techniques.

Irradiations of fuel material prepared in the manner described above have been completed or are in progress in the NRX, MTR, and ORR. A summary of these tests is presented in Table 4.2. The more salient features of this program are as follows:

1. A comparison is being made between oxides produced by the sol-gel and arc-fusion routes (MTR Group I and NRX Group II capsules).
2. Type 304 stainless steel fuel tubes, 0.312-in. o.d x 0.025-in. wall, are specified as the cladding for the MTR and NRX experiments. This approximates the 0.304-in.-o.d. x 0.0205-in.-wall geometry of the fuel pins for the Consolidated Edison Thorium Reactor, CETR, at Indian Point, New York. The capsule design is schematically illustrated in Fig. 4.16. Fuel rod lengths

Table 4.1. Summary of Properties of Uranium-Thorium Oxides Used in Fabrication of Irradiation Specimens

	Sol-gel A	Sol-gel B	Sol-gel C[a]	Sol-gel D[a]	Sol-gel E[a]	Arc Fused	Sol-gel S	Sol-gel Batch 26
Total uranium, wt %	4.31	4.39	4.01	2.50	4.0	3.96	5.21	5.35
Uranium enrichment, %	93	93	93	93	93	93	93	93
Carbon, ppm	110	100	60	40	130	120	80	40
Nitrogen, ppm	22	21	55	29	31	1130	30	13
Iron, ppm	100	50	265	140	160	130	300	215
Silicon, ppm	600	500	<20	<10	<10	20	20	<25
BET surface area (N_2), m^2/g	0.20	0.26	0.03	0.008	0.011	0.11	0.17	0.047
O/U ratio	2.0	2.0	2.03	2.02	2.02	2.01	2.01	2.02
Volatile matter released in vacuum at 1200°C, cc/g	0.125	0.151	0.055	0.012	0.027	0.24	0.284	0.244
Lattice parameter, A	5.591	5.592	5.593	--	5.593	5.594	5.594	--
Crystalline size, A	2400	1700	2200	--	--	--	1800	--
Particle density, g/cc[b]	9.94	9.92	9.76	9.97	9.92	10.11	10.0	--
Packed density, g/cc[c]	8.69	8.69	8.36	8.74	8.74	8.6	8.8	--

[a] Cooled in pure argon after calcination in hydrogen.

[b] Toluene intrusion, pycnometric method. Theoretical density: 10.04 g/cc.

[c] NAVCO air vibrator, 1/25-in. piston; 5/16-in.-o.d. x 11-in. stainless steel tube.

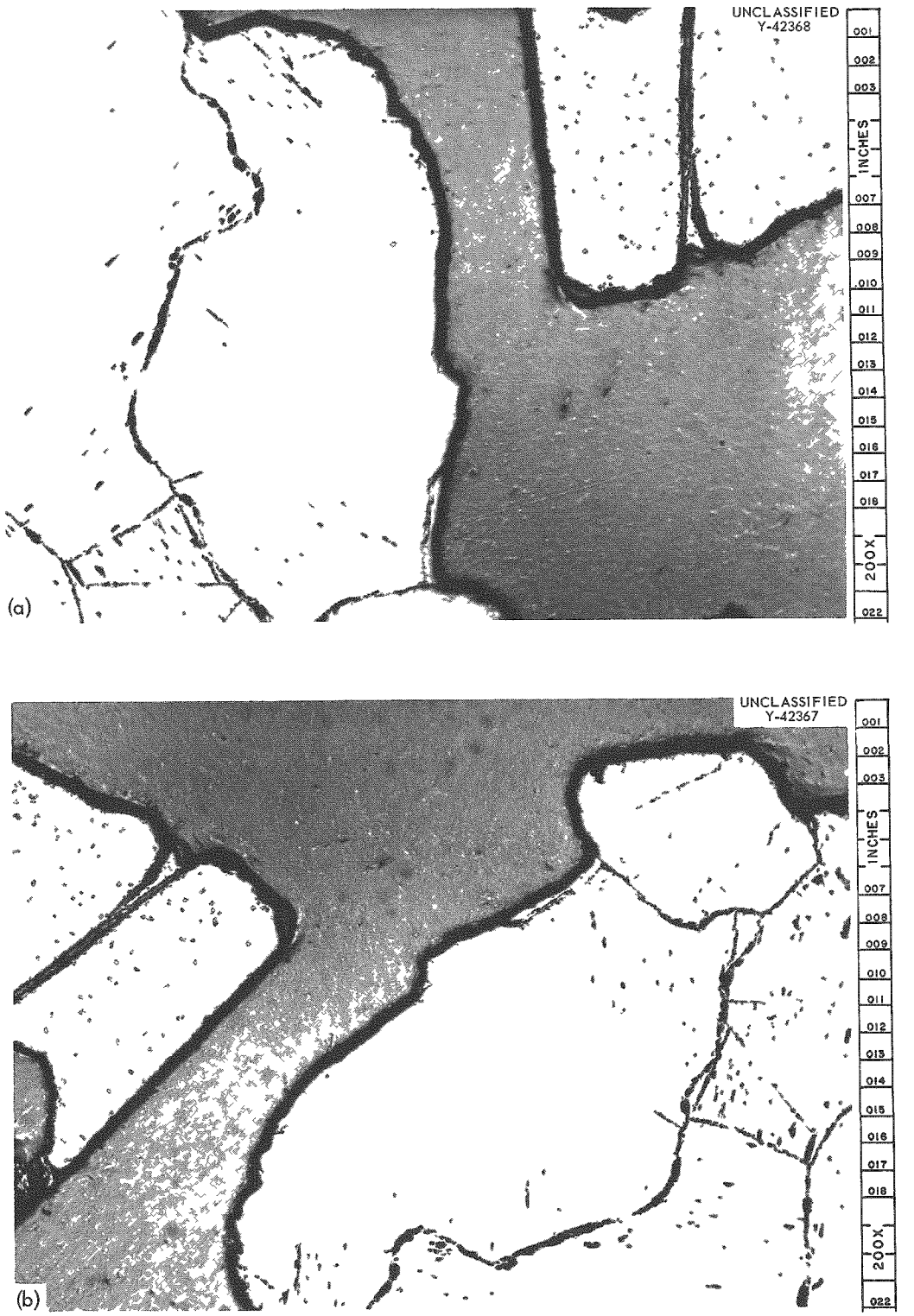

Fig. 4.14. Spencer Arc-Fused ThO_2–4.5 Wt % UO_2 Powder. The white second-phase precipitate, found in varying percentages in the particles, is probably uranium. The particles exhibit both transgranular and intergranular cracking. (a) As-polished. (b) No microstructural change was observed after etching for UO_2 (7 parts H_2O, 1 part HNO_3, 2 parts 30% H_2O_2 for 2-1/2 min). Reduced 18%.

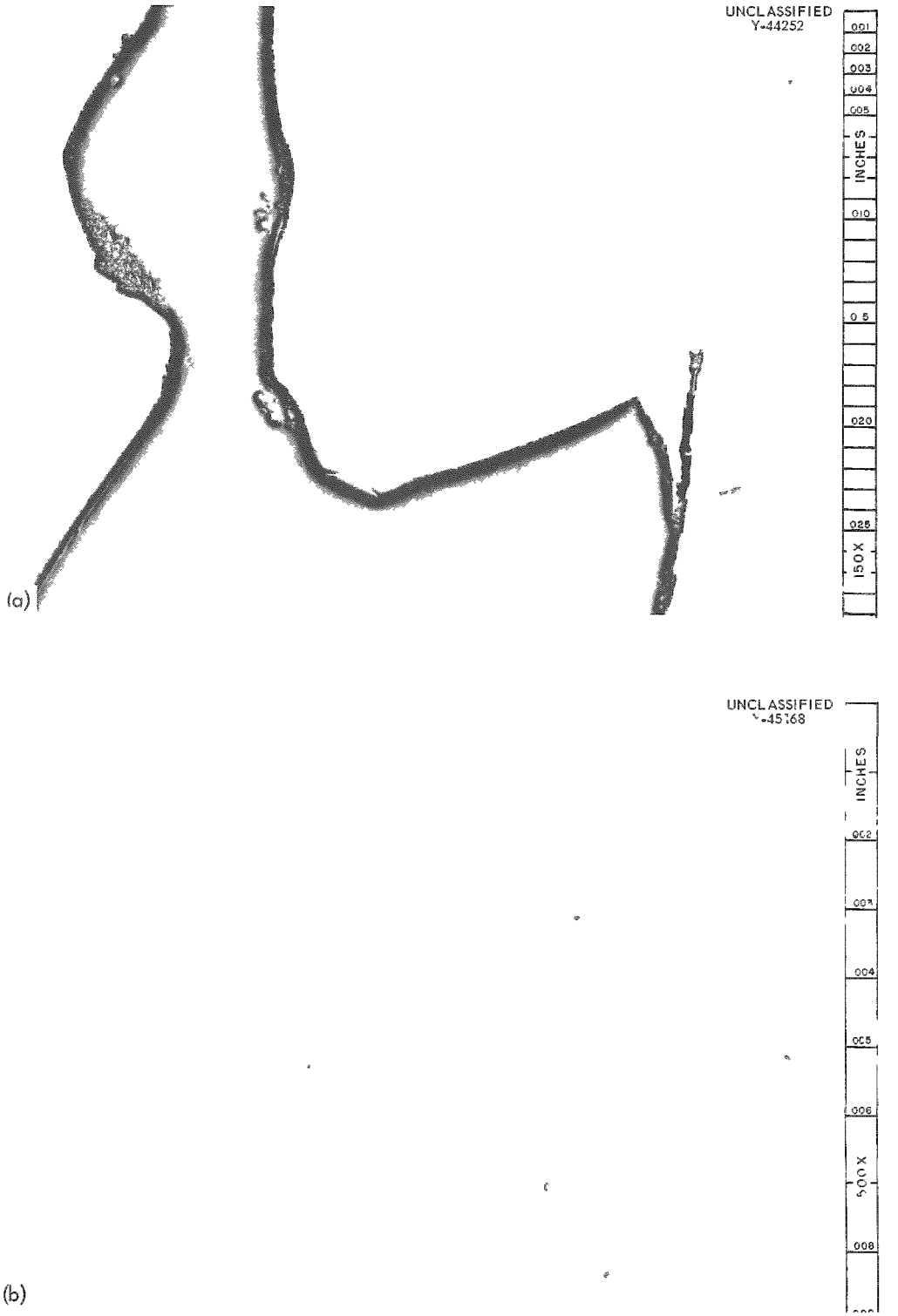

Fig. 4.15. ORNL (Chemical Technology Division) Sol-Gel E ThO_2-4.5 Wt % UO_2 Powder. No impurities were found in this material. Small surface cracks may be seen in the particles. (a) 150X. As-polished. (b) 500X. Etchant: boiling HNO_3-HF. At higher magnification the particles show a very fine natural porosity and extremely fine crystallites (spheroidal white particles) may be observed. No large grain boundaries are evident. Reduced 19%.

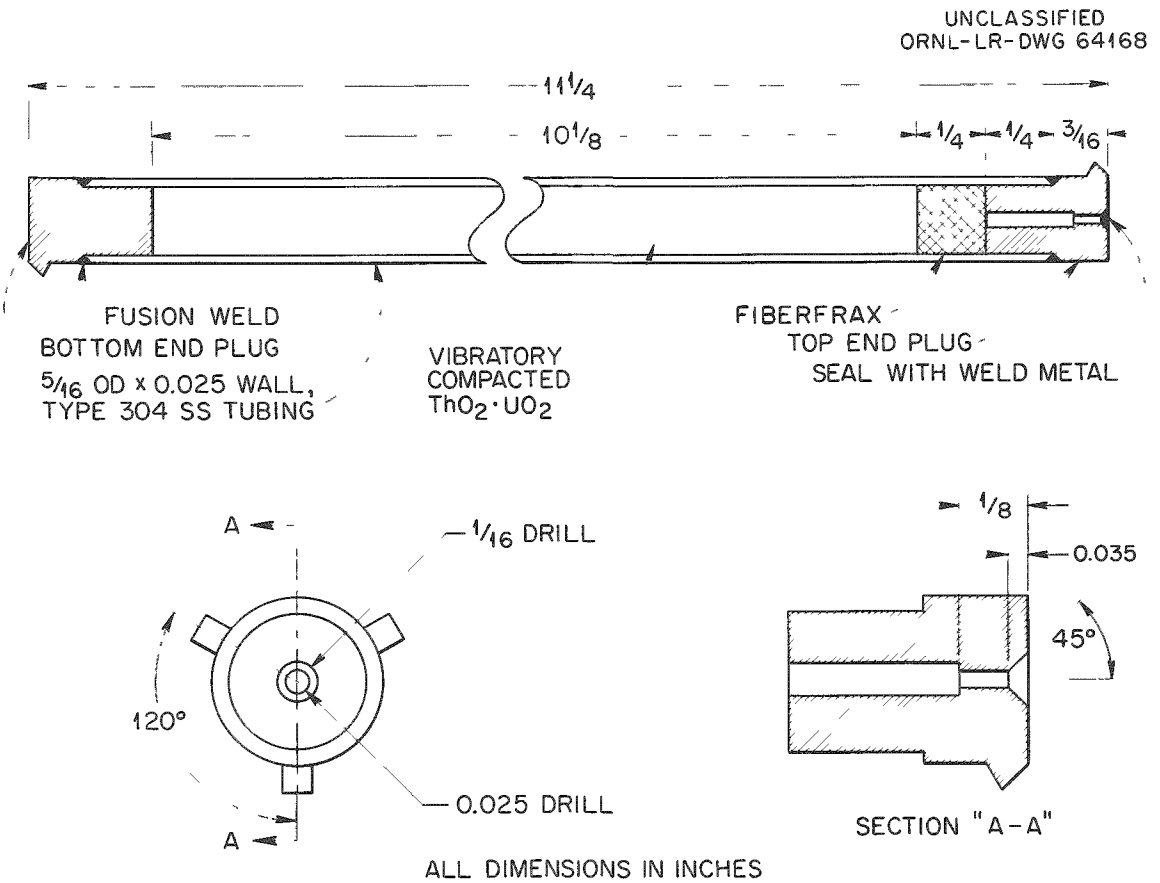

Fig. 4.16. ThO_2-UO_2 Fuel Cycle Capsule for NRX and MTR Irradiations.

Table 4.2. Summary of Fuel Cycle Irradiaitions[a]

Experimental Facility	No. of Capsules	Type of Oxide	Vibrated Density (% theoretical)	Clad Temp (°F)	Average External Pressure (psia)	Fuel Rod Dimensions (in.)			Linear Heat Rating (Btu/hr·ft)	Estimated Burnup (Mwd/MT metal)	Status
						Outside Length	Diameter	Wall			
ORR Poolside	2	Sol-gel D	85–86	1000, 1300	315	7	0.625	0.020	40,000	7,000	Out 9-23-62
NRX (Group I)	8	Sol-gel A, Sol-gel B	84–86	~200	130	11	0.312	0.025	24,000	20,000	Out 5-22-62
NRX (Group II)	4	Arc-fused, Sol-gel C	84–86	~200	130	22.5	0.312	0.025	20,000	3,500	Out 2-16-62
MTR (Group I)	7	Arc-fused, Sol-gel E	86–87	~200	40	11	0.312	0.025	41,800–47,600	12,300–100,000	5 in-pile 2 out 4-2-62
NRX (Group III)	6	Sol-gel S	88–89	~200	130	39	0.312	0.025	28,000	23,000	In 5-24-62
NRX (Group III)	3	Sol-gel ThO_2-PuO_2	74–76[b]	~200	130	11	0.312	0.025	27,000	22,000	In 5-24-62
ORR Loop (L-1)	3-rod cluster	Sol-gel 26	84–85	~500	1750	21.5	0.460	0.015	43,000–52,300	2,500–3,000	Out 10-31-62

[a] Fuel = ThO_2-UO_2 except for three (NRX Group III) ThO_2-PuO_2 bearing capsules.

Clad = Type 304 stainless steel except for experiment L-1 (one clad with type 304 stainless steel and two with Zircaloy-2).

[b] Tamp packed.

were 11, 22 1/2, and 39 in. The longer 39-in. rods were helically wire wrapped to preclude bowing.

3. The experimental peak linear heat ratings of 47,600 Btu/hr·ft (ref 8) for the sol-gel oxide may be compared with 37,000 Btu/hr ft in the CETR.
4. Maximum burnups of 100,000 Mwd/MT metal (2.06×10^{21} fissions/cc) are anticipated in the ORNL program, as compared to 60,000 Mwd/MT metal expected in the CETR.
5. Two instrumented capsules were irradiated in the ORR Poolside Facility (06-5 and 03-5) to investigate the suitability of sol-gel oxide for advanced gas-cooled reactors with high surface temperatures. Each capsule (Fig. 4.17) had an axial molybdenum thermowell containing a tungsten-rhenium thermocouple to continuously measure the center-line temperature. Nominal clad temperatures were 1000°F (540°C) and 1300°F (700°C). The external pressure was 300 psi. This experimental arrangement furnished some indication of the effective in-pile thermal conductivity of the sol-gel fuel material.
6. The ThO_2-PuO_2 fuel-bearing capsules were placed in-pile in May, 1962. For expediency, these powders were simply tamp packed in the rods. This powder also had been made by the sol-gel process.
7. A trefoil cluster (Fig. 4.18) was irradiated in an ORR pressurized-water loop operating at 500°F (260°C) and 1750 psi with a predicted thermal neutron flux of $2.67–3.26 \times 10^{13}$ neutrons cm^{-2} sec^{-1}. The estimated peak heat flux was 330,000–400,000 Btu/hr·ft^2. The mechanically assembled bundle contained two rods that were clad with 0.460-in.-o.d. x 0.015-in.-wall Zircaloy-2 tubes, and the other was clad with type 304 stainless steel of the same geometry. The thickness of the clad is such that collapse onto the fuel would occur at a coolant pressure of 1750 psi,

---

[8] This corresponds to a heat generation rate of 1350 w/cc and a surface heat flux of 590,000 Btu/hr·ft^2 for 0.312-in.-diam x 0.025-in.-wall clad pins.

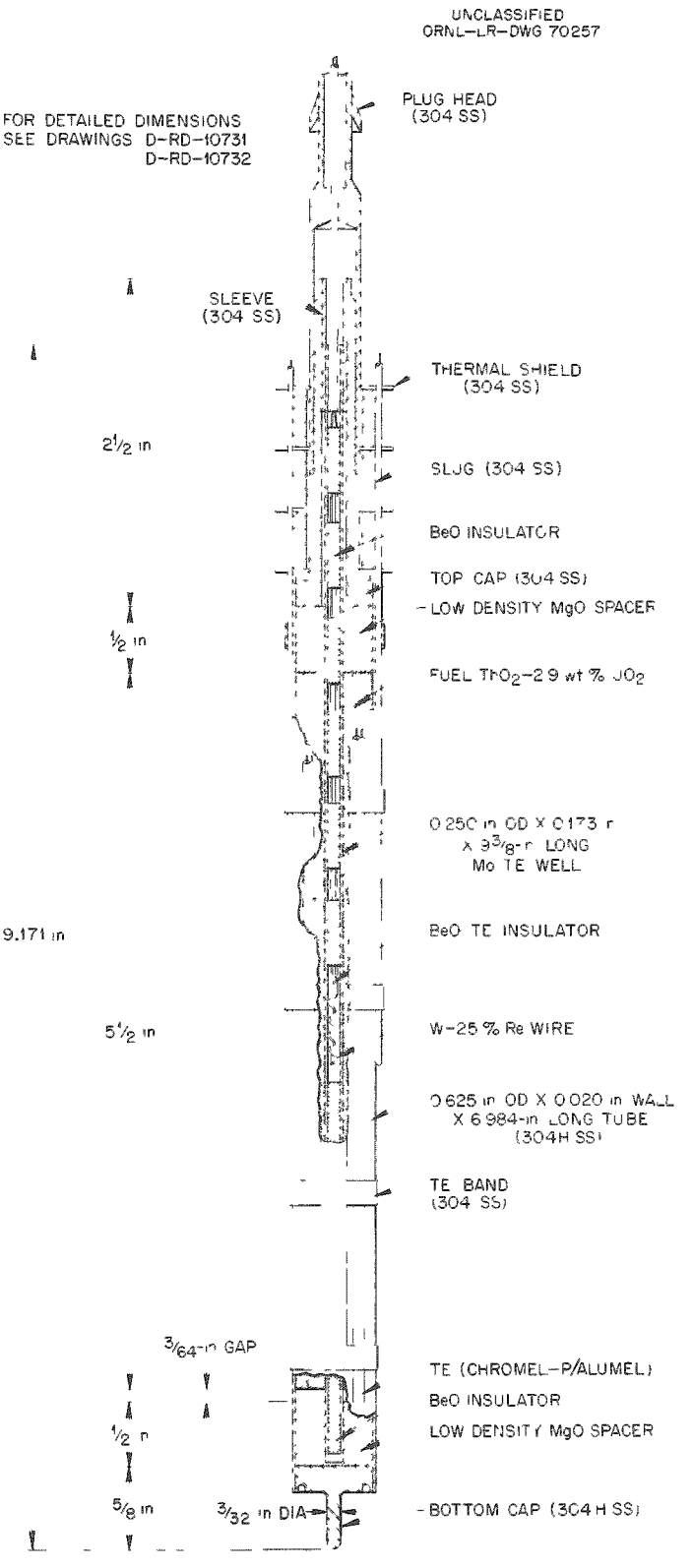

Fig. 4.17. Vertical Cross Section of Fuel Cycle; ORR Irradiation Capsule.

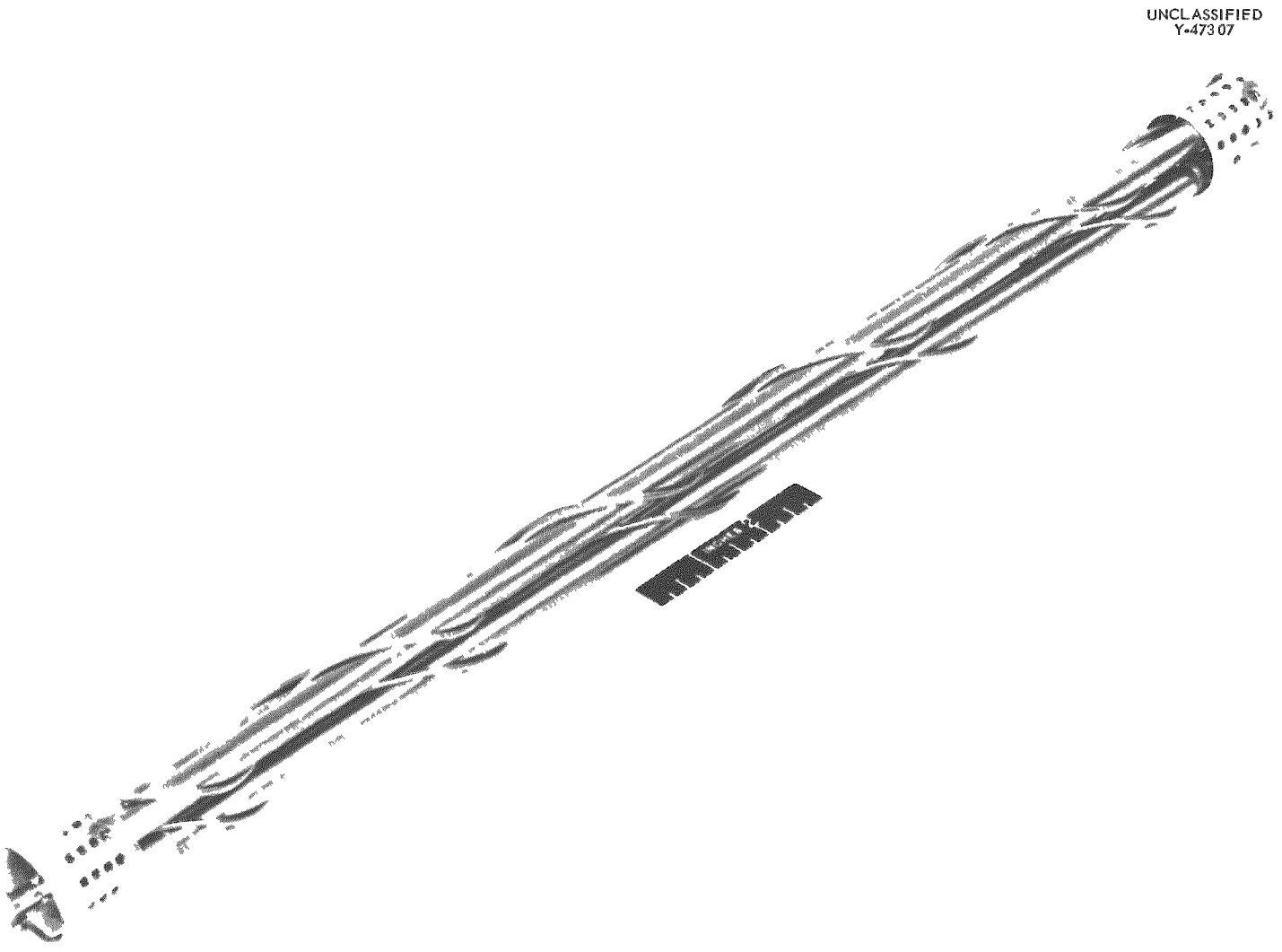

Fig. 4.18. Overall View of Trefoil Cluster for ORR Pressurized Water Loop Experiment L-1.

thereby assuring intimate contact. Each rod was spirally wrapped with a wire of the same material to assure that the rods did not bow together. The primary objective of the test was to examine fuel-clad and clad-coolant interactions at elevated temperatures. This element has since been removed from the reactor due to a fuel rod failure.

4.4.2 Irradiation Behavior and Examination

Postirradiation examination of the first two MTR irradiated rods has virtually been completed. Work on the twelve NRX irradiated rods is complete except for metallographic examinations and burnup determination. These examinations included dimensional measurements, gamma radioactivity scans, fission-gas analysis, burnup measurement of the fuel, and metallographic examination of the fuel and clad.

The two MTR capsules (U-1, Z-5) behaved without incident and were removed according to schedule. Burnup analyses are shown in Table 4.3.

Table 4.3. Burnup Analyses for Capsules U-1 and Z-5

Capsule No.	Type of Oxide	Neutron Dose (nvt)	Burnup (Mwd/MT Th+U)			Specific Power (kw/kg)
			Cs^{137}	Ce^{144}	Mass Spectrograph	
U-1	Arc-fused	6.0×10^{20}	9,380	8,290	12,300	112
Z-5	Sol-gel E	7.0×10^{20}	14,800	12,900	14,000	127

Radiochemical and mass spectrometric burnup measurements on the fuel agreed fairly well with the neutron dose received by the stainless steel clad, which was determined by measurement of the cobalt activation.

No significant changes in the dimensions of the rods were found. Rod bowing was about the same as that before irradiation. Most of the observed diameter changes were increases, the maximum being three mils. Gamma scans reflected the neutron flux gradients along the rods, but did not indicate any significant shifting of the fuel.

Each rod was pierced for collection and analysis of the contained gases. The fission-gas-release fraction was determined by comparison of the Kr^{85} counting data with total Kr^{85} generation based on measured fuel burnup. Gas-release data are shown in Table 4.4. These data show that sol-gel batches A, B, and C are comparable to arc-fused material in retaining fission gases and that batch E is clearly superior. This effect is tentatively attributed to the structural differences between the two materials (see Figs. 4.14 and 4.15) but requires further experimental validation.

Table 4.4. Fuel Cycle Experiment Gas Data

Capsule No.	Type of Oxide	Per Cent of Kr^{85} Atoms Released
MTR-I (U-1)	Arc-Fused	2.4
MTR-I (Z-5)	Sol-gel E	0.50
NRX-I	Sol-gel A	2.06[a]
NRX-I	Sol-gel B	2.76[a]
NRX-II	Sol-gel C	4.07
NRX-II	Arc-Fused	3.43[a]

[a]Average of two samples.

There was no evidence of sintering, grain growth, or central void formation in either rod, as attested in Figs. 4.19 and 4.20. Structurally, the oxide is characterized by a tightly packed fine powder surrounding the coarser fuel particles. The aforementioned metallic inclusions also were found in the irradiated material. There were more large granules of fuel in Z-5 than in U-1 and, consequently, less fine powder. The fuel had a speckled appearance due to uniformly distributed fine porosity; however, this phenomenon has been observed in unirradiated sol-gel oxide (Fig. 4.15b) and appears to be a characteristic of the material rather than the irradiation. There were no indications of reaction at the fuel-clad interfaces.

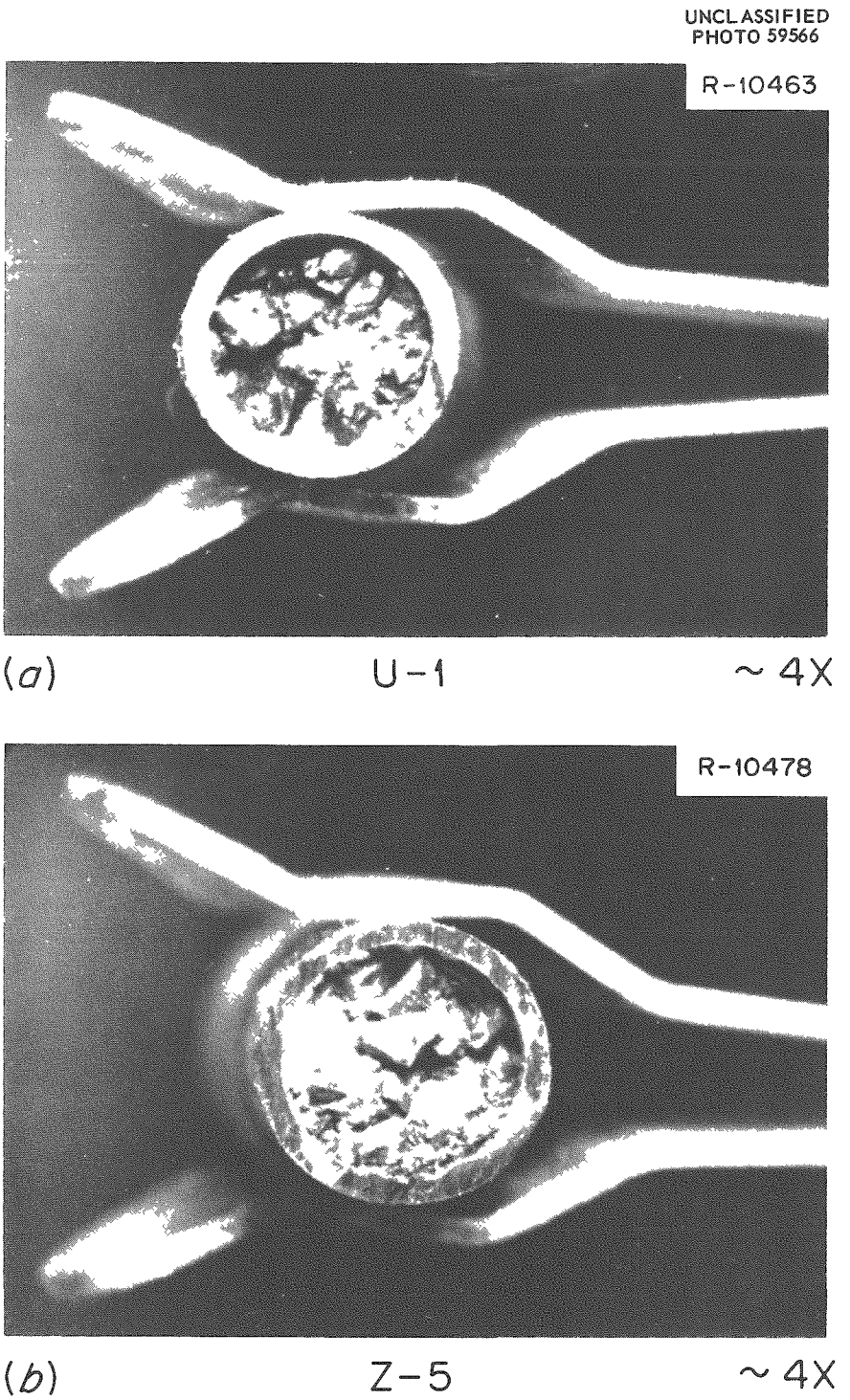

Fig. 4.19. (a) Transverse Cut 3/5 in. from Bottom of Capsule U-1. (b) Transverse Cut 1 in. from Top End of Capsule Z-5.

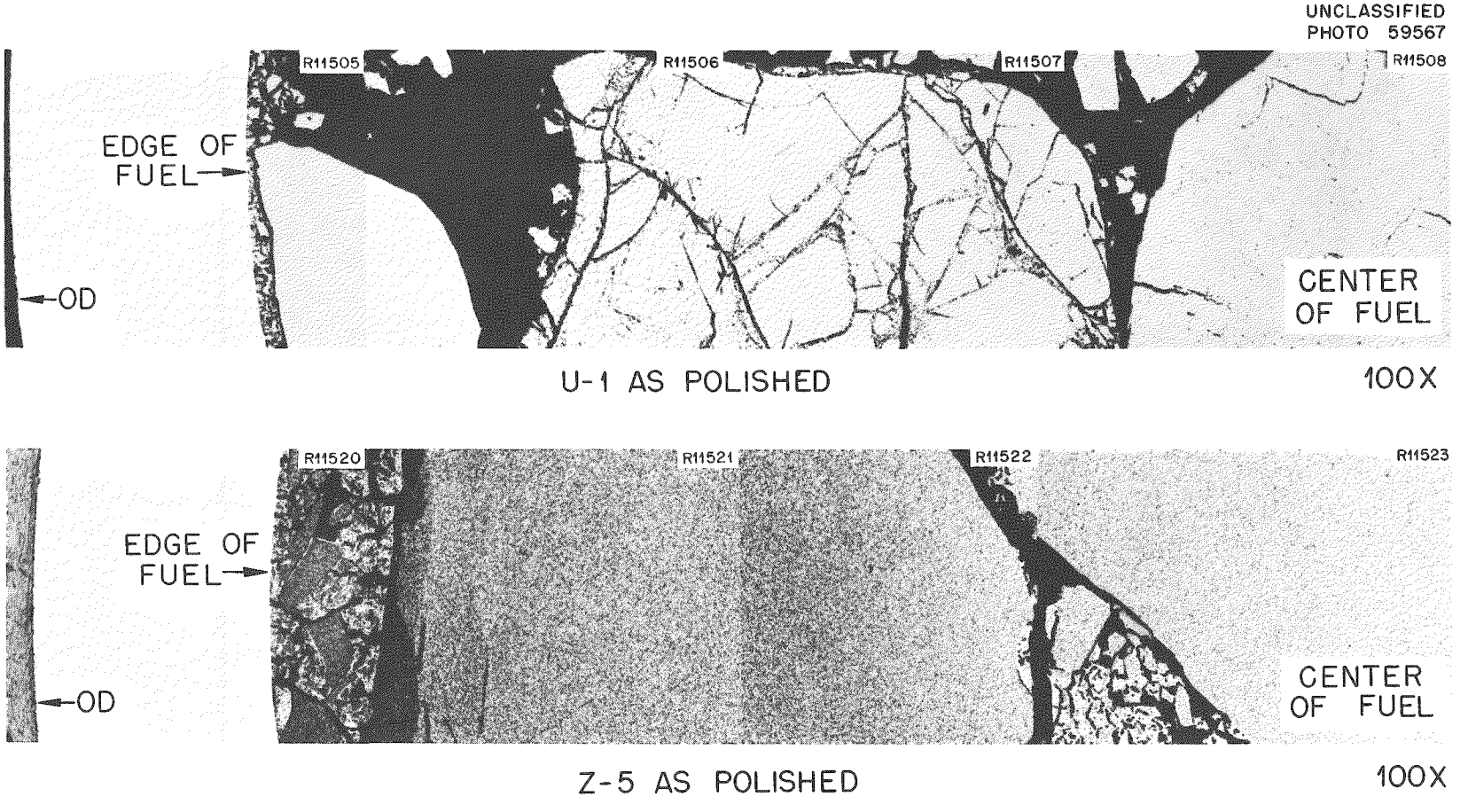

Fig. 4.20. Composite Photomicrographs Showing Typical Transverse Sections of Capsules U-1 and Z-5. Reduced 9%.

The eight NRX Group I capsules, which were irradiated in tandem, also performed satisfactorily in-pile. No deterioration was evident from visual examination. Dimensional measurements showed negligible changes as a result of irradiation.

Gamma scans of the rods did reveal an anomaly. The three capsules containing sol-gel A gave a normal scan with very few peaks and valleys. However, the five capsules containing sol-gel B exhibited an extremely erratic activity profile. This phenomenon is depicted in Fig. 4.21. Since all eight capsules were in one holder, these unusual effects apparently are related to the fuel itself. However, the cause of this anomaly is presently unknown and further examination is in progress.

No microstructural changes in the fuel and clad were apparent as a result of the irradiation, and there is no evidence of sintering or void formation.

The four NRX Group II specimens were prematurely discharged due to leakage of fission products from the holder that contained these rods. Since there were also 100 pellet fuel pins for the power reactor fuel reprocessing program in the same holder, it was not known whether a compacted rod was responsible. Capsule C-3 was suspect because it presumably was stuck to the wall of the holder, apparently having bowed and created a hot spot on the cladding. However, subsequent visual, leak-test, and Zyglo dye-penetrant examinations showed no indications of failure in any of the vibratory-compacted rods.

The results of the vacuum-leak-testing experiments conducted are summarized in Table 4.5. As a result of these tests, a rather interesting phenomenon was observed. The original hole made in each capsule at ORNL to measure fission-gas release was sealed with an epoxy resin and cured for a suitable length of time. Each rod was then punctured at the opposite end and the system pressure allowed to come to equilibrium. The leak rate was then measured and diffusion of gas into the vacuum system was found to be insignificant (Table 4.5). This indicates that no leak was present that would permit diffusion of gas into or out of the capsules at room temperature.

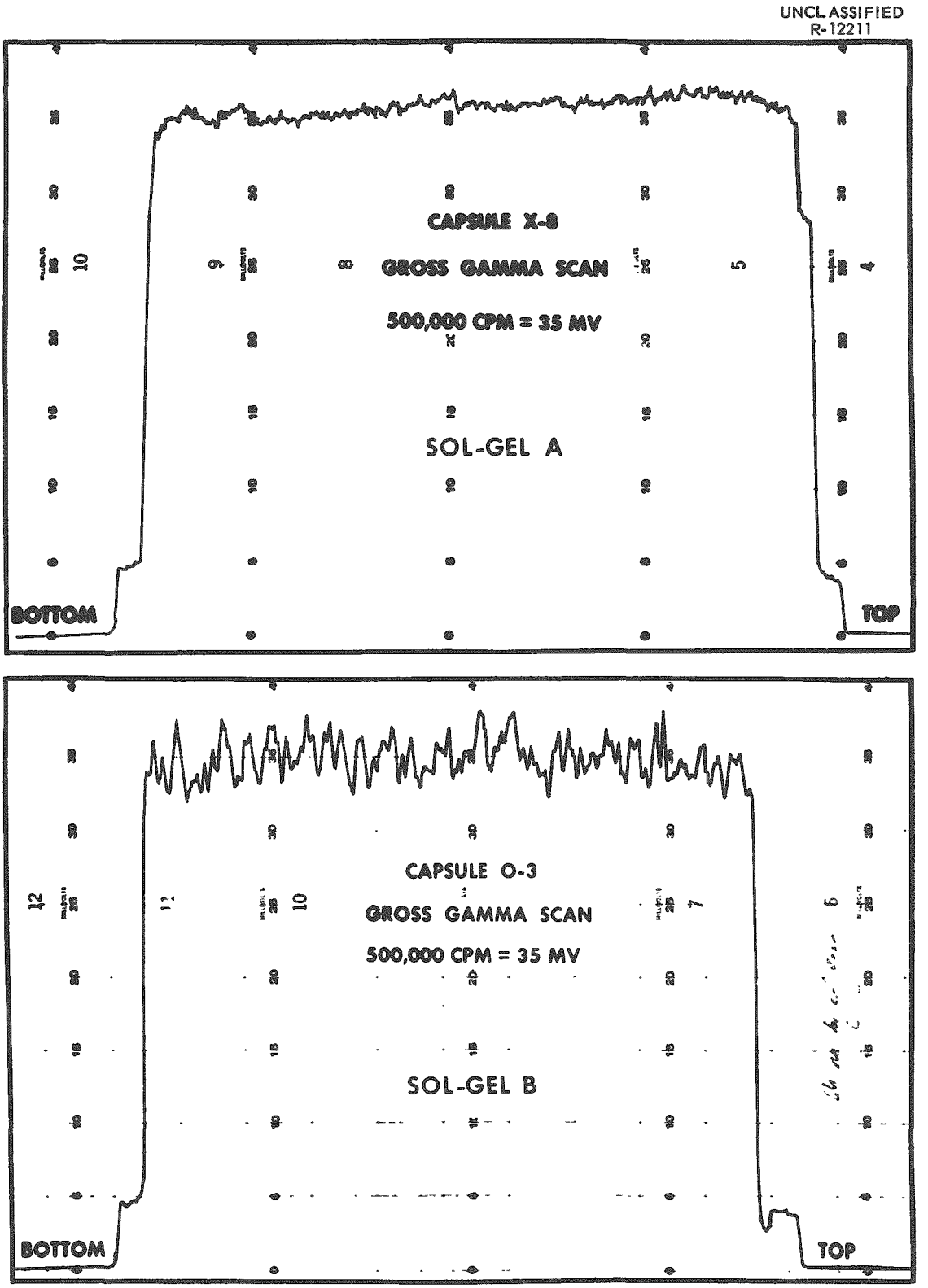

Fig. 4.21. Gamma Scans of Fuel Rods X-8 and O-3 Showing Regular and Erratic Profiles, Respectively.

Table 4.5. Leak Detection on NRX-II Capsules

Rod	Leak Rate[a] Through Cladding (μ/min)	Kr^{85} Activity Atoms Total	Diffusion[b] Rate Through Capsule (μ/min)	Measured Volume of Gas at STP (cc)
A-1	0.2	4.3×10^{13}	1.6	2.52
A-2	1.0	9.5×10^{13}	1.0	2.43
C-3	0.9	2.2×10^{14}	0.9	2.24
C-4	0.9	1.5×10^{14}	c	7.57

[a]After system reached equilibrium.

[b]Both ends pierced.

[c]Rose to atmospheric pressure in 2 hr.

A gas sample was then removed from each rod and analyzed for Kr^{85} activity to determine whether the fission gases had been removed after the initial puncture. Despite the fact that the capsules had been punctured and exposed to the atmosphere for several months, a measurable quantity of Kr^{85} remained (Table 4.5). The rods were then repunctured at the original end and the diffusion rate of air along the length of each rod was measured. As shown in Table 4.5, diffusion was unexpectedly slow except for capsule C-4. From these data, it would appear that gas diffusion was poor through these vibratory-compacted rods. This situation warrants further investigation as the practical implications in terms of fuel element design may be profound.

As was the case with other rods examined, there was no evidence of sintering or void formation. The appearance of the fuel material was similar in each rod.

Preliminary effective thermal conductivity values for the ThO_2-UO_2 fuel in the two ORR poolside capsules were calculated on the basis of the measured parameters given in Table 4.6 and the nominal capsule dimensions (Fig. 4.17).

Table 4.6. Data on ORR Poolside Capsules

Capsule No.	Fuel Bulk Density (g/cc)	Neutron Flux (neutrons cm^{-2} sec^{-1}) Design	Neutron Flux (neutrons cm^{-2} sec^{-1}) Actual	Power Density (w/cc)	Temperature (°F) Clad	Temperature (°F) Center	Temperature (°F) Av Core
06-5	8.54	3.0×10^{13}	2.5×10^{13}	192	1000	2600	1815
03-5	8.60	3.0×10^{13}	3.3×10^{13}	253	1300	3500	2415

Two problems were encountered in the temperature measurements. First, in capsule 03-5, the thermocouple indicated a downward drift which presumably is a result of fuel sintering or a gradual change in thermocouple response. Second, occasional cladding temperature oscillations of ±150°F and ±100°F occurred for 03-5 and 06-5, respectively. These oscillations have been attributed to sporadic convective movement of the NaK surrounding the capsule.[9]

These conductivities include the gradient at the fuel-sheath interface and are averaged over the temperature gradient across the fuel. In performing the calculations, the following assumptions were made:

1. Uniform heat generation occurred in the fuel (neglect flux depression).
2. The internal thermocouple was in contact with the wall of the thermowell.
3. There was no temperature change across the wall of the thermowell.
4. The thermal conductivity of stainless steel was not significantly affected by the irradiation.
5. Energy release was 185 Mev/fission deposited locally, with no additional gamma heating.

The results are listed in Table 4.7 together with some comparative values from the literature for pressed and sintered bodies of ThO_2 and ThO_2–10% UO_{2+x}. It is notable that the conductivities compare favorably.

[9] F. R. McQuilkin, V. A. DeCarlo, R. L. Senn, "GCR Quar. Prog. Rep. March 31, 1962," ORNL-3302, pp 59–61.

However, until burnup analyses are obtained and the flux more accurately determined, these conductivities must be regarded as estimates.

Table 4.7. Thermal Conductivity of Thoria-Base Fuels

Source	Composition	Average Temperature (°C)	Average Temperature (°F)	Thermal Conductivity[a] (w/cm·°C)	Thermal Conductivity[a] (Btu/hr·ft·°F)
ORNL (06-5)	ThO_2–2.9% UO_2	990	1815	0.025[b]	1.44
ORNL (03-5)	ThO_2–2.9% UO_2	1325	2415	0.024[b]	1.38
Kingery[c]	ThO_2	600	1112	0.046	2.66
Kingery[c]	ThO_2	800	1472	0.036	2.08
Kingery[c]	ThO_2	1000	1832	0.033	1.91
Kingery[c]	ThO_2–10% UO_{2+x}	600	1112	0.032	1.87
Kingery[c]	ThO_2–10% UO_{2+x}	800	1472	0.029	1.66
Kingery[c]	ThO_2–10% UO_{2+x}	1000	1832	0.025	1.44

[a]Data corrected to same density as vibrated ThO_2–2.9% UO_2 using the relationship $k_m = k_t$ (1-P) where P = pore volume fraction, k_m is the measured conductivity, and k_t is the value corrected to theoretical density.

[b]Based on flux measurement during test.

[c]W. D. Kingery, "Thermal Conductivity: XIV, Conductivity of Multicomponent Systems," J. Am. Ceram. Soc. 42(12): 617 (1959).

As previously mentioned, the trefoil cluster (L-1) was removed from the ORR pressurized-water loop when leakage of fission products was detected. The fuel rods were blanketed by a dark deposit which was loosely adherent and readily removed with steel wool and soap. After disassembling and scraping the rods, a failure was located on rod L1B approximately 2 1/2 in. from the top end. This area is situated midway along the length of the plenum, or about 1 1/4 in. above the top of the fuel column. The appearance of this area (Fig. 4.22) indicates that the failure occurred as a result of some corrosion reaction; also, a circumferential crack propagated around the surface of the rod. Diametral

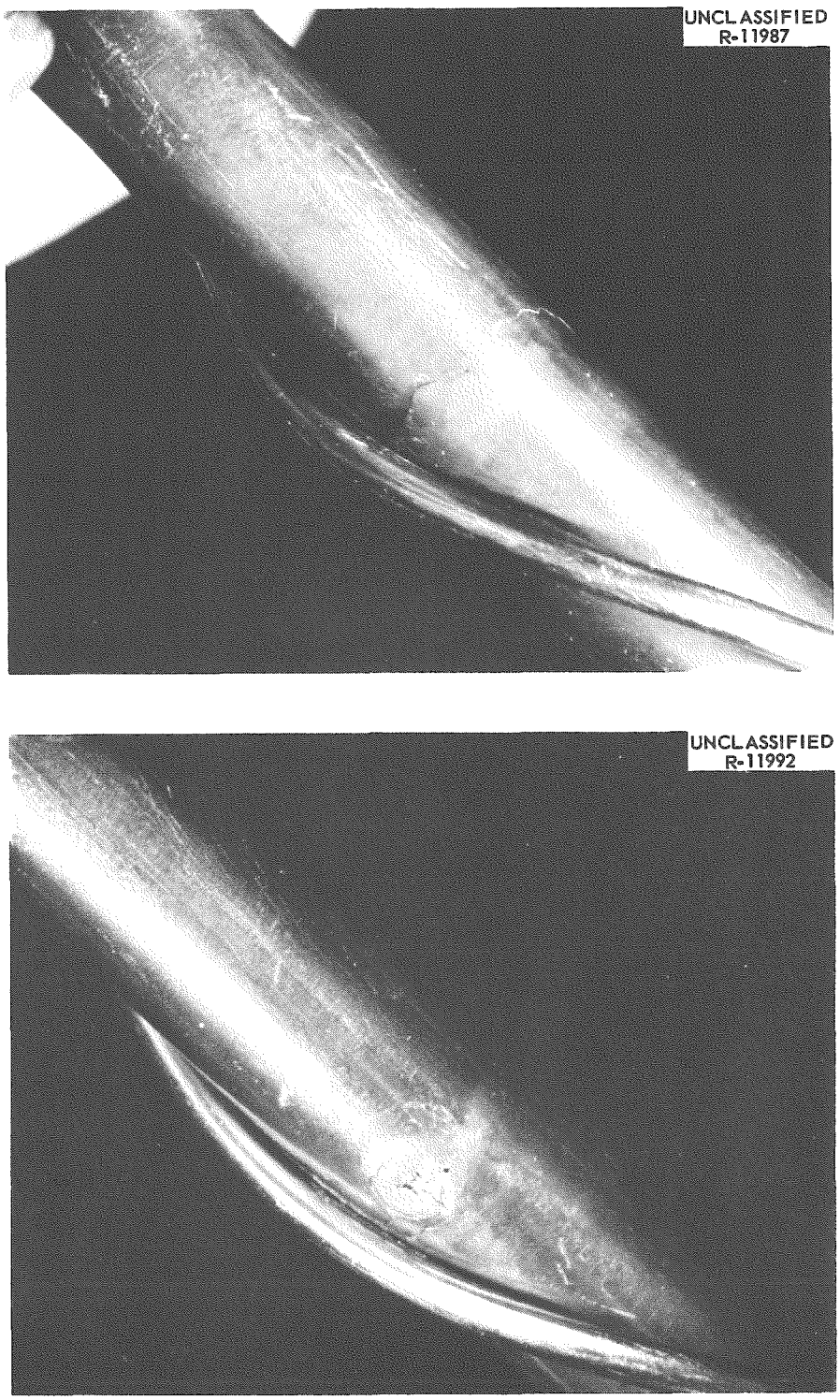

Fig. 4.22. Defective Area Approximately 2-1/2 in. from Top End of Zircaloy-2 Clad Fuel Rod L1B.

measurements at this location in comparison with the surrounding regions revealed that swelling up to 25 mils had occurred. Contrast dye-penetrant inspection of this area indicated a leak. An explanation, however, of the location and causes of this failure awaits further examination.

4.4.3 Fission-Gas-Release Studies

In conjunction with in-pile irradiation studies, neutron-activation (D')[10,11] studies are under way to characterize fission-gas release from sol-gel and arc-fused oxide. Individual samples containing 0.2–0.6 mg of U^{235} were irradiated in the graphite reactor to an integrated dose of 6.77×10^{17} nvt and then vacuum-induction annealed. Then the release of Xe^{133} was continuously monitored in a charcoal-filled bulb.

In the case where diffusion is the primary release mechanism, several important relationships can be derived. After irradiation, the fraction of a stable isotope released during annealing under isothermal conditions may be expressed by

$$F = \frac{6}{\sqrt{\pi}} \sqrt{\frac{Dt}{a^2}} , \qquad (1)$$

where

F = fraction released,

D = diffusion coefficient (cm^2/sec),

t = annealing time (sec),

a = radius of equivalent sphere (cm).

The above equation is correct for small values of F. Because of uncertainties in measuring the equivalent radius, it is more convenient to determine the quantity $D' = (D/a^2)$ which is the release-rate parameter.

---

[10] D. F. Toner and J. L. Scott, "GCR Quar. Prog. Rep. Dec. 31, 1959," ORNL-2888, pp 68–72.

[11] A. H. Booth and G. T. Rymer, "Determination of the Diffusion Constant of Fission Xenon in UO_2 Crystals and Sintered Compacts," AECL-692 (August 1958).

Equation 1 then becomes

$$F = \frac{6}{\sqrt{\pi}} \sqrt{D't} \quad . \tag{2}$$

For diffusion-controlled release, a plot of F vs $t^{1/2}$ at a given temperature will be linear and D' can be readily determined from the slope of the curve. Further, it is known that for a diffusion process the temperature dependence of release rate will be given by the Arrhenius relationship

$$D' = D'_o \, e^{-Q/RT} \quad ,$$

where

D'_o = a constant,

Q = activation energy for process (cal/mole),

R = universal gas constant (1.987 cal/g·mole·°C),

T = absolute temperature.

By determining D' at several temperatures and plotting the log D' vs 1/T, the activation energy can be determined from the slope of the plot.

Available data for sol-gel ThO_2–5 wt % UO_2, sol-gel ThO_2–5.9 wt % UO_2, arc-fused ThO_2–4.5 wt % UO_2, and arc-fused UO_2 are compiled in Table 4.8.[12-15]

The fraction of Xe^{133} released as a function of temperature for the sol-gel oxide is shown in Fig. 4.23. Note that after an initial burst of gas, which has also been observed for UO_2,[16] the release mechanism

---

[12] J. L. Scott and D. F. Toner, "GCR Quar. Prog. Rep. March 31, 1961," ORNL-3102, pp 93–7.

[13] J. L. Scott, D. F. Toner, R. E. Adams, "GCR Quar. Prog. Rep. June 30, 1961," ORNL-3166, pp 89–91.

[14] J. L. Scott, D. F. Toner, R. E. Adams, "GCR Quar. Prog. Rep. Dec. 31, 1961," ORNL-3254, pp 153–5.

[15] R. B. Fitts, Oak Ridge National Laboratory, Private Communication, November 1962.

[16] B. Lustman, "Irradiation Effects in Uranium Dioxide," Uranium Dioxide: Properties and Nuclear Applications, pp 431–666, ed. J. Belle, U. S. Government Printing Office, Washington, D. C., 1961.

Table 4.8. Neutron-Activation Studies on Ceramic Fuel Powders

Material	Preparation	Particle Size (mesh)	Test Temperature (°C)	Total Xe^{133} Fraction Released (cumulative)	Total Test Time (hr)	Release-Rate Parameter D' (sec^{-1})
ThO_2–5 wt % UO_2	Sol-gel (similar to B)	Coarse chunks	1440	4.43×10^{-3}	18.8	4.64×10^{-12}
			1640	9.38×10^{-3}	22.7	7.32×10^{-11}
			1760	1.23×10^{-2}	19.6	1.10×10^{-10}
			2015	3.47×10^{-2}	48.0	1.27×10^{-9}
			2200	3.06×10^{-1}	25.0	b
ThO_2–5.9 wt % UO_2	Sol-gel S	-10 +16	Irrad.[a]	4.81×10^{-4}	--	To be determined
			1000	2.30×10^{-3}	2.0	
			1200	2.40×10^{-3}	2.0	
			1400	2.56×10^{-3}	2.0	
			1800	1.29×10^{-2}	2.0	
			2000	1.30×10^{-2}	2.0	
		-325	Irrad.[a]	1.86×10^{-2}	--	
			1000	5.14×10^{-2}	2.0	
			1200	1.30×10^{-1}	2.0	
ThO_2–4.5 wt % UO_2	Arc-fusion	-70 +100	1000	2.9×10^{-3}	25.0	1.7×10^{-12}
			1200	8.9×10^{-3}	25.0	6.1×10^{-12}
			1400	3.2×10^{-3}	25.0	1.4×10^{-11}
			1600	3.94×10^{-2}	25.0	3.5×10^{-11}

Table 4.8 (continued)

Material	Preparation	Particle Size (mesh)	Test Temperature (°C)	Total Fraction Xe^{133} Released (cumulative)	Total Test Time (hr)	Release-Rate Parameter D' (sec^{-1})
ThO_2–4.5 wt % UO_2	Arc-fusion	-10 +16	1000	3.2×10^{-4}	25.0	5.5×10^{-14}
			1200	8.6×10^{-4}	25.0	1.5×10^{-13}
			1400	2.3×10^{-3}	25.0	1.4×10^{-12}
UO_2	Arc-fusion	-70 +100	1400	5.91×10^{-3}	22.5	1.13×10^{-11}
			1600	1.67×10^{-2}	24.5	2.66×10^{-10}
UO_2	Pellet fuel	--	1900	Complete	25.0	b

[a]Release on puncture after neutron activation.

[b]Release not controlled by diffusion.

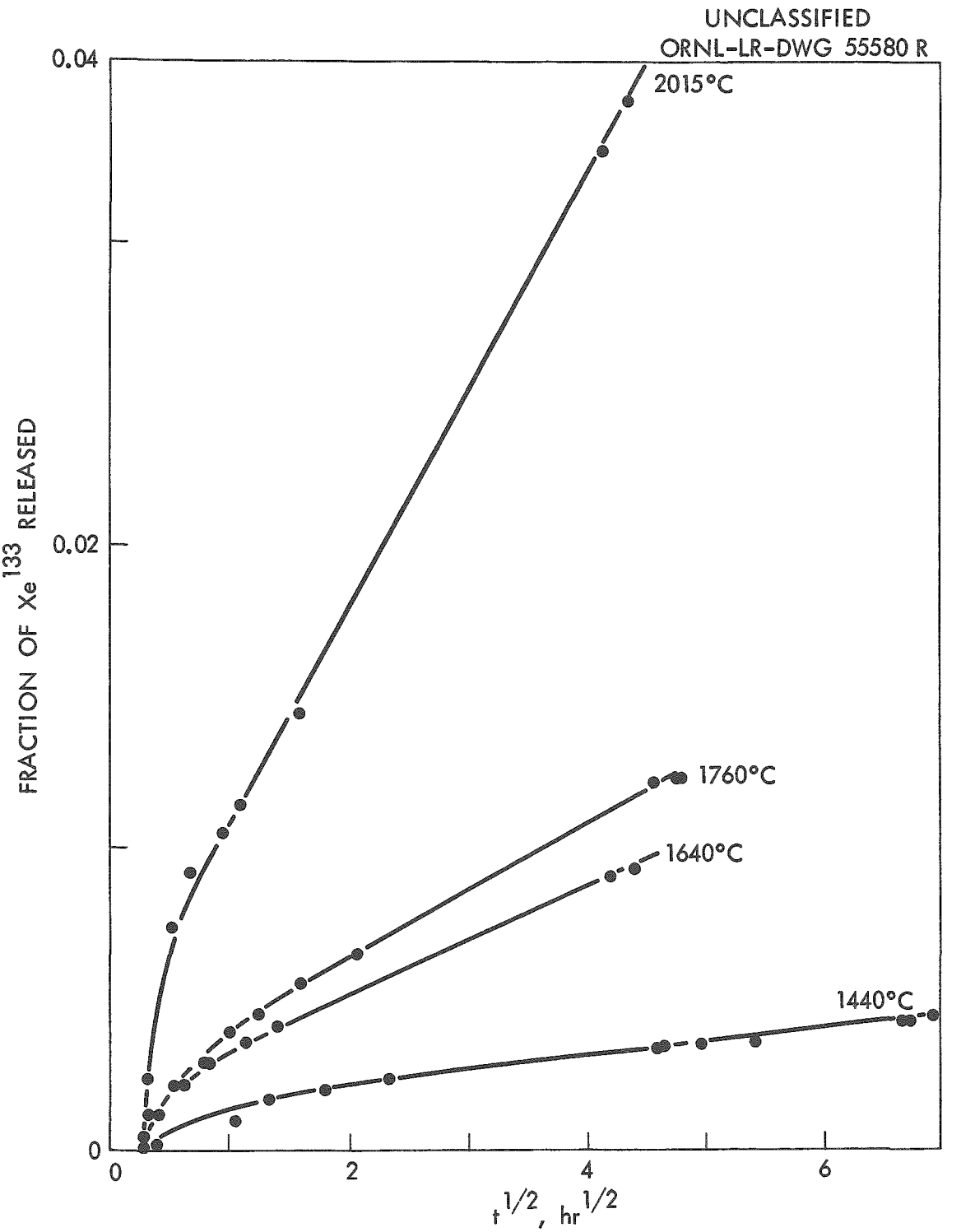

Fig. 4.23. Release of Xe^{133} from ThO_2–5 Wt % UO_2 Prepared by the Sol-Gel Process. Results obtained by neutron-activation technique.

was diffusion. Results for the arc-fused ThO_2-UO_2 were comparable. Release was lower by a factor of ten for the coarse fraction than for the medium size fraction. Increased release with decreasing particle size was also noted for sol-gel S, which is the expected effect of decreasing particle size. It is also notable that whereas 30.6% of the Xe^{133} was released from the sol-gel ThO_2-UO_2 at 2200°C after 25 hr, Xe^{133} was completely released from UO_2 at 1900°C for a comparable time and the UO_2 sample vaporized. This clearly illustrates the greater stability of ThO_2-UO_2 compared to UO_2, which is to be expected, since the melting point of ThO_2 is 3300°C compared to 2750°C for UO_2.

From the slope of the curve of log D' vs the reciprocal of the absolute temperature (Fig. 4.24), the activation energy for diffusion of Xe^{133} from sol-gel and arc-fused ThO_2-UO_2 was calculated to be 75.9 kcal/mole and 25 kcal/mole, respectively. These values compare to 70–80 kcal/mole reported for diffusion of xenon from UO_2.[17] The difference in activation energy between sol-gel and arc-fused ThO_2-UO_2 may be due to the structural differences between the two materials (Figs. 4.14 and 4.15).

Since the NRX and MTR capsules ran at relatively low central temperatures, it would be expected that a significant portion of the fission-gas release occurred by a mechanism other than diffusion. This quantity can be estimated from the neutron-activation data by adding the fraction released during the low-temperature irradiation to the burst release upon subsequent annealing. This is being done for sol-gel S and will be conducted on other powders.

4.4.4 Other Experiments to be Conducted

The experiments currently or soon to be in-pile (Table 4.2) provide comparisons and assessments in the following areas: (1) type of oxide,

---

[17] W. B. Cottrell, J. L. Scott, H. N. Culver, M. M. Yarosh, "Fission Products Release from UO_2," ORNL-2935 (Sept. 13, 1960).

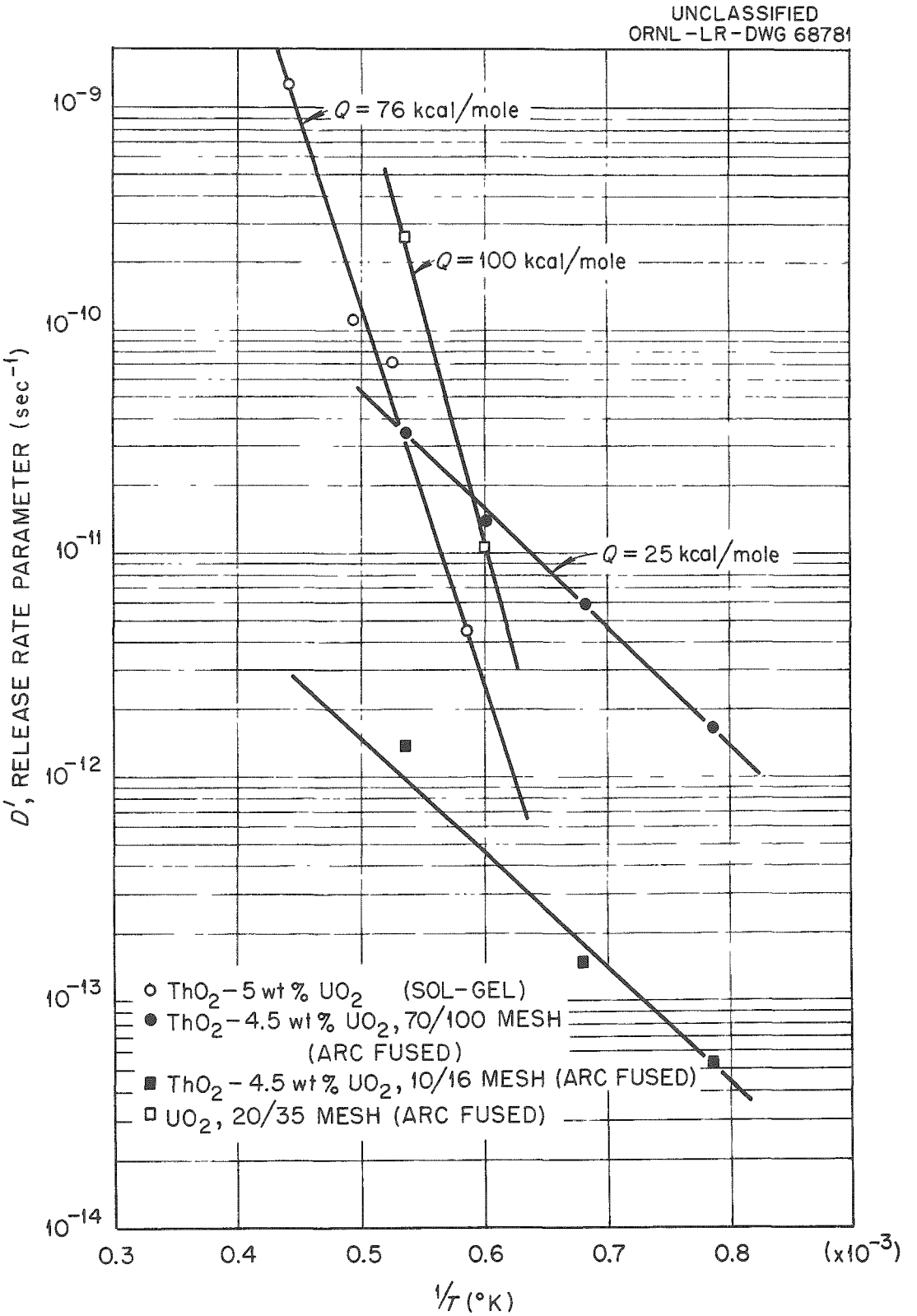

Fig. 4.24. Log D' vs 1/T' for Various Oxide Fuels.

(2) content of fissile material, (3) fuel rod length, (4) irradiation temperature, (5) heat-generation rate, and (6) burnup. In addition to concluding this work, it is necessary that the scope of the program be broadened by embarking upon new areas of investigation.

Among the in-pile experiments under consideration are the following: (1) exposure at higher heat ratings; (2) variations in fuel chemistry, which include testing fuel with a higher uranium content and a comparison of air-fired vs H_2-fired sol-gel oxides; (3) irradiation of larger diameter specimens; (4) remote fabrication and irradiation of fuel rods and a large fuel rod bundle containing U^{233}; (5) constant power irradiation tests; and (6) evaluation of new fuel systems. Finally, additional out-of-pile studies appear warranted in such areas as: (1) characteristics of sol-gel powder particles and the relation to irradiation performance; (2) sintering behavior of arc-fused and sol-gel oxide; (3) thermal conductivity; (4) neutron activation to evaluate fission-gas release; and (5) waterlogging susceptibility.

4.5 Thoria Pellet Development (R. A. Potter, A. J. Taylor)

Techniques were developed for preparing and characterizing coated and uncoated ThO_2 pellets suitable for use in fluidized-blanket systems where high attrition resistance is required. During this report period, 1/8-in.-diam pellets of two different geometries were considered: (1) round-edged right-circular cylinders with a length-to-diameter ratio (L/D) of 1, and (2) spheroids, both coated and uncoated.

The specifications for the pellets are that they be of such quality, size, and geometry to exhibit minimum attrition losses during periodic arrangement of the blanket in reactor operation. For coated pellets, the permissible amount of coating material is determined by its poison effect on neutrons and should not exceed 0.01 absorption per absorption in thorium.

Fabrication methods were developed whereby pellet density and grain size could be controlled. The effects of these properties on attrition

resistance were investigated. Some consideration was given to the properties of the ThO_2 powder from which the pellets were made; however, a complete evaluation and correlation of these properties were not effected. Coatings of Al_2O_3 and Zr metal were evaluated on the basis of spouted bed tests.

Although the pellet development project has been terminated, provisions are in effect for an orderly close-out. Coated spheroids are presently being examined by metallographic techniques. The forthcoming information will be used in conjunction with the data obtained during spouted bed tests for an evaluation of the coatings. Additional data concerning the effect of pellet grain size and density on attrition resistance also will be obtained.

4.5.1 Fabrication

Thoria Powder. The powder used for the fabrication of pellets was a Chemical Technology Division Pilot Plant oxide,[18] designated DT-102, which was made by precipitation of thorium oxalate from a nitrate solution followed by calcination at 800°C tc the oxide. The characteristics of this powder are given in Tables 4.9, 4.10, and 4.11.

Table 4.9. Some Physical Properties of Batch DT-102 ThO_2 Powder

Crystallite Size,[a] A	261
Surface Area,[b] m^2/g	15.5
Mean Particle Size,[c] μ	1.15

[a]Determined from x-ray line broadening.
[b]Determined by BET method using N_2.
[c]Determined by sedimentation method.

[18]A. Taboada et al., "HRP Prog. Rep. Nov. 30, 1960," ORNL-3061, p 101.

Table 4.10. Particle-Size Analysis for Batch DT-102 ThO_2 Powder

Apparent Stokes Diam, d_g (μ)	Amount of Material With Size Equal to or Less Than That Given in First Column (wt %)
25.60	99.0
7.10	99.0
5.11	99.0
4.20	99.0
3.66	99.0
3.00	99.0
2.60	98.1
2.03	91.5
1.84	90.3
1.65	81.7
1.50	76.4
1.40	67.7
1.30	61.8
1.20	52.5
1.10	41.8
1.00	33.6
0.70	11.4

Table 4.11. Chemical Analysis of Batch DT-102 ThO_2 Powder

Element	Amount Present (%)
Th	87.45
Al	0.0006
Ca	0.0062
Cl	<0.001
CO_3	0.15
Cr	<0.001
F	<0.001
Fe	0.002
K	0.001
Li	0.004
Mg	0.0007
Na	0.0025
Ni	0.004
NO_3	0.003
Pb	<0.001
PO_4	0.004
Si	0.001
SO_4	0.006
Loss on ignition	0.21

Forming and Sintering Techniques. During the initial stages of the investigations, the procedures for cold forming the pellets were modified to accommodate specific batches of powder. However, toward the end of the program, the procedure as outlined below was adopted as standard.

1. Prepress powder at 15,000 psi and granulate to pass 100 mesh.
2. Cold press in steel dies to form either cubes or cylinders of 4.1 g/cm^3 density.
3. Isostatically press at some pressure in the range 12,500–35,000 psi, predetermined according to desired density.
4. Tumble pellets in a cylindrical jar mill. (In the case of cubes, tumble until spheroids of the desired size are formed. In the case of cylinders, tumble until all edges are removed.)
5. Sinter at 1750°C in H_2 for a predetermined time according to desired grain size.
6. Polish sintered pellets by tumbling with Al_2O_3 grog.

Slight modifications of this procedure afford the flexibility necessary when using different batches of oxide under different conditions. For example, it was found in previous work[19] with a different batch of oxide formed into cubes on an automatic press that the addition of an organic binder was necessary in order to produce a free flowing powder adaptable to the automatic operation. The addition of this binder then preceded Step 1 cited in the general procedure.

Pellets were sintered in a hydrogen-atmosphere continuous furnace at 1750°C. Grain size was systematically varied by varying the sintering time. Sintering periods of 2/3, 16, and 65 hr resulted in grain sizes of approximately 35, 60, and 100 μ, respectively.

4.5.2 Characterization of Pellets

A series of round-edged right-circular cylindrical pellets was prepared in accordance with the standard preparation procedure which was

---

[19] A. Taboada et al., "HRP Prog. Rep. May 31, 1961," ORNL-3167, p 111.

somewhat modified. Tumbling (Step 4) was changed to follow sintering (Step 5) and 1/4-in. Al_2O_3 balls and water were added to the charge. Density and grain size of these pellets were controlled by varying isostatic pressure and sintering time. Fabrication variables and properties of these pellets are given in Table 4.12. The results showed that grain size is a major controlling factor with regard to attrition resistance and that bulk density per se in the range 91 to 97% of theoretical is much less important. This correlation is consistent with the data obtained from a previous set of pellets (Code P-82) of relatively small grain size (10–15 μ).[20] The attrition resistance as displayed by the fine-grained Code P-82 pellets was very good compared with other pellets made during these investigations.

4.5.3 Evaluation of Coated ThO_2 Spheroids

Spheroids of 1/8-in. diam with an average bulk density of 96.0% of theoretical prepared by the standard procedure were coated with two different materials by Battelle Memorial Institute under a subcontract arrangement. Some characteristics of the as-coated spheroids are shown in Table 4.13 and the results of attrition tests are given in Table 4.14.

As shown in Table 4.14, pellet attrition resistance may be increased considerably with the proper application of a coating such as Al_2O_3. Code P-171 pellets show particular promise; for these pellets the weight-loss rate compared with the uncoated control sample (Code P-169) was better by a factor of six. Furthermore, the Al_2O_3 coating of 80 μ is within the limits of coating specifications based on neutron absorption, which allow an Al_2O_3 coating of 84-μ thickness on a 1/8-in. sphere. The lack of integrity displayed by some of the coated pellets suggests that close control must be maintained during the coating process.

---

[20] A. Taboada et al., "HRP Prog. Rep. May 31, 1961," ORNL-3167, p 84.

Table 4.12. Effects of Grain Size and Density on Attrition Resistance of ThO_2 Pellets

Code No.	Pressing Pressure (psi)	Sintering Time at 1750°C in H_2 (hr)	Bulk Density (% of theoretical)	Approximate Grain Size (μ)	Overall Weight Loss Rate During Spouted Bed Test[a] (%/hr)
P-165	12,500	2/3	91.4	35	0.63
P-159	18,000	2/3	92.6	35	0.65
P-162	35,000	2/3	94.3	35	0.61
P-166	12,500	16	95.3	60	0.95
P-160	18,000	16	95.5	60	0.83
P-163	35,000	16	96.8	60	0.87
P-167	12,500	65	96.6	100	1.3
P-161	18,000	65	96.8	100	1.2
P-164	35,000	65	96.7	100	1.2

[a]Six-hour test conducted using 0.3 fps superficial velocity. Pellets in static autoclave for 72 hr in 260°C H_2O between second and third hour of spouted bed test. Attrition-resistance tests were performed by S. Reed, Reactor Chemistry Division, ORNL.

Table 4.13. Characteristics of Coated ThO_2 Spheroids

Batch No.	Coating	Coating Thickness[a] (μ)	Appearance[b]	Average Hardness KHN 50-g Load	
				Coating	ThO_2
19245-5	Al_2O_3	80	Dense, void-free, smooth surface, slightly translucent	2750	875
19245-6A	Al_2O_3	130	Dense, void-free, knobby surface, several layers	2600	780
19245-7B	Al_2O_3	180	Dense, void-free, smooth surface, white-opaque	2200	760
19245-9	Al_2O_3	195	Dense, void-free, smooth surface, inner layer white-opaque, outer layer more translucent	2550	860
19245-10	Al_2O_3	100	Dense, void-free, smooth surface, white-opaque	2300	915
15755-32	Zr	45	Porous, continuous	510	c
15755-35	Zr	75	Porous, continuous	c	c
15755-36	Zr	60	Inner 20 μ, fairly dense, balance porous	c	c
15755-38	Zr	10	Fairly dense coating	c	c

[a]Based on measurement of the coating thickness of one ball.

[b]Based on visual observation of sectioned spheroids.

[c]Not determined.

Table 4.14. Weight-Loss Data for Coated ThO_2 Pellets During Spouted Bed Tests[a]

Code	Identification No.	Type Coating	Superficial Velocity (fps)	Overall Weight Loss Rate During Spouted Bed Tests[b] (%/hr)
P-168	15755-36	Zr	0.16	0.26
P-169[c]	257-L1	None	0.18	0.22
P-170[c]	257-L2	None	0.16	0.20
P-171	19245-5	Al_2O_3	0.18	0.033
P-172	19245-6A	Al_2O_3	(Two pellets broken after autoclave test)	
P-173	19245-7B	Al_2O_3	0.18	0.28
P-174	19245-9	Al_2O_3	(One pellet broken into two pieces after first test)	
P-175	19245-10	Al_2O_3	(Coating gone from one pellet after first test)	

[a]Tests performed by S. Reed, Reactor Chemistry Division, ORNL.

[b]Two 1-hr tests, pellets in static autoclave in 260°C H_2O between tests.

[c]Control samples.

4.6 Thorium Metal Development

Thorium metal has several characteristics which make it an attractive fuel material for converter or breeder reactor systems. Its value would be considerably enhanced if it were more resistant to irradiation damage. Increasing the elevated-temperature strength is one method by which improved performance can be achieved. Two approaches are under study to effect an increase in the strength of thorium metal. One technique is to use alloying elements which provide solid-solution strengthening. Zirconium, indium, and beryllium in conjunction with carbon have exhibited promising results. A second approach is to utilize dispersion hardening. For several reasons this seems to offer more potential than solid-solution alloying. For instance, a stable oxide dispersoid provides greater creep resistance at elevated temperatures. These particles may also act as nucleation sites and alleviate the tendency to form large bubbles with attendant metal swelling. On the debit side, thorium alloys can readily be produced, whereas, achieving the fine particle, uniform dispersion of stable oxide particles is difficult. Much of the effort in the past year has been directed toward developing fabrication techniques to obtain the desired structure.

The procedure which appears most promising consists of blending and milling powders of thorium hydride and thorium oxide. The mixed powders are hot pressed under vacuum which simultaneously compacts and reduces the hydride to the metal. The compacts are then extruded. Hot-hardness tests have been performed on compacts of several different mixtures. The results on Th–10 vol % AlO(OH), Th–10 vol % ZrO_2, and Th-ThO_2 are compared in Fig. 4.25 with that obtained for arc-melted thorium metal. The highest hardness values at all temperatures were obtained from the compact containing AlO(OH). However, both the AlO(OH) and ZrO_2 reacted with thorium and formed large agglomerates of thoria. This instability and coarsening of the particles will most certainly tend to reduce the effectiveness of the hard particle in increasing the creep strength of thorium.

In order to obtain a finer and more uniform dispersion of ThO_2 in thorium, studies have been made of the effects of milling variables on the

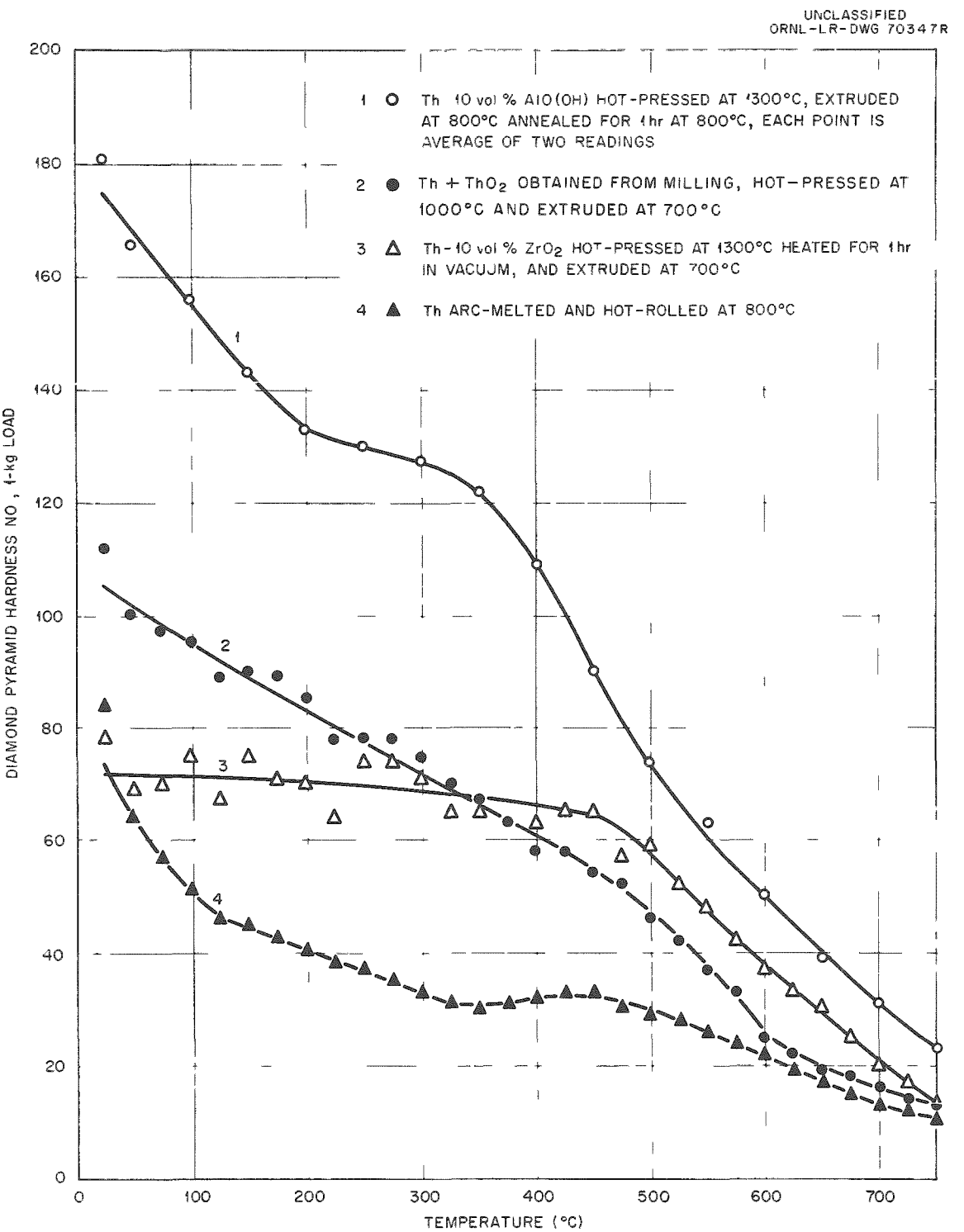

Fig. 4.25. Hot-Hardness Curves of Thorium and Thorium Containing Dispersions of Hard Particles.

particle size of thorium hydride. Also, a source of ultrafine thoria powder has been found which can supply powders having an average particle size of 0.05 μ. The ball-milling results indicated that milling times of one and twenty-four days produced a minimum particle size of thorium hydride of 1.8 μ as measured by neutron activation-sedimentation analysis. Proceeding from the milling studies a series of hot-pressed compacts has been prepared containing 10 vol % of the ultrafine thoria. The powder mixtures were ball milled for times varying between one and twenty-four days. Hot-hardness results on some as-pressed compacts indicate hardness values significantly greater than those obtained from the compact containing AlO(OH)at temperatures above 400°C. It is expected that extrusion of the compacts will give even greater improvement in hot hardness because of increased densification and better distribution of the oxide.

The performance of thorium as a fuel material may be improved by introducing the fissile material as stable particles in the thorium matrix, as in a dispersion-type fuel. Compatibility studies were made to determine the degree of reaction between thorium and particles of UC, UC_2, and UO_2. Also, the effectiveness of coatings of pyrolytic carbon and niobium to prevent reaction was investigated. The most stable particles at temperatures to 1100°C were found to be UC and UC_2 coated with pyrolytic carbon. Niobium coatings were ineffective and uncoated UO_2 proved the least resistant to reaction.

ORNL-3385
UC-25 — Metals, Ceramics, and Materials
TID-4500 (22nd ed.)

INTERNAL DISTRIBUTION

1. Biology Library
2-4. Central Research Library
5. Reactor Division Library
6-7. ORNL — Y-12 Technical Library Document Reference Section
8-27. Laboratory Records Department
28. Laboratory Records, ORNL R.C.
29. R. E. Adams
30. G. M. Adamson
31. R. E. Biggers
32. R. E. Blanco
33. J. C. Bresee
34. R. E. Brooksbank
35. K. B. Brown
36. J. A. Burka
37. W. H. Carr
38. W. L. Carter
39. S. D. Clinton
40. F. L. Culler
41. J. E. Cunningham
42. F. W. Davis
43. J. H. Day
44. O. C. Dean
45. D. A. Douglas
46. W. S. Ernst, Jr.
47. D. E. Ferguson
48. J. H Frye, Jr.
49. H. E. Goeller
50. C. E. Guthrie
51. Paul Haas
52. J. P. Hammond
53. W. O. Harms
54. C. C. Haws
55. D. M. Hewette
56. M. R. Hill
57. A. R. Irvine
58. J. L. Kelly
59. E. M. King
60. A. T. Kleinsteuber
61. T. Koizumi
62. C. E. Larson
63. C. F. Leitten
64. A. L. Lotts
65. H. G. MacPherson
66. A. H. Malone
67. W. D. Manly
68. J. P. McBride
69. R. V. McClung
70. K. H. McCorkle
71. E. C. Moncrief
72. C. S. Morgan
73. L. E. Morse
74. P. Patriarca
75. F. L. Peishel
76. S. A. Rabin
77. J. L. Scott
78. J. D. Sease
79. M. J. Skinner
80. G. M. Slaughter
81. J. W. Snider
82. J. A. Swartout
83. R. E. Thoma
84. D. G. Thomas
85. W. C. Thurber
86. J. W. Ullmann
87. A. M. Weinberg
88. J. R. Weir
89. W. J. Werner
90. M. E. Whatley
91. W. R. Whitson
92. R. E. Whitt
93. R. G. Wymer
94. P. H. Emmett (consultant)
95. J. J. Katz (consultant)
96. T. H. Pigford (consultant)
97. C. E. Winters (consultant)
98. A. A. Burr (consultant)
99. J. R. Johnson (consultant)
100. C. S. Smith (consultant)
101. R. Smoluchowski (consultant)

EXTERNAL DISTRIBUTION

102. Research and Development Division, AEC, ORO
103-687. Given distribution as shown in TID-4500 (22nd ed.) under Metals, Ceramics, and Materials category (75 copies — OTS)